CHAPTER ONE

INTRODUCTION AND BASIC CONCEPTS

INTRODUCTION 1.1

Water is essential to life. It is part of the physiological process of nutrition and waste removal from cells of all living things. It is one of the controlling factors for biodiversity and the distribution of Earth's varied ecosystems, communities of animals, plants, and bacteria and their interrelated physical and chemical environments. In terrestrial ecosystems, organisms have adapted to large variations in water availability (Stephen J. et al. 2002).

Water use by organisms in desert ecosystems is vastly different from those in forest ecosystems. For example, some seeds lie dormant for years in arid climates waiting to be awakened by a rare precipitation event. In contrast, a large oak tree in a temperate climate returns about 4,000 gallons of water a year to the atmosphere. Through the process of transpiration, plants give off moisture largely through their leaves. Aquatic ecosystems, such as wetlands, streams, and lakes, are especially sensitive to changes in water quality and quantity. These ecosystems receive sediment, nutrients, and toxic substances that are produced or used within their water shed the land area that drains water to a stream, river, lake or ocean. As a result, an aquatic ecosystem is indicative of the conditions of the terrestrial habitat in its watershed. Wetland ecosystems provide habitat to a great variety of birds, plants and animals. These transitional areas between dry and wet habitats help reduce floods and abate water pollution. They also support many recreational activities and commercial fisheries and provide a number of other important functions. Nearly every activity that occurs on land ultimately affects ground waters or surface waters. Water plays a major role in shaping the land surface of the Earth. Canyons, flood plains, terraces, and watersheds are formed by the action of water flowing across the land surface. As a result, watersheds have many different shapes and sizes. Some contain parts of mountains and hills, and others are nearly flat (Stephen J. et al. 2002).

Water either is used in the stream (in stream use) or it may be diverted from a stream or reservoir or taken from a well, then transferred to a place of use (off stream use). Examples of in stream water use include recreation, hydroelectric power generation, fisheries, ecosystem and channel maintenance, and transportation. Water-use estimates for these categories are difficult to obtain because water is used numerous times as it flows down a river. Water flowing from an upstream hydroelectric power plant is used by the power plants downstream, and because very little water is consumed by in stream uses, near-continual water reuse is possible. Domestic, commercial, agricultural, industrial, mining, and thermoelectric power generation are examples of off stream uses. Only a portion of the water removed for an off stream use is actually consumed. The remaining water returns to the stream or the aquifer and can be used again (Stephen J. et al. 2002).

The need for water resources, combined with their environmental importance and variable availability, necessitates that we manage them wisely. Historically, management focused only on supplying water to areas of need. Effective management of water resources is a complex task that requires knowing where water is located, where it is needed, its physical and legal availability, its quality and its contents, the effects of its use on ecosystems, the risk of contamination, and the cost of meeting the demand. Modern management of surface water resources addresses concerns throughout the water shed. By assessing land and water-use practices within a watershed, water managers are able to determine the human activities and natural processes that affect both the quantity and quality of water within it. Part of that is the characterization of water resources which is very important to manage the use of water. Activities in one part of a watershed can influence the water resources in other parts of the water shed. Groundwater resources do not necessarily correspond to surface watershed boundaries. However, surface waters and groundwater generally are connected. Besides recently fallen precipitation, most of the water we see flowing in streams day to day is

water that is returning to the surface from groundwater and not just runoff from the land surface. Thus, land and water-use activities, such as withdrawing or contaminating groundwater, can affect either resource in more than one watershed. The availability of groundwater as a water source depends largely upon surface and subsurface geology as well as climate. The porosity and permeability of a geologic formation control its ability to hold and transmit water. Porosity is measured as a ratio of voids to the total volume of rock material and is usually described as a percentage. Water moves through an aquifer from areas of recharge to areas of discharge. Recharge of groundwater occurs from precipitation that infiltrates soils or that seeps from the bottom of surface water bodies such as lakes and streams. Discharge areas include streams, lakes, wetlands, coastal areas, springs, or where the groundwater flow is intercepted by wells. Water between the recharge and discharge areas is said to be in storage. The effect that a contaminant has on water depends upon the characteristics of the water itself and the quantity and characteristics of the contaminant. Each body of water can be described according to its physical, chemical, and biological characteristics. Collectively, these characteristics give each water body an ability to absorb or assimilate some contaminants without becoming degraded (Xuesong Song, et. al., 2013).

THE STUDY OBJECTIVES 1.2

:The objectives of this study are

(1) Appling laser Raman spectroscopyfor the first time to characterize and identify the groundwater components collected from different places of western Saudi Arabia.

(2) Comparing the results obtained from this study with the results obtained from other studies.

THESIS STRUCTURE 1.3

This thesis contains four chapters:

Chapter one presents: the use of water, groundwater and contaminated water, and the use of laser in spectroscopy.

Chapter Two discuses the fundamentals and applications of Raman spectroscopy in classical and quantum images, Raman spectrometers, types of Raman spectroscopy, applications of Raman spectroscopy and literature review.

Chapter Three covers the practical side, methods of collection of samples, Raman setup and procedure.

Chapter Four deals with the obtained results, the analysis of Raman spectra, the discussion of the results, the comparison with other results, conclusions and recommendations.

LASERS IN SPECTROSCOPY 1.4

Laser spectroscopy is a branch of optical spectroscopy whose methods are based on the use of laser radiation. By employing monochromatic laser radiation, quantum transitions can be induced between specific atomic and molecular energy levels. The main categories of using laser in spectroscopy are: laser absorption spectroscopy and laser emission spectroscopy beside laser scattering spectroscopy.

1.4.1 Laser Absorption Spectroscopy

In classical absorption spectroscopy, radiation sources with a broad emission continuum are preferred (e.g., high-pressure Hg arcs, Xe flash lamps, etc.) (Fig.1.1. a). The radiation is collimated by the lens L_1 and passes through the absorption cell. Behind a dispersing instrument for wavelength selection (spectrometer or interferometer), the power of the transmitted light $P_T(\lambda)$ is measured as a function of the wavelength λ. By comparison with the reference beam $P_R(\lambda)$, which can be realized, for instance, by shifting the absorption cell alternatively out of the light beam, the absorption spectrum

$$P_A(\lambda) = a[P_0(\lambda) - P_T(\lambda)] = a[bP_R(\lambda) - P_T(\lambda)], \quad (1.1)$$

can be obtained, where the constants *a* and *b* take into account wavelength independent losses of P_R and P_T (e.g., reflections of the cell walls) (Wolfgang D., 2008).

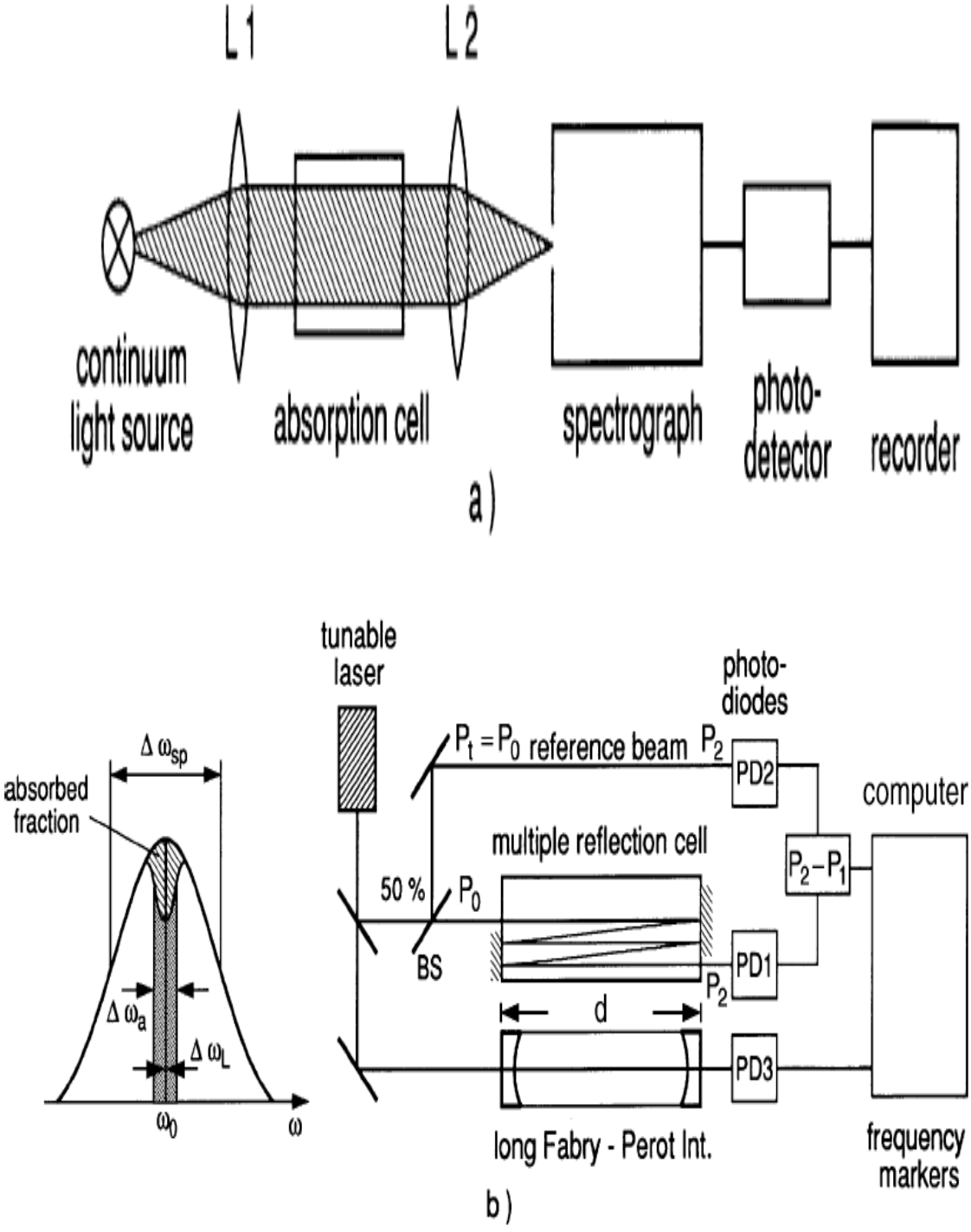

Figure 1.1: Comparison between absorption spectroscopy with a broadband incoherent source (**a**) and with a tunable single-mode laser (**b**)

1.4.1.1 Intracavity Setup

The spectral resolution is generally limited by the resolving power of the dispersing spectrometer. Only with large and expensive instruments (e.g., Fourier spectrometers) may the Doppler limit be reached (J. Kauppinen, J. Partanen, 2001).

The detection sensitivity of the experimental arrangement is defined by the minimum absorbed power that can still be detected. In most cases it is limited by the detector noise and by intensity fluctuations of the radiation source. Generally, the limit of the detectable absorption is reached at relative absorptions $\Delta P/P \geq 10^{-4}-10^{-5}$. This limit can be pushed further down only in favorable cases by using special sources and lock-in detection or signal averaging techniques (Wolfgang D., 2008).

Contrary to radiation sources with broad emission continua used in conventional spectroscopy, tunable lasers offer radiation sources in the spectral range from the UV to the IR with extremely narrow bandwidths and with spectral power densities that may exceed those of incoherent light sources by many orders of magnitude.

1.4.1.2 Advantages and Applications of Laser Absorption Spectroscopy

In several regards laser absorption spectroscopy corresponds to microwave spectroscopy, where klystrons or carcinotrons instead of lasers represent tunable coherent radiation sources. Laser spectroscopy transfers many of the techniques and advantages of microwave spectroscopy to the infrared, visible, and ultraviolet spectral ranges (Wolfgang D., 2008).

The advantages of absorption spectroscopy with tunable lasers may be summarized as follows:

• No monochromator is needed, since the absorption coefficient and its frequency dependence can be directly measured from the difference between the intensities of the reference beam with $P_R = P_2$ and transmitted beam with $P_T = P_1$ (Fig.1.1.b). The spectral resolution is higher than in conventional

spectroscopy. With tunable single mode lasers it is only limited by the linewidths of the absorbing molecular transitions. Using Doppler-free techniques, even sub-Doppler resolution can be achieved.

• Because of the high spectral power density of many lasers, the detector noise is generally negligible. Power fluctuations of the laser, which limit the detection sensitivity, may essentially be suppressed by power stabilization. This furthermore increases the signal-to-noise ratio and therefore enhances the sensitivity.

• The detection sensitivity increases with increasing spectral resolution $\omega/\Delta\omega$ as long as $\Delta\omega$ is still larger than the linewidth $\delta\omega$ of the absorption line.

• Because of the good collimation of a laser beam, long absorption paths can be realized by multiple reflections back and forth through the multiple-path absorption cell. Disturbing reflections from cell walls or windows, which may influence the measurements, can essentially be avoided. Such long absorption paths enable measurements of absorbing transitions even with small absorption coefficients.

• If a small fraction of the laser output is sent through a long Fabry–Perot interferometer with a separation d of the mirrors (Fig.1.1. b), the photodetector PD3 receives intensity peaks each time the laser frequency ν_L is tuned to a transmission maximum at $\nu = ½\ mc/d$. These peaks serve as accurate wavelength markers, which allow one to calibrate the separation of adjacent absorption lines.

• The laser frequency may be stabilized onto the center of an absorption line. it is possible to measure the wavelength λ_L of the laser with an absolute accuracy of 10^{-8} or better. This allows determination of the molecular absorption lines with the same accuracy.

• It is possible to tune the laser wavelength very rapidly over a spectral region where molecular absorption lines have to be detected. With electro-optical components, for instance, pulsed dye lasers can be turned over several wave numbers within a microsecond. This opens new perspectives for

spectroscopic investigations of short-lived intermediate radicals in chemical reactions. The capabilities of classical flash photolysis may be considerably extended using such rapidly tunable laser sources.

• An important advantage of absorption spectroscopy with tunable single mode lasers stems from their capabilities to measure line profiles of absorbing molecular transitions with high accuracy. In case of pressure broadening, the determination of line profiles allows one to derive information about the interaction potential of the collision partners. In plasma physics this technique is widely used to determine electron and ion densities and temperatures (Wolfgang D., 2008).

1.4.2 Laser in Emission Spectroscopy

1.4.2.1 Laser-Induced Fluorescence

Laser-induced fluorescence (LIF) is the optical emission from molecules that have been excited to higher energy levels by absorption of laser radiation as shown in figure (1.2) (J.R. Lakowicz 1991).

The fluorescence spectrum emitted from a selectively populated rovibronic level (v'_k ,J'_k) (v_k ,J_k : a rovibronic level in an excited electronic state of a diatomic molecule) consists of all allowed transitions to lower levels (v''_m ,J''_m) (Fig.1.2). The wavenumber differences of the fluorescence lines immediately yield the term differences of these terminating levels (v''_m ,J''_m).

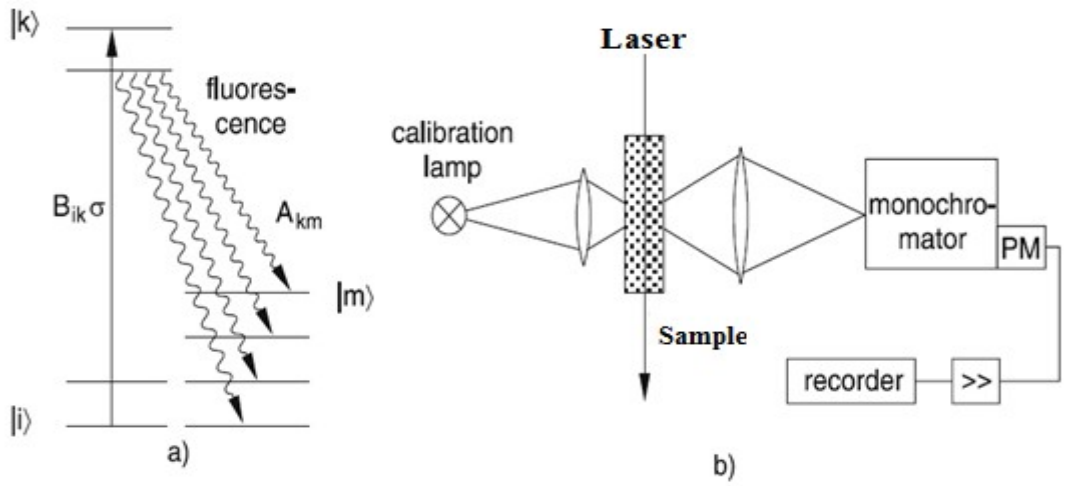

Figure1.2: Laser-induced fluorescence: (a) level scheme and (b) experimental arrangement for measuring LIF spectra.

Laser-induced fluorescence (LIF) has a large range of advantages (J.L. Kinsey 1977). First, LIF serves as a sensitive monitor for the absorption of laser photons in fluorescence excitation spectroscopy. Second, it is well suited to gain information on molecular states if the fluorescence spectrum excited by a laser on a selected absorption transition is dispersed by a monochromatic. A third aspect of LIF is the spectroscopic study of collision processes. If the excited molecule is transferred by inelastic collisions from the level (v'_k ,J'_k) into other rovibronic levels, the fluorescence spectrum shows new lines emitted from these collisionally populated levels which give quantitative information on the collision cross sections. Another aspect of LIF concerns its application to the determination of the internal-state distribution in molecular reaction products of chemical reactions. Under certain conditions the intensity I_{Fl} of LIF excited on the transition $|i\rangle \rightarrow |k\rangle$ is a direct measure of the population density *Ni* in the absorbing level $|i\rangle$.

1.4.2.2 Laser-Induced Breakdown Spectroscopy

The Physical principle of laser-induced breakdown spectroscopy is shown schematically in Figure (1.3). A pulsed laser beam is focused onto the surface of a substance to be analyzed, see step (1) in Fig. 1.3. Radiation energy is locally coupled into the material (2) and the material starts to evaporate (3). Within this material vapor and the surrounding gas atmosphere a plasma is generated (4), leading to the excitation of the material constituents and their spontaneous emission of radiation. The plasma decays and emits element-specific radiation (5)–(7). This emission is resolved spectrally and is detected by a spectrometer (Reinhard Noll, 2012).

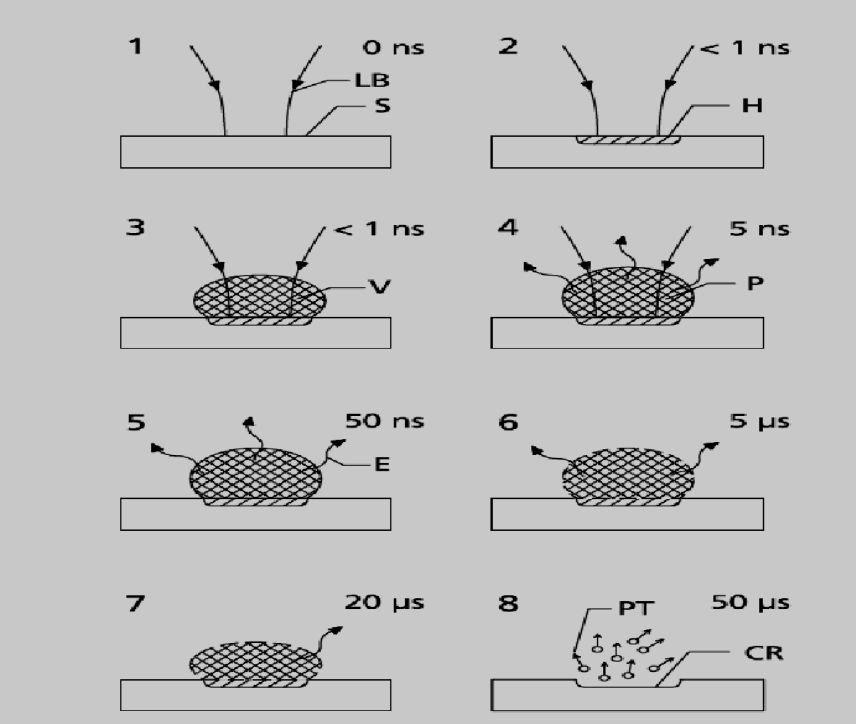

Figure 1.3: Principle of laser-induced breakdown spectroscopy shown in phases 1–8; LB = incoming laser beam, S = sample, H = region of energy deposition, V = material vapor, P = plasma, E = element-specific emission, CR = crater, PT = particles. The times given depict the temporal evolution after start of irradiation of the laser pulse.

For solid substances, a crater is formed finally (8). The evaporated material is removed partially from the interaction zone driven by the intrinsic dynamics of the plasma expansion and by an externally impressed gas flow. The process denoted in phase (3) as “evaporation” is a simplified description and refers to solid inorganic substances. In general, there is no pure sublimation from the solid phase to the gaseous phase. Depending on the laser parameters – e.g., the pulse duration – and the material properties a transient liquid phase may also exist. Besides the evaporation and dissociation processes also particles are ablated, e.g., small particulates or droplets, which are ejected due to the impact of the pressure exerted by the plasma and the accompanying shock waves on a melt layer. For organic substances, the initial material is disintegrated, fragmented, and dissociated**.** The life time of the plasma depends on the laser beam parameters chosen, the conditions of the surrounding gas atmosphere, and the substance to be analyzed. The life time lies typically in the range of 0.5–10 µs. The whole process depicted in

Figure (1.3) can be repeated with frequencies of 10Hz up to 1 kHz Figure (1.4) shows the principle setup for laser-induced breakdown spectroscopy. A mirror guides the pulsed laser radiation to a focusing lens. The sample to be analyzed is placed in a measuring chamber. As a rule the incident direction of the laser radiation is oriented perpendicularly to the sample surface. The focused radiation generates plasma at the sample surface. The emission of this plasma is observed in a direction, which includes an angle to the incident direction of the laser radiation. In Fig.1.4, the measuring radiation is transmitted via a fiber optics to a spectrometer, where it is spectrally dispersed and converted to electrical signals. The measuring chamber is gas tight. Laser radiation and measuring radiation are transmitted via built-in windows. Via gas fittings the type of gas filling as well as the gas pressure and gas exchange rate can be adjusted in a defined manner. A translation stage moves the sample in relation to the incident laser beam to measure at different locations on the sample surface. The use of a measuring chamber is not a necessary precondition for laser-induced breakdown spectroscopy.

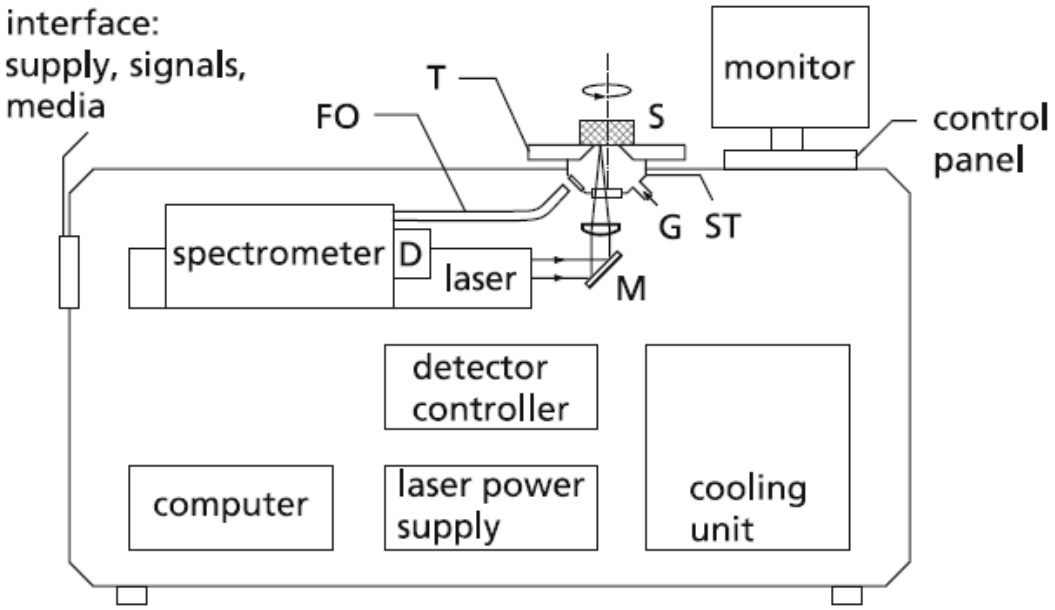

Figure1.4: Arrangement of components in a LIBS-based analyzing system; T = sample table, S = sample, ST = sample stand, FO = fiber optics, G = gas supply, D = detector, M = mirror

Laser-induced breakdown spectroscopy is a versatile tool to analyze solid, liquid, or gaseous substances.

The laser beam is focused onto a solid sample. By translation of the sample in a direction perpendicular to the optical axis of the irradiated laser beam the sample surface is scanned to obtain spatially resolved information about the chemical composition. The laser beam can be guided via fiber optics to a measuring head and then be focused to analyze a liquid. The laser beam can also be focused through a window into a closed tube to analyze gases. A methodical extension is the combination of LIBS with separation techniques such as capillary electrophoresis (CE) or high-pressure liquid chromatography (HPLC). LIBS can be combined with other laser spectroscopic methods such as laser-induced fluorescence (LIF). The laser is a multipurpose tool allowing to locally ablate surface layers and to perform chemical analysis of the underlying bulk material.

1.4.3 Laser Raman Spectroscopy

Raman spectroscopy is based on the scattering phenomenon. In this context, scattering occurs due to collisions between photons and molecules. Generally, a photon collides with a substance, not necessarily only with a molecule; but for simplicity the photon-molecule collision is considered (Richard L., 2000).

For many years Raman spectroscopy has been a powerful tool for the investigation of molecular vibrations and rotations. In the pre-laser however, its main drawback was a lack of sufficiently intense radiation sources. The introduction of lasers, therefore, has indeed revolutionized this classical field of spectroscopy. Lasers have not only greatly enhanced the sensitivity of spontaneous Raman spectroscopy but they have furthermore initiated new spectroscopic techniques, based on the stimulated Raman effect., such as coherent anti-Stokes Raman scattering (CARS) or hyper-Raman spectroscopy. The research activities in laser Raman spectroscopy have recently shown an impressive expansion and a vast literature on this field is available (W. Demtroder, 2008).

Raman scattering may be regarded as an inelastic collision of an incident photon $\hbar\omega_i$ with a molecule in the initial energy level E_i (Fig.1.5.a). Following the collision, a photon $\hbar\omega_s$ with lower energy is detected and the molecule is found in a higher-energy level E_f, this process called stokes scattering.

$\hbar\omega_i + M(E_i) \rightarrow M*(E_f) + \hbar\omega_s$, with $\hbar(\omega i - \omega s) = E_f - E_i > 0$ (1.2)

The energy difference $\Delta E = E_f - E_i$ may appear as vibrational, rotational, or electronic energy of the molecule.

If the photon $\hbar\omega_i$ is scattered by a vibrationally excited molecule, it may gain energy and the scattered photon has a higher frequency ω_{as} (Fig.1.5.c), where

$$\hbar\omega_{as} = \hbar\omega_i + E_i - E_f \text{ , with } E_i > E_f . \quad (1.3)$$

This “superelastic” photon scattering is called anti-Stokes radiation.

In the energy level scheme (Fig.1.5.b), the intermediate state $E_v = E_i + \hbar\omega_i$ of the system “during” the scattering process is often formally described as a virtual level, which, however, is not necessarily a “real” stationary eigenstate of the molecule. If the virtual level coincides with one of the molecular eigenstates, one speaks of the resonance Raman Effect.

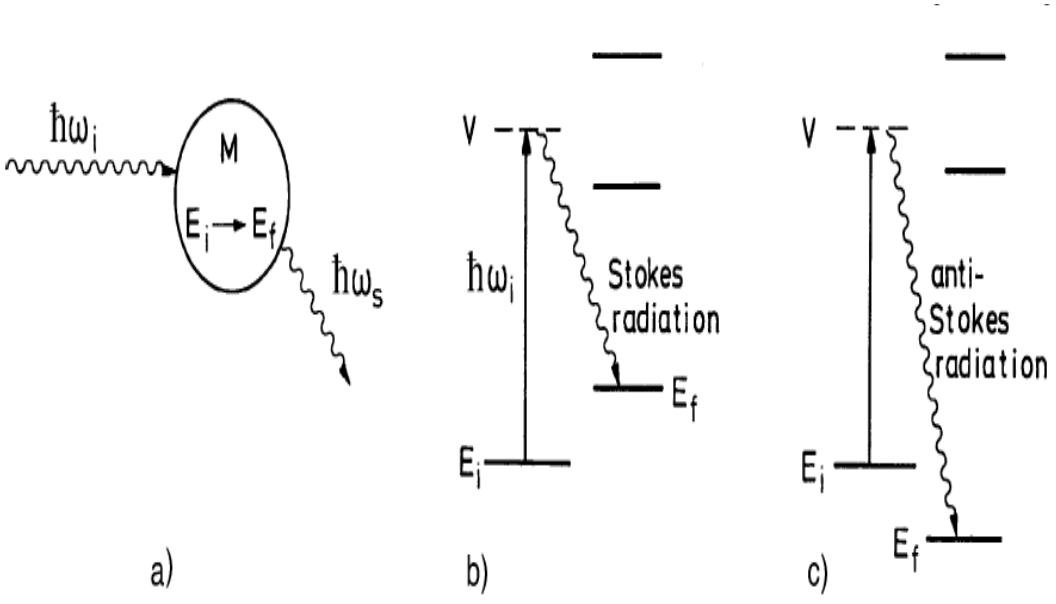

Figure 1.5: Schematic level diagram of Raman scattering

CHAPTER TWO

RAMAN SPECTROSCOPY, PRINCIPLES AND APPLICATIONS

INTRODUCTION 2.1

This chapter presents the fundamentals and applications of Raman spectroscopy in classical and quantum images, selection rules, Raman spectrometers, types and applications of Raman spectroscopy, and finally literature review.

2.2 HISTORY

The phenomenon of inelastic scattering of light was first postulated by Smekal in 1923 and first observed experimentally in 1928, when Sir Chandrasekhra Venkata Raman discovered the phenomenon that bears his name which based on the wavelength shift of the scattered light. Sir Raman used sunlight as the source and a telescope as the collector; the detector was his eyes. The difference in the wavelength between the incident and the scattered light (called Raman shift) is a finger print of the material under study (Ewen S., Geoffery D., 2005).

Gradually, improvements in the various components of Raman instrumentation took place. Early research was concentrated on the development of better excitation sources. Various lamps of elements were developed (e.g., helium, bismuth, lead, zinc). These proved to be unsatisfactory because of low light intensities. Mercury sources were also developed. An early mercury lamp which had been used for other purposes in 1914 by Kerschbaum was developed. In the 1930s mercury lamps suitable for Raman use were designed. Hibben developed a mercury burner in 1939, and Spedding and Stamm experimented with a cooled version in 1942. Further progress was made by Rank and McCartney in 1948, who studied mercury burners and their backgrounds. Hilger Co. developed a commercial mercury excitation source system for the Raman instrument, which consisted of four lamps surrounding the Raman tube. Welsh *et al.* introduced a mercury source in 1952, which became known as the Toronto Arc (John R. et al. 2003). The

lamp consisted of a four-turn helix of Pyrex tubing and was an improvement over the Hilger lamp. Improvements in lamps were made by Ham and Walsh, who described the use of microwave-powered helium, mercury, sodium, rubidium and potassium lamps. Stammreich also examined the practicality of using helium, argon, rubidium and cesium lamps for colored materials. In 1962 laser sources were developed for use with Raman spectroscopy. Eventually, the Ar+ (351.l-514.5nm) and the Kr+ (337.4-676.4 nm) lasers became available, and more recently the Nd- YAG laser (1064 nm) has been used for Raman spectroscopy (John R. et al. 2003).

Progress occurred also in the detection systems for Raman measurements. Whereas original measurements were made using photographic plates with the cumbersome development of photographic plates, photoelectric Raman instrumentation was developed after World War II. The first photoelectric Raman instrument was reported in 1942 by Rank and Wiegand, who used a cooled cascade type RCA IP21 detector. The Heigl instrument appeared in 1950 and used a cooled RCA C-7073B photomultiplier. In 1953 Stamm and Salzman reported the development of photoelectric Raman instrumentation using a cooled RCA IP21 photomultiplier tube. The Hilger E612 instrument was also produced at this time, which could be used as a photographic or photoelectric instrument. In the photoelectric mode a photomultiplier was used as the detector. This was followed by the introduction of the Cary Model 81 Raman spectrometer. The source used was the 3 kW helical Hg arc of the Toronto type. The instrument employed a twin-grating, twin-slit double monochromators.

Developments in the optical train of Raman instrumentation took place in the early 1960s. It was discovered that a double monochromator removed stray light more efficiently than a single monochromator. Later, a triple monochromator was introduced, which was even more efficient in removing stray light. Holographic gratings appeared in 1968, which added to the efficiency of the collection of Raman scattering in commercial Raman

instruments. These developments in Raman instrumentation brought commercial Raman instruments to the present state of the art of Raman measurements. Now, Raman spectra can also be obtained by Fourier transform (FT) spectroscopy. FT-Raman instruments are being sold by all Fourier transform infrared (FT-IR) instrument makers, either as interfaced units to the FT-IR spectrometer or as dedicated FT-Raman instruments (John R. et al. 2003).

2.3 PRINCIPLES OF RAMAN SPECTROSCOPY

Raman spectroscopy is a spectroscopic technique based on inelastic scattering of monochromatic light, usually from a laser source. Inelastic scattering means that the frequency of photons in monochromatic light changes upon interaction with a sample. Photons of the laser light are absorbed by the sample and then reemitted. Frequency of the reemitted photons is shifted up or down in comparison with original monochromatic frequency, which is called the Raman Effect. This shift provides information about vibrational, rotational and other low frequency transitions in molecules. Raman spectroscopy can be used to study solid, liquid and gaseous samples (Ewen S., Geoffery D., 2005).

The Raman effect is based on molecular deformations in electric field E determined by molecular polarizability α. The laser beam can be considered as an oscillating electromagnetic wave with electrical vector E. Upon interaction with the sample it induces electric dipole moment $P = \alpha E$ which deforms molecules. Because of periodical deformation, molecules start vibrating with characteristic frequency υ. Amplitude of vibration is called a nuclear displacement. In other words, monochromatic laser light with frequency υ_0 excites molecules and transforms them into oscillating dipoles. Such oscillating dipoles emit light of three different frequencies when:

1. A molecule with no Raman-active modes absorbs a photon with the frequency υ_0. The excited molecule returns back to the same basic vibrational

state and emits light with the same frequency υ_0 as an excitation source. This type if interaction is called an elastic Rayleigh scattering.

2. A photon with frequency υ_0 is absorbed by Raman-active molecule which at the time of interaction is in the basic vibrational state. Part of the photon's energy is transferred to the Raman-active mode with frequency υ and the resulting frequency of scattered light is reduced to $\upsilon_0 - \upsilon$. This Raman frequency is called Stokes frequency.

3. A photon with frequency υ_0 is absorbed by a Raman-active molecule, which, at the time of interaction, is already in the excited vibrational state. Excessive energy of excited Raman active mode is released, molecule returns to the basic vibrational state and the resulting frequency of scattered light goes up to $\upsilon_0 + \upsilon$. This Raman frequency is called Anti- Stokes frequency.

2.3.1 Raman Scattering

The Raman effect arises when a photon is incident on a molecule and interacts with its electric dipole. In quantum mechanics, the scattering is described as an excitation to a virtual state lower in energy than a real electronic transition with nearly coincident de-excitation and a change in vibrational energy. The scattering event occurs in 10^{-14} seconds or less (Ewen S., Geoffery D., 2005). The virtual state description of the scattering is shown in Figure 2.1.

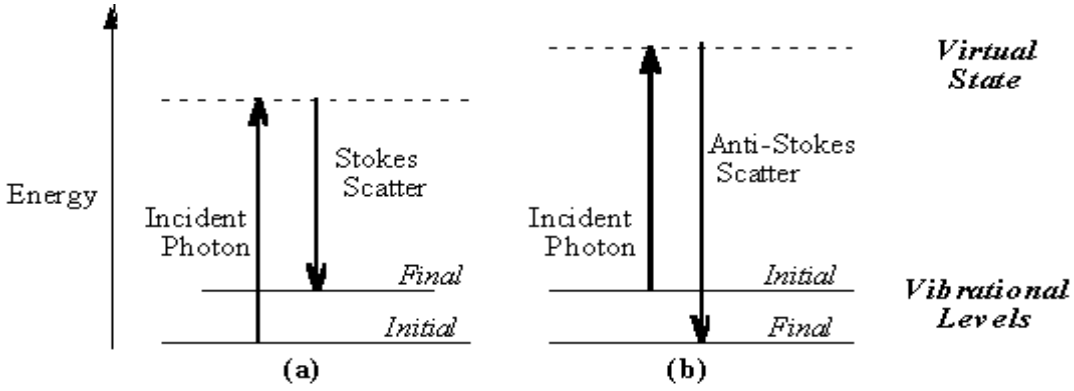

Figure 2.1: Energy level diagram for Raman scattering; (a) Stokes scattering, (b) Anti-Stokes scattering.

The energy difference between the incident and scattered photons is represented by the arrows of different lengths in Figure 2.1. Numerically, the Raman shift in wavenumbers (cm^{-1}), is calculated through Eq.,

$$\bar{\nu} = \frac{1}{\lambda_{incident}} - \frac{1}{\lambda_{scattered}} \quad (2.1)$$

In which the λ's are the wavelengths (in cm) of the incident and Raman scattered photons, respectively.

At room temperature the thermal population of vibrational excited states is low, although not zero. Therefore, the initial state is the ground state, and the scattered photon will have lower energy (longer wavelength) than the exciting photon. This Stokes shifted scatter is what is usually observed in Raman spectroscopy, Figure 2.1(a).

A small fraction of the molecules are in vibrationally excited states. Raman scattering from vibrationally excited molecules leaves the molecule in the ground state. The scattered photon appears at higher energy, as shown in Figure 2.1(b). The Stokes and anti-Stokes spectra contain the same frequency information. The anti-Stokes spectrum can be used when the Stokes spectrum is not directly observable, for example, because of poor detector response at lower frequencies.

2.3.2 Origin of Raman Spectra

The origin of Raman spectra is markedly different from that of IR spectra. In Raman spectroscopy, the sample is irradiated by intense laser beams in the UV-visible region (υ_0), and the scattered Light is usually observed in the direction perpendicular to the incident beam (John R., et al., 2003).

According to classical theory, Raman scattering can be explained as follows: The electric field strength *(E).* Of the electromagnetic wave (laser beam) fluctuates with time (t) as shown by Eq:

$$E = E_0 \cos 2\pi \upsilon_0 t \quad (2.2)$$

Where E_0 is the vibrational amplitude and υ_0 is the frequency of the laser. If a diatomic molecule is irradiated by this light, an electric dipole moment *P* is induced:

$$p = \alpha E = \alpha E_0 \cos 2\pi \upsilon_0 t \quad (2.3)$$

Here, α is a proportionality constant and is called polarizability. If the molecule is vibrating with a frequency υ_m, the nuclear displacement q is written

$$q = q_o \cos 2\pi \upsilon_m t \quad (2.4)$$

Where q_o is the vibrational amplitude. For small amplitude of vibration, α is a linear function of q. Thus, we can write

$$\alpha = \alpha_o + \left(\frac{d\alpha}{dq}\right)_o q_o + \ldots \quad (2.5)$$

Here, α_o is the polarizability at the equilibrium position, and $(d\alpha / dq)_0$ is the rate of change with respect to the change in q, evaluated at the equilibrium position.

Combining the three equations (2.3), (2.4), and (2.5), we obtain

$$P = \alpha E_0 \cos 2\pi V_o t \quad (2.6)$$

$$= \alpha_0 E_0 \cos 2\pi V_o t + \left(\frac{d\alpha}{dq}\right)_o q E_0 \cos 2\pi V_o t$$

$$= \alpha_0 E_0 \cos 2\pi V_o t + \left(\frac{d\alpha}{dq}\right)_o q_o E_0 \cos 2\pi V_o t \cos 2\pi V_m t$$

$$= \alpha_0 E_0 \cos 2\pi Vo t + \tfrac{1}{2} \left(\frac{d\alpha}{dq}\right)_o q_o E_0 [\cos \{2\pi (V_0 + V_m)t\} + \cos \{2\pi (V_o - V_m)t\}]$$

Figure (2.2) illustrates Raman scattering in terms of a diatomic energy levels. In normal Raman spectroscopy, the exciting line (V_o) is chosen so that its energy is far below the first electronic excited state. The dotted line indicates a "virtual state" to distinguish it from the real excited state. The population of molecules at V = 0 is much larger than that at V = 1 (Maxwell-Boltzmann distribution law). Thus, the Stokes *(S)* lines are stronger than the anti-Stokes *(A)* lines under normal conditions. Since both give the same information, it is customary to measure only the Stokes side of the spectrum.

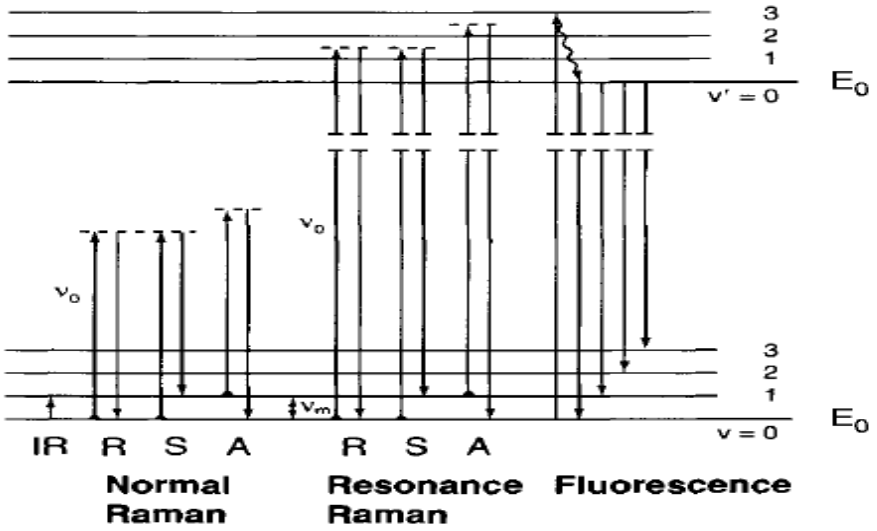

Figure 2.2: Comparison of energy levels for the normal Raman, resonance Raman, and fluorescence spectra.

Resonance Raman (RR) scattering occurs when the exciting line is chosen so that its energy intercepts the manifold of an electronic excited state. In the liquid and solid states, vibrational levels are broadened to produce a continuum. In the gaseous state, a continuum exists above a series of discrete levels. Excitation of these continua produces RR spectra that show extremely strong enhancement of Raman bands originating in this particular electronic transition. Because of its importance. The term "pre-resonance" is used when the exciting line is close in energy to the electronic excited state. Resonance fluorescence (RF) occurs when the molecule is excited to a discrete level of the electronic excited state. This has been observed for gaseous molecules such as I_2, Br_2. Finally, fluorescence spectra are observed when the excited state molecule decays to the lowest vibrational level via radiationless transitions and then emits radiation. The lifetime of the excited state in RR is very short (~ 10^{-14} s), while those in fluorescence are much longer (~10^{-8} to 10^{-5}s) (Ewen S., Geoffery D., 2005, John R., et al., 2003).

2.3.3 Selection Rules for Raman Spectra

To determine if the vibration is active in the Raman spectra, the selection rules must be applied to each normal vibration. Since the origins of Raman

spectra are markedly different than IR spectroscopy, their selection rules are also distinctively different. According to quantum mechanics a vibration is Raman-active if the polarizability is changed during the vibration (John R., et al., 2003).

To discuss Raman activity, let us consider the nature of the polarizability. When a molecule is placed in an electric field (laser beam), it suffers distortion since the positively charged nuclei are attracted toward the negative pole, and electrons toward the positive pole (Fig. 2.3). This charge separation produces an induced dipole moment (P) given by

$$P = \alpha E \qquad (2.7)$$

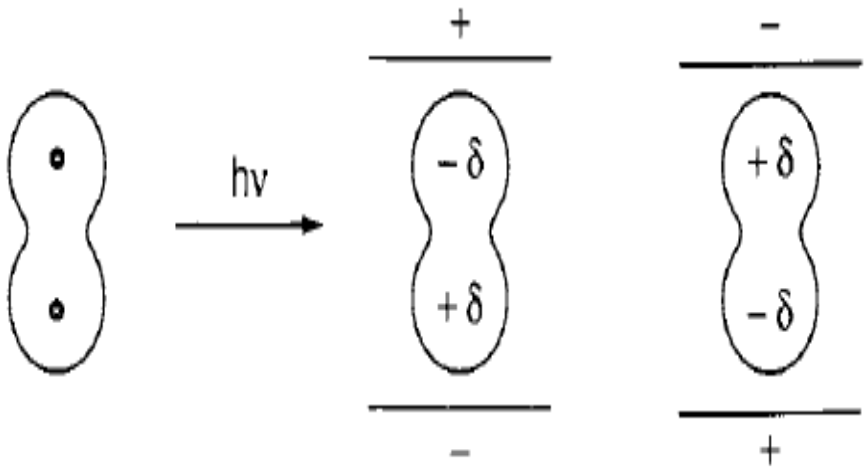

Figure 2.3: Polarization of a diatomic molecule in an electric field.

In actual molecules, such a simple relationship does not hold since both P and E are vectors consisting of three components in the x, y and z directions. Thus, Eq. (2.7) must be written as

$$p_x = \alpha_{xx} E_x + \alpha_{xy} E_y + \alpha_{xz} E_z , \qquad (2.8)$$

$$p_y = \alpha_{yx} E_x + \alpha_{yy} E_y + \alpha_{yz} E_z ,$$

$$p_z = \alpha_{zx} E_x + \alpha_{zy} E_y + \alpha_{zz} E_z ,$$

In matrix form, this is written as

$$\begin{bmatrix} P_x \\ P_y \\ p_z \end{bmatrix} = \begin{bmatrix} \alpha_{xx} & \alpha_{xy} & \alpha_{xz} \\ \alpha_{yx} & \alpha_{yy} & \alpha_{yz} \\ \alpha_{zx} & \alpha_{zy} & \alpha_{zz} \end{bmatrix} \begin{bmatrix} E_X \\ E_Y \\ E_Z \end{bmatrix} \qquad (2.9)$$

The first matrix on the right-hand side is called the polarizability tensor. In normal Raman scattering, this tensor is symmetric; $\alpha_{xy} = \alpha_{yz}$, $\alpha_{xz} = \alpha_{zx}$ and $\alpha_{yz} = \alpha_{zy}$. According to quantum mechanics, the vibration is Raman-active if one of these components of the polarizability tensor is changed during the vibration.

In the case of small molecules, it is easy to see whether or not the polarizability changes during the vibration. Consider diatomic molecules such as H_2 or linear molecules such as CO_2. Their electron clouds have an elongated water melon like shape with circular cross-sections. In these molecules, the electrons are more polarizable (a larger α) along the chemical bond than in the direction perpendicular to it. If we plot α_i (α in the i-direction) from the center of gravity in all directions, we end up with a three-dimensional surface. Conventionally, we plot $1/\sqrt{\alpha_i}$ rather than α_i itself and call the resulting three-dimensional body a polarizability ellipsoid. Figure 2.4 shows the changes of such an ellipsoid during the vibrations of the CO_2 molecule. In terms of the polarizability ellipsoid, the vibration is Raman-active if the size, shape or orientation changes during the normal vibration. The size of the ellipsoid is changing in υ_1 vibration and υ_3 vibration, although the diagonal elements (α_{xx}, α_{yy} and α_{zz}) are changing simultaneously. Thus, it is Raman-active. The difference between the υ_1 and υ_3 is shown in Fig. 2.5.

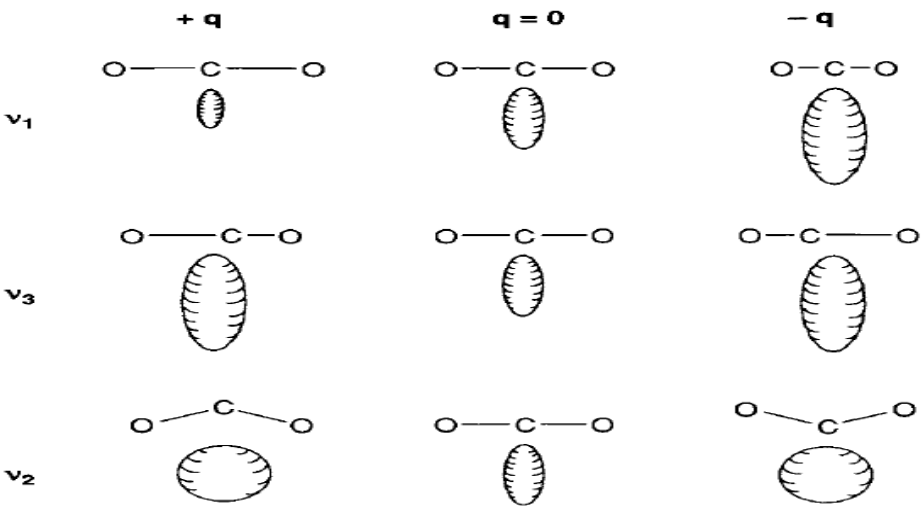

Figure (2.4): Changes in polarizability ellipsoids during vibration of CO_2 molecule.

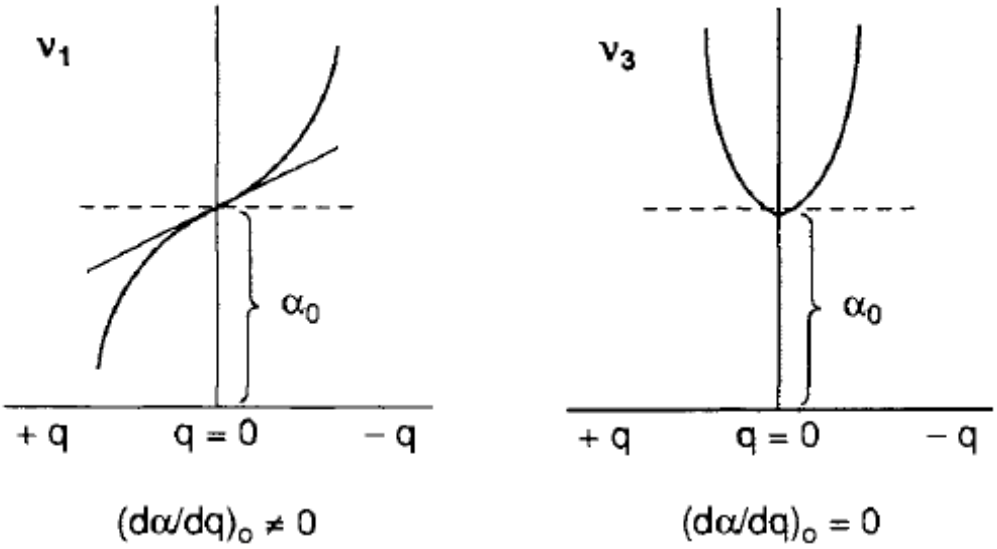

Figure 2.5: Difference between υ_1 and υ_3 vibrations in CO_2 molecule.

Figure (2.6) illustrates the changes in the polarizability ellipsoid during the normal vibrations of the H_2O molecule. Its υ_1 vibration is Raman-active, as is the υ_1 vibration of CO_2. The υ_2 vibration is also Raman-active because the shape of the ellipsoid is different at +q and -q. In terms of the polarizability tensor, α_{xx}, α_{yy} and α_{zz} are all changing with different rates. Finally, the υ_3 vibration is Raman-active because the orientation of the ellipsoid is changing during the vibration.

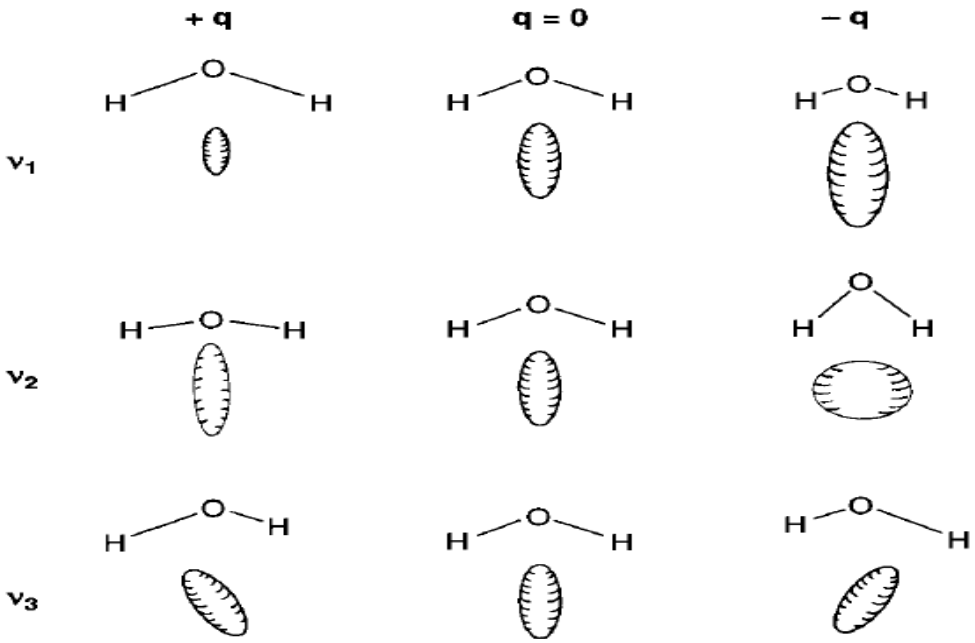

Figure 2.6: Changes in polarizability ellipsoid during normal vibrations of H_2O molecule.

2.4 TYPES OF RAMAN SPECTROSCOPY AND APPLICATION

The types of Raman spectroscopy include high pressure Raman spectroscopy, Raman microscopy, surface-enhanced Raman spectroscopy, Raman spectroelectrochemistry, time-resolved Raman spectroscopy, matrix-isolation Raman spectroscopy, two-dimensional correlation Raman spectroscopy, Raman imaging spectrometry, Coherent anti-Stokes Raman spectroscopy, Linear Laser Raman Spectroscopy and Nonlinear Raman Spectroscopy (John R., et al.,2003).

2.4.1 High-Pressure Raman Spectroscopy

The pressure technique involves a pressure device diamond anvil cell (DAC) that can transmit the pressure to the sample under study. If spectroscopic methods are chosen for diagnostic purposes, it is a requirement to use windows on the pressure device that are hard and transmit the irradiating light in the particular wavelength of the electromagnetic spectrum being studied. The window of choice for IR and Raman studies is type of diamond. It is the hardest material known and is transmissive for laser Raman studies. Additionally, it is an excellent thermal conductor as well. The pressure device must be compact and fit into the sample compartment of the spectrometer. The DAC fulfills all of these criteria and has been extensively used since its discovery by Weir and Van Valkenburg in 1959. The interface to the Raman spectrometer is readily accomplished (unlike the IR experiment where beam condensers are required in the dispersive instrument, although presently this requirement is unnecessary in the Raman/DAC experiment), and normal commercial Raman instrumentation can be used (John R., et al., 2003).

A few applications illustrating the pressure effects on materials using Raman spectroscopy as the diagnostic tool, like:

1. Phase Transitions in Solids.
2. Pressure Changes in Solid Coordination Compounds.
3. Evidence for Metallization of hydrogen at Mega bar Pressures.

2.4.2 Raman Microscopy

The major limitations in the design of a Raman microprobe are related to the feeble Raman Effect and the minute sample size. It is necessary to optimize the Raman signal, and this is accomplished by taking care in the development of the fore optical configuration to provide a high numerical operative and detector system. The fore optical configuration is extremely important in optimization of the Raman microprobe. A high numerical aperture (NA) is necessary to collect the light scattered over a large solid angle to assure that more Raman scattered light from the sample is detected. A large-aperture collector is used, which minimizes elastic and inelastic scattering from the substrate (John R. et al. 2003, W. Demtroder, 2008). The Raman microprobe has provided applications in a number of diverse areas of science. Generally, the areas of applications fall into two major categories:

(1) finger-print identification of microscopic contaminants, and

(2) Characterization of new materials: (a) Surface Contaminant Identification: The presence of organic contaminants as small as 1 μm or films as thin as 1 μm on silicon wafers during the manufacturing process of integrated circuits can be readily identified. (b) Biological compounds: The Raman microprobe has been used to detect foreign bodies in various tissues. (c) Inclusions in solid inorganic materials: The nature of solid, liquid or gaseous inclusions that may be found within transparent inorganic glass or crystalline materials can be determined by Raman microprobe techniques without breaking up the sample. (d) Fourier Transform (FT) Raman Microscopy: use a microscope to obtain the FT-Raman effect. (e) Raman mapping: Two modes of illumination are available for Raman illumination. One is "point illumination", and the other is "area (or global) illumination" (W. Demtroder, 2008).

2.4.3 Surface-Enhanced Raman Spectroscopy (SERS)

Surface-Enhanced Raman Spectroscopy utilizes the following effect. Raman signal from molecules adsorbed on certain metal surfaces can be 5-6 orders of magnitude stronger then the Raman signal from the same molecules in bulk volume. The exact reason for such dramatic improvement is still under discussion. However, since intensity of Raman signal is proportional to the square of electric dipole moment $P = \alpha E$, there are two possible reasons - the enhancement of polarizability α, and the enhancement of electrical field E.

The first enhancement of polarizability may occur because of a charge-transfer effect or chemical bond formation between metal surface and molecules under observation. This is a so-called chemical enhancement. The second one takes into account interaction of the laser beam with irregularities on the metal surface such as metal micro-particles or roughness profile. It is believed that laser light excites conduction electrons at the metal surface leading to a surface plasma resonance and strong enhancement of electric field E. It is also called electromagnetic enhancement. In all cases choice of appropriate surface substrate is very important. The most popular and universal substrates used for SERS are electrochemically etched silver electrodes as well as silver and gold colloids with average particle size below 20 nm. One disadvantage of SERS is the difficulty of spectra interpretation. The signal enhancement is so dramatic that Raman bands that are very weak and unnoticeable in spontaneous Raman spectra can appear in SERS. Some trace contaminants can also contribute additional peaks (John R. et al. 2003, W. Demtroder, 2008).

2.4.4 Raman Spectroelectrochemistry

Raman spectroelectrochemistry is a field in which studies electrogenerated species on electrode surfaces, in electrode diffusion layers and bulk solution by Raman spectroscopy. Thus, the surface-enhanced Raman scattering (SERS) is part of Raman spectroelectrochemistry. Here, we discuss Raman

spectroscopic studies on electrogenerated species in bulk solution and in electrode diffusion layers. Since no enhancement from SERS is expected and since the concentrations of these electrogenerated species are rather low, it is imperative to take advantages of resonance Raman (RR) scattering (John R. et al. 2003, W. Demtroder, 2008).

(a) Bulk solution: measured the RR spectrum of the tetracyanodimethane anion radical ($TCNQ^{-}$).

(b) Diffusion Layer: The RR spectrum of tetramethyl-*p*-phenylenediamine $TMPD^{+}$, confined to the diffusion layer, was obtained by applying a square-wave voltage (repetition rate, 10 Hz).

2.4.5 Time-Resolved Raman (TRR) Spectroscopy

Developments in laser Raman spectroscopy have made it possible to measure the Raman spectra of short-lived transient species, such as electronically excited molecules, radicals and exciplexes, which have life times on the order of nano- (10^{-9}) and pico- (10^{-12}) seconds. These short lived species may be generated by electron pulse radiolysis, photo-excitation and rapid mixing. However, the application of electron pulse radiolysis is limited in its adaptability and selectivity, while rapid mixing is limited by mixing rates, normally to a resolution on the order of milliseconds.

Molecules are excited from S_o (singlet ground state) to S_1(singlet excited state) by a pump laser of frequency υ_0. Molecules excited to S_1 undergo nonradiative decay to T_1 (triplet state). Since the pump pulse width is much narrower than the lifetime of the T_1 state (milli ~ microseconds), excitation to the S_1 state by a pump laser increases the population of molecules on T_1, which may become sufficient to observe the Raman spectrum of the T_1 state molecule with a probe laser (υ_1).

Heme proteins such as hemoglobin (Hb), myoglobin (Mb) and cytochromes contain the heme group (iron protoporphyrin) as the active site of their biological functions. porphyrin rings are ideal for Resolved Raman studies because strong resonance enhancement is produced without interference from

the rest of the protein when the laser wavelength is chosen to coincide with different transitions of the porphyrin ring (John R. et al. 2003, W. Demtroder, 2008).

2.4.6 Matrix-Isolation Raman Spectroscopy

Technically, Raman spectroscopy is more difficult to apply to low-temperature matrices than IR spectroscopy for the following reasons: (1) Since Raman signals are inherently weak, relatively high concentrations of the sample or relatively wide slit widths are required. The former may cause the formation of dimeric and polymeric species, while the latter leads to the loss of resolving power of the monochromator. (2) If one increases the laser power to obtain stronger Raman signals, the matrix temperature will rise because of local heating by the laser beam, and this will accelerate the diffusion of solute molecules in the matrix. (1) and (2) can be circumvented if Raman spectra are obtained under resonance conditions. (3) The quality of the Raman spectra obtained depends on the quality of the matrix prepared; "clear matrices" give better results. (4) The matrix itself or oil contamination from the diffusion pump may cause fluorescence (John R. et al. 2003).

In some cases, matrix-isolation laser-Raman spectroscopy can be utilized to produce unstable species via laser photolysis and to measure their resonance Raman spectra simultaneously in the same matrix using the same laser.

2.4.7 Two Dimensional Correlation Raman Spectroscopy

The concept of two-dimensional (2D) correlation spectroscopy has been applied to a number of systems to separate overlapped bands, to make band assignments, and to study intensity variations of individual bands due to external perturbations. The first step is to measure a series of spectra (Raman) of a system by changing the external perturbation (temperature, pressure, concentration etc.). Then, a series of dynamic spectra are calculated by subtracting a reference spectrum from each perturbed spectrum. An average of observed spectra is generally used as the reference spectrum (John R. et al. 2003, W. Demtroder, 2008).

Two Dimensional correlation spectroscopy is highly effective in separating overlapped bands which cannot be resolved by conventional one-dimensional spectroscopy.

2.4.8 Raman Imaging Spectrometry

In Raman images, Raman spectra are measured at the various spatial locations. After all the data are collected, it is possible to display individual Raman spectra for each spatial location or to display a false color image based on the intensities at a selected Raman frequency.

The ability to obtain Raman images of chemical and biological samples is of great importance to the scientific community. The improvements and increased use of charge couple devices (CCD) for detection of Raman spectra has made such measurements practical. Imaging spectrometer used to measure Raman images of a biological system (W. Demtroder, 2008).

2.4.9 Coherent anti-Stokes Raman spectroscopy (CARS)

The CARS process can be physically explained by using either a classical oscillator model or by using a quantum mechanical model that incorporates the energy levels of the molecule. Classically, the Raman active vibrator is modeled as a (damped) harmonic oscillator with a characteristic frequency of ω_v. In CARS, this oscillator is not driven by a single optical wave, but by the difference frequency (ω_p-ω_S) between the pump and the Stokes beams instead.

The first exploits the selectivity of vibrational spectroscopy whereas the latter is aimed to temperature measurements; the CARS signal is temperature dependent. The strength of the signal scales (non-linearly) with the difference in the ground state population and the vibrationally excited state population. Since the population of states follows the temperature dependent Boltzmann Distribution, the CARS signal carries an intrinsic temperature dependence as well. This temperature dependence makes CARS a popular technique for monitoring the temperature of hot gases and flames. More recently, CARS has been utilized as a method for non-invasive imaging of lipids in biological

samples, both in vivo and in vitro. Moreover, RP-CARS, a particular implementation of the Coherent anti-Stokes Raman spectroscopy microscopy, is used to study myelin and myelopathies (John R. et al. 2003, W. Demtroder, 2008).

2.4.10 Linear Laser Raman Spectroscopy

The scattering cross sections in spontaneous Raman spectroscopy are very small, typically on the order of $10-30$ cm^2. The experimental problems of detecting weak signals in the presence of intense background radiation are by no means trivial. The achievable signal-to-noise ratio depends both on the pump intensity and on the sensitivity of the detector. Recent years have brought remarkable progress on the source as well as on the detector side. The incident light intensity can be greatly enhanced by using multiple reflection cells, intracavity techniques, or a combination of both. Figure 2.7 depicts as an example of such advanced equipment a Raman spectrometer with a multiple-reflection Raman cell inside the resonator of an argon laser. The laser can be tuned by the Brewster prism with reflecting backside (LP + M) to the different laser lines. A sophisticated system of mirrors CM collects the scattered light, which is further imaged by the lens L_1 onto the entrance slit S of the spectrometer. A Dove prism DP turns the image of the line source by 90° to make it parallel to the entrance slit as shown in Figure 2.7. (W. Demtroder, 2008).

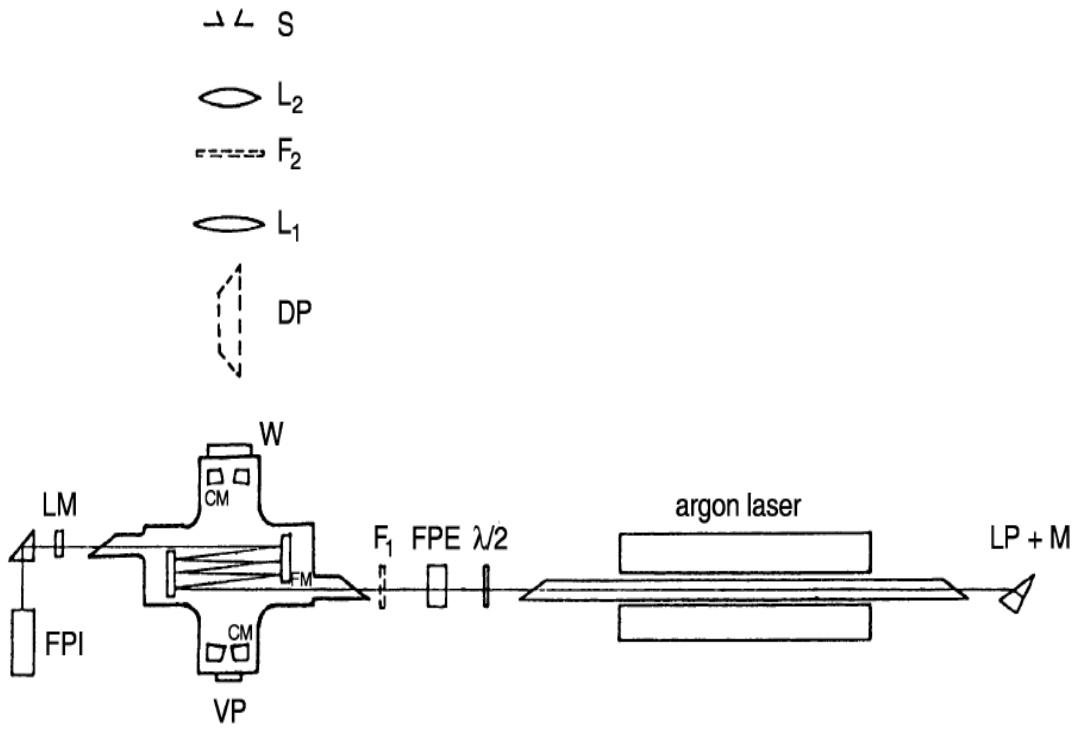

Figure 2.7: Raman spectroscopy with an argon laser: CM=multiple reflection four-mirror system for efficient collection of scattered light; LM= laser-resonator mirror; DP= Dove prism, which turns the image of the horizontal interaction plane by 90◦ in order to match it to the vertical entrance slit S of the spectrograph; FPE=Fabry–Perot etalon to enforce single-mode operation of the argon laser; LP= Littrow prism for line selection.

2.4.11 Nonlinear Raman Spectroscopy

When the intensity of the incident light wave becomes sufficiently large, the induced oscillation of the electron cloud surpasses the linear range. This implies that the induced dipole moments p of the molecules is no longer proportional to the electric field E and we have to generalize (W. Demtroder, 2008). The function p (E) can be expanded into a power series of E^n (n = 0, 1, 2, . . .), which is generally written as

$$p(E) = \mu + \tilde{}\alpha E + \tilde{}\beta E \cdot E + \tilde{}\gamma E \cdot E \cdot E \qquad (2.10)$$

where ˜α is the polarizability tensor, ˜β is named hyper-polarizability, and ˜γ is called the second hyper-polarizability. The quantities α, β, and γ are tensors of rank two, three, and four, respectively.

In component notation (i = x, y, z) written as

$$p_i(E) = \mu_i + \Sigma_k \alpha_{ik} E_k + \Sigma_k \Sigma_j \beta_{ikj} E_k E_j + \Sigma_k \Sigma_j \Sigma_l \gamma_{ikjl} E_k E_j E_l \qquad (2.11)$$

This gives for the polarization P = N p of a medium with N oriented dipoles

$$Pi\ (E) = \varepsilon_0)\ \chi_i + \Sigma_k\ \chi_{ik} Ek + \Sigma_{k,j}\ \chi_{ik\,j}\ E_k E_j + . . .) \quad (2.12)$$

For sufficiently small electric field amplitudes E the nonlinear terms can be neglected, and we then obtain for the linear Raman spectroscopy.

2.5 LITERATURE REVIEW

In 2002 Kazuhiro Ito, et.al., studied the quantification of the average particle diameter of latex as water-based emulsions by Fourier transform Raman spectroscopy. Their results showed that the wavenumbers, at 1000, 1668 and 3053 cm^{-1} can be assigned to ring breathing, C=C stretch and CH stretch of styrene and butadiene, respectively. The wavenumbers at 1732 and 2239 cm^{-1} may be due to C=O stretch of methyl methacrylate and C≡N stretch of acrylonitrile. The broad peak around 3300 cm^{-1}can be assigned to the OH stretch of water present in the latex emulsions since drying of the emulsions caused a weakening of this peak. They concluded that, a single FT-Raman instrument can be sufficient to control many aspects of product quality on-line (Kazuhiro Ito, et.al., 2002).

Monsuru O. Gborigi, et.al., in 2005 studied the Raman spectroscopy of a hydrated CO_2/water composite. A typical Raman spectrum collected from the composite after the water had been drained from the pressure vessel. Two pairs of peaks (four intotal) were observed which correspond to the well-known CO_2 Fermi-diad peaks from both liquid CO_2 and CO_2 in hydrate.They concluded that, flowrate ratios of CO_2 and water are the determining factors in the formation of sinking hydrate composite. Raman spectroscopy can be used to determine the presence of CO_2 in both liquid and hydrate form of the composite (Monsuru O. Gborigi, et.al., 2005).

In 2006, P. Schmidt, J. Dybal, M. Trchova investigated the hydrophobic and hydrophilic interactions in polymer–water systems by Raman spectroscopy. Their results showed that the peak positions of the bands in the C–H stretching were in the region (3000 – 2800 cm^{-1}) and the Amide I and Amide II in the region (1800–1500 cm^{-1}). The evaluation of the peak positions of

both the infrared and Raman CH_3 stretching vibrational bands of thermotropic polymers showed that the wavenumbers of the maxima decrease in the sequence: water solution (below Tt)–water suspension (above Tt)–solid. They concluded that, Parts of molecules of organic compounds in aqueous solutions undergo different types of interactions with the neighboring molecules of water (P. Schmidt, J. Dybal, M. Trchova, 2006).

Vincenza Crupi. et.al., in 2007 studied the hydrogen bonding structures of nanoconfined water using Raman spectroscopy. Their results showed that in liquid water each molecule is surrounded by four nearest neighbours in a tetrahedral fashion like in the ice structure. This fully H-bonded five molecule structural unit can be considered as the ‘building block’ of the spatial network of H-bonds. Temperature and confinement in restricted geometry are two common causes that can affect the water arrangements. the size of the geometrical confinement and changing the interaction of H_2O molecules with the solid substrate were determined (Vinceza Crupi. et. al. , 2007).

In 2007, K. A. Vereschagin. et.al, used the Coherent anti-stokes Raman spectroscopy to investigate the collisional broadening of the hydrogen Q-branch transitions by water at high temperatures. The CARS spectra recorded in the channel of the measurement complex were processed as follows. First, temperature estimation was done (temperature range 2500 – 3500 K). For identical values of temperatures and pressures, the data from another channel on the widths of spectral lines were selected. The standard deviation for a series of temperature measurements was typically 100–200 K, which makes up 3–5% from the measured values of temperatures. They concluded that, the broadening coefficients for hydrogen Q-branch lines are due to collisions with water molecules at temperatures from 2100 up to 3500 K inside a high-pressure hydrogen–oxygen combustion chamber (K. A. Vereschagin. et.al, 2007).

P. Sobron, et.al, in 2007 studied the modeling of physico-chemistry of the acid sulfate waters through Raman spectroscopy using the system $FeSO_4$–H_2SO_4–H_2O The ($FeSO_4$–H_2SO_4–H_2O) formed when groundwater flows through the cracks in the crushed sulfides or sulfur-rich minerals. The recorded spectrum of solution was in the region 850–1200 cm^{-1}. Processing of the original Raman spectra was performed with software developed in the group. The spectra were first filtered, smoothed and baseline-corrected in order to remove both sample fluorescence and noise. These operations are required to perform further spectral analysis such as band-fitting. They concluded that, Raman spectroscopy is a powerful tool that allows to carry out an accurate quantitative analysis of concentrations of species present in the system iron(II)–sulfuric acid–water (P. Sobron, et.al., 2007).

In 2008, Martin Mulvihill, et.al, used the Surface-Enhanced Raman Spectroscopy for Trace Arsenic Detection in Contaminated Water. The results indicated that the substrates to be useful in the field detection of arsenic in groundwater must show good sensitivity for arsenate (the most abundant arsenic contaminant) at concentrations of 10 ppb or less. Although other SERS substrates, including sputtered silver films and silver colloidal solutions, can improve detection of the arsenate ion at high concentrations, their close-packed arrays of nano crystals were the first to demonstrate SERS sensitivity significantly below 10 ppb. The study showed that, the Langmuir–Blodgett assemblies of polyhedral Ag nanocrystals were highly active in SERS substrates that can perform low-level arsenate and arsenite sensing in aqueous solutions. They achieved arsenate detection at 1 ppb an order of magnitude below the current standard set by the WHO. This SERS chip was robust, reproducible, highly portable, and could be easily implemented in field detection (Martin Mulvihill, et.al., 2008).

M. Pastorczak, et.al, studied in 2009 the Water–Polymer interactions in Poly(vinyl methyl ether) (PVME) hydrogels. Their results showed that in the low frequency part of the spectra (2700–3100 cm-1) there were well visible

CHx groups stretching vibrations of PVME; in the high frequency part one can see broad multimode band connected with OH stretching of liquid water. Shapes of the water stretching bands in the equilibrium swollen hydro gel and those of the distilled water do not differ. They concluded that: (1) Formation of water–polymer hydrogen bonds (seen as shifts of the υ_s (CH_3) bands) directly influences supramolecular structure of water absorbed by the hydro gel. However, for high swelling degree (for SD > 3–4, i.e. for ca.10–13 water molecules per monomer unit) the additionally absorbed water does not interact with the polymer network. (2) Hydrophobic water–polymer interactions, which manifest in perturbation of symmetry of the υ (CH_2) vibrations, are in equilibrium with hydrophilic interactions over wide range of swelling degrees at room temperature. (3) Cross linking density of the polymer network influences the availability of the hydrophilic sites to water molecules what reduces the equilibrium SD of the hydro gel (M. Pastorczak, et.al., 2009).

In 2009, Qiang Sun, studied the Raman OH stretching bands of liquid water. Three-dimensional hydrogen bonding network was formed between water molecules. They concluded that, the OH stretching vibration is closely related to local hydrogen bonding, and this can be applied to investigate the OH stretching region in the Raman spectrum of liquid water (Qiang Sun, 2009).

In 2010, Ivana –Duriˇckovi´c, et.al., studied the Water–ice phase transition probed by Raman spectroscopy. They recorded the water spectra in the temperature range from 10 to −15 C°, paying special attention to the OH–stretching region. The study showed that the OH–stretching modes of water fall in the 2900–3700 cm^{-1} range of the Raman spectrum. Besides the intramolecular O–H pairs, intermolecular O–H linked by hydrogen bonds contribute to the stretching. Thus, the effects of both intramolecular and intermolecular vibrational couplings of the OH–sb are mingled. However, it is primarily the intermolecular coupling that characterizes the spectral response of water. The role of the hydrogen bonds is therefore of great

importance for the understanding of this spectral range. This bond being flexible, it is sensitive to temperature, explaining why the OH–sb was selected as relevant for the phase transition determination. Variations in the temperature of water significantly contributed to the differences in Raman spectra of this region. The changes detected in this range in both phases were attributed to the changes in the water structure (expansion, bond elongation) (Ivana –Duriˇckovi´c, et.al., 2010).

S. Burikov, et.al., in 2010 studied the identification and determination of concentration of salts in natural waters by Raman spectroscopy using artificial neural networks. Their results showed that, when both low-frequency (200-1830 cm^{-1}) and valence (2700-3900 cm^{-1}) bands of spectra were used as input data, the obtained accuracy of determination of salts concentration was 0.02-0.03 M in the concentration range 0-2.5M. These results significantly outperform those obtained with the same experimental data by water Raman valence band only, and they are several folds better than the results obtained before for 3-component solutions in narrower concentration range (S. Burikov, et.al., 2010).

In 2011 Anna Yu. Likhacheva, et.al., studied the Raman spectroscopy of natural cordierite at high water pressure up to 5 GPa. Their results showed that the O–H stretching region in the Raman spectrum showed a sharp band at 3600 cm^{-1} and another weak and broad band at around 3580 cm^{-1}. Upon increasing the pressure up to about 4.5 GPa, all the framework bands in the region of 400–1200 cm^{-1} showed positive linear pressure dependence. They concluded that, the high-pressure Raman data indicated the existence of a reversible, low-kinetics phase transition in natural cordierite at about 4.5 GPa. The observed abrupt shifts of all the framework and O–H stretching modes indicate this transition to be of first order (Anna Yu. Likhacheva, et.al, 2011).

Xuesong Song , et.al., in 2013 studied the detection of herbicides in drinking water by surface-enhanced Raman spectroscopy coupled with gold

nanostructures. Their results showed that pure atrazine and arsenic trioxide can be analyzed using Raman spectroscopy by directly applying the samples on a gold slide. The atrazine spectra are highly consistent with a previous study using a hydroxylamine hydrochloride-reduced silver colloid as substrate. They concluded that, a SERS method, coupled with gold nanosubstrates can be developed to detect atrazine and arsenic trioxide in drinking water (Xuesong Song, et. al., 2013).

Fangyuan Han, Weimin Liu, Chong Fang, studied in 2013 the excited-state proton transfer of photo excited pyranine in water observed by femtosecond stimulated Raman spectroscopy. The ground-state Femtosecond Stimulated Raman Spectroscopy (FSRS) spectrum of 8-hydroxypyrene-1,3,6-trisulfonic acid (HPTS) has been measured at two grating positions of the spectrograph, in order to cover the wide spectral range of 50–2000 cm^{-1}. The slit width in Raman pump generation is set below 0.1 mm still with enough output power to induce the Raman transition, enabling the observation of the narrow linewidth of the Raman peak close to the natural linewidth seen in the continuous wave (cw) excitation case. They concluded that, the newly developed femtosecond stimulated Raman spectroscopy (FSRS) can be used to study the excited-state structural dynamics of HPTS in pure H_2O and D_2O following 400 nm photo excitation. The simultaneously high spectral and temporal resolution of the apparatus enable the collection of time-resolved excited state FSRS spectra of the photo excited chromophore as it transfers its phenolic proton to the labile molecular water H-bonded network in real time. The non-equilibrium spectroscopic approach reveals the multidimensional reaction coordinate on the excited-state PES for intermolecular ESPT, where in the sequentially emerged low-frequency skeletal motions gate and/or facilitate ESPT in H_2O on multiple timescales of 620 ± 50 fs, ~ 4.5 ps, and ~ 100 ps (Fangyuan Han, Weimin Liu, Chong Fang, 2013).

Yang Zhaoa, et.al., in 2014 studied the ultrafast vibrational dynamics in distilled water at room temperature using Raman Spectroscopy or CARS. The pump and probe pulses have the same wavelength, λ_{pr}= λ_{pu}= 638 nm,630 nm, 625 nm, 622 nm. The Stokes pulse was set to a longer wavelength λ_{st}= 800 nm, in such a way that the difference between pump and Stokes pulses was resonant with a vibrational Raman transition in 3100–3700 cm^{-1}. The time-resolved CARS signal was at λ_{CARS} = 530 nm, 520 nm, 513 nm, 509 nm. This was a result of time-resolved femtosecond CARS measurements for vibration modes in water at Raman shift of 3170 cm^{-1}, 3370 cm^{-1}, 3500 cm^{-1}, 3570 cm^{-1}.They concluded that through the femtosecond time-resolved CARS experimental platform, ultrafast dynamics process of the OH-stretching modes between 3100 $cm^{-1}$and 3700 cm^{-1} in water can be studied. The duration of the laser beams was obtained by two-beam CARS. The dephasing times of four Raman modes between 3100 cm^{-1} and 3700 cm^{-1}in water were detected and compared (Yang Zhaoa, et.al., 2014).

In 2014 Phodchanee Phongpa-Ngan, et.al, used Raman spectroscopy to assess water holding capacity in chicken breast muscle from fast and slow growing broilers. Their results showed that muscles from the low growth rate population showed significantly lower pH measured at 15 min post-mortem (pH15); pH measured at 24 h post-mortem (pHu). Muscles from high growth rate population showed significantly lower color values than muscle from low growth population both in lightness, and blue to yellow. There was no statistical difference between the low- and high-growth rate between pHDiff (difference in pH15 and pHu), green to red (a), chroma (C), drip loss (DL), and cook yield (CY). They concluded that Raman spectroscopy provides good predictive information for specific wavenumbers related to growth rate of broilers and water holding capacity (WHC) of chicken breast muscle (Phodchanee Phongpa-Ngan, et.al., 2014).

CHAPTER THREE

MATERIALS AND METHODS

3.1 Introduction

This chapter presents the materials used, the equipments and tools, the collection of the samples and the experimental procedure.

3.2 The Raman Spectrometer

Instrumentation for the measurement of Raman spectra usually consists of four components, namely: excitation source, illumination and light collection optics, wavelength selector unit, and the detector. The excitation source plays an important role in the performance of a Raman spectrometer, including its sensitivity and stability. Two important parameters of the excitation source are its bandwidth and power. The wavelength selector is the most critical component in a Raman spectrometer, through which the intensity information of individual frequencies is extracted. There are basically two types of wavelength selection mechanisms, dispersive and non-dispersive. A dispersive spectrometer relies on dispersive components to separate light spatially according to the wavelength, such as the diffraction grating and prism. For the non-dispersive spectrometer, light can be selected either by an optical filter. The detectors exploit the photoelectric effect which uses the incoming light energy to generate charge carriers that are separated and can subsequently be measured as a current at the terminals (Zhiyun Li, et. al., 2014).

In this work a Raman Spectrometer model (LIRA – 300) was used. LIRA – 300 laser Raman spectrometer is a useful instrument for the identification of a wide range of substances in physics and chemistry laboratories. It is a straightforward, non-destructive technique requiring no sample preparation, and it involves illuminating a sample with monochromatic light and using a spectrometer to examine the light scattered by a sample. The schematic

diagram of the LIRA – 300 laser Raman spectrometer is shown in figure (3.1).

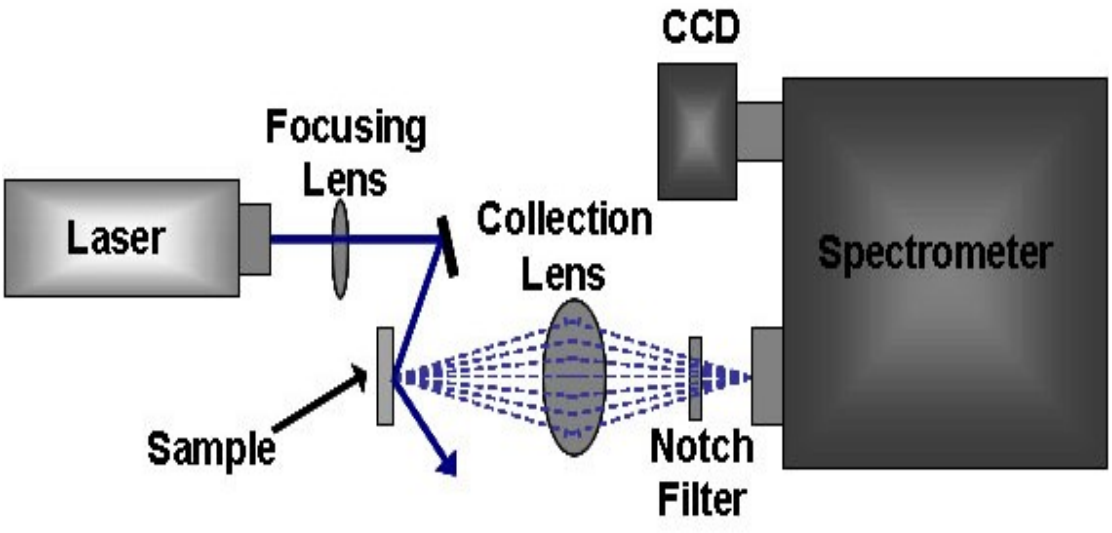

Figure 3.1: Diagram of LIRA – 300 laser Raman spectrometer.

When a light beam emitted from a laser device passes into external optic path and irradiates the sample, the scattered light enters the monochromator. When the grating in the monochromator is rotating, the spectrum message is transformed by a photomultiplier into current pulses which are enlarged and counted by photocounter and sent into computer for processing, while a spectrum curve is being displayed on a monitor. Specifications in details of laser Raman Spectrometer model LIRA – 300 are listed in table 3.1.

Table 3.1 Specifications of laser Raman Spectrometer model LIRA – 300

Specifications	
Wavelength Range	200 – 800 nm
Wavelength Accuracy	≤ 0.4 nm
Wavelength Repeatability	≤ 0.2 nm
Stray Light	≤ 10^{-3}
Reciprocal of Line Dispersion	2.7 mm
Parameters	
Momochromoator	Relative Aperture Ratio D/F = 1/5.5, Optical Grating 1200 lines/mm, blazed 500 nm, Slit Width 0 ~ 2 mm continuous, resolution 0.01 nm
Receiver	Photomultiplier R6249 Electrical Source 0 ~ 1500 V

	Broadband Amplifier Bandwidth > 100MHz
Notch Filter	Wavelength 532 nm Spectral Bandwidth < 10 nm
Single – Photon Counter	Integration time 0 ~ 30 min, Max count 10^7, Threshold Voltage 0 ~ 2.6 V, ~ 256 black (10 mV/ Block)
Light Source	Diode Pump Solid State (DPSS) Green Laser 532 nm Output power ≥ 40 mW Stability ≤ 2%

3.2.1Raman Software

LIRA – 300 is supplied with software designed for data processing. The main areas of the application window are: Title bar, Menu bar, Main toolbar, Auxiliary toolbar, Workspace, Parameter setup area, Channel information area, etc. as shown in Figure (3.2).

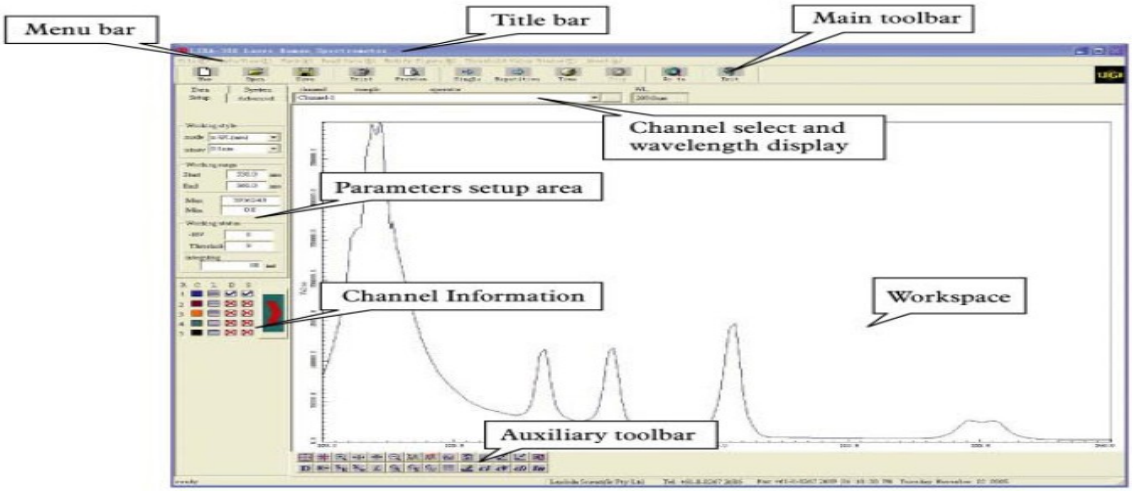

Figure 3.2: Raman Software window.

Menu bar: the menu bare is a collection of file, info/View, work, read data, modify figure, threshold value window, etc. Toolbars: the software offers two toolbars (Main toolbar and auxiliary toolbar). A certain number of function buttons compose each toolbar. Workspace: workspace is where spectral lines are drawn, browsed and edited; up to 5 spectral lines can be displayed at the same time. Parameters setup area: parameter setup area is for setting the instrument operation parameters. Channel information: channel information

area is to display information of every channel. Channel select and wavelength display: Channel select and wavelength display bar is to select present channel and display present position of wavelength (Lambda Scientific Pty Ltd, 2016).

3.2.2 The Tools

In this study, numbers of tools were used to carry out the analysis of water samples and to record the results, these tools are:

1. Cuvette tube (sample cell)
2. Some tools to adjust the alignments of laser (tracer, cutter, ruler, pen, adhesive and paper).
3. A syringe for sampling.
4. Samples Containers.

3. 3 The Samples

The samples investigated in this study are underground water samples collected from some wells in the western region of Saudi Arabia. These samples were taken from wells directly. Different areas and depths were chosen to ensure accurate results. The collected are listed in table (3.2):

Table 3.2: collection samples codes and locations.

Sample Code	Location
S_1	Ground wells in Jeddah region (Ajuad)
S_2	Ground wells in Jeddah region (Almazara)
S_3	Ground wells in Jeddah region (Safa)
S_4	Ground wells in Jeddah region (Omalgoura)
S_5	Ground wells in Jeddah region (Shakreen)
S_6	Ground wells in Makah region (Alawaly)
S_7	Ground wells in Makah region (Alzaher)
S_8	Ground wells in Makah region (Alhasanya)
S_9	Ground wells in Makah region (Alhasanya2)
S_{10}	Ground wells in Makah region (Kakya)
S_{11}	Ground wells in Madina region (Alarak)
S_{12}	Ground wells in Madina region (Aldeara)
S_{13}	Ground wells in Madina region (Almaboath)
S_{14}	Ground wells in Madina region (Alabar)

3.4 The Methods

Laser Raman Spectrometer model LIRA – 300 is easy use, no sample preparation is needed. Figure 3.3 shows the optical components and the optical components. To run the Raman device perfectly, the work was divided to stages, carried out in order to get the best results. Reviewing the power supply and connections well, then the laser module was operated. The Raman switch was open after that. Out cover was open to see the laser path, and make it linear on all tracks, this is done in two phases, The first phase was the adjusting of the laser path vertical on the sample holder in the middle of the hole, and using the manual adjustment and simple tools (such as Cutter, ruler, paper, and gum). After making sure that the laser has become in the center of the sample holder, the second phase was started by moving the unit lenses to get a sharp line of the laser on the region of magnification and recording signal, use screws to make adjustment, see Figure (3.3). After that the scattering laser line was centered at the hole of the magnification unit.

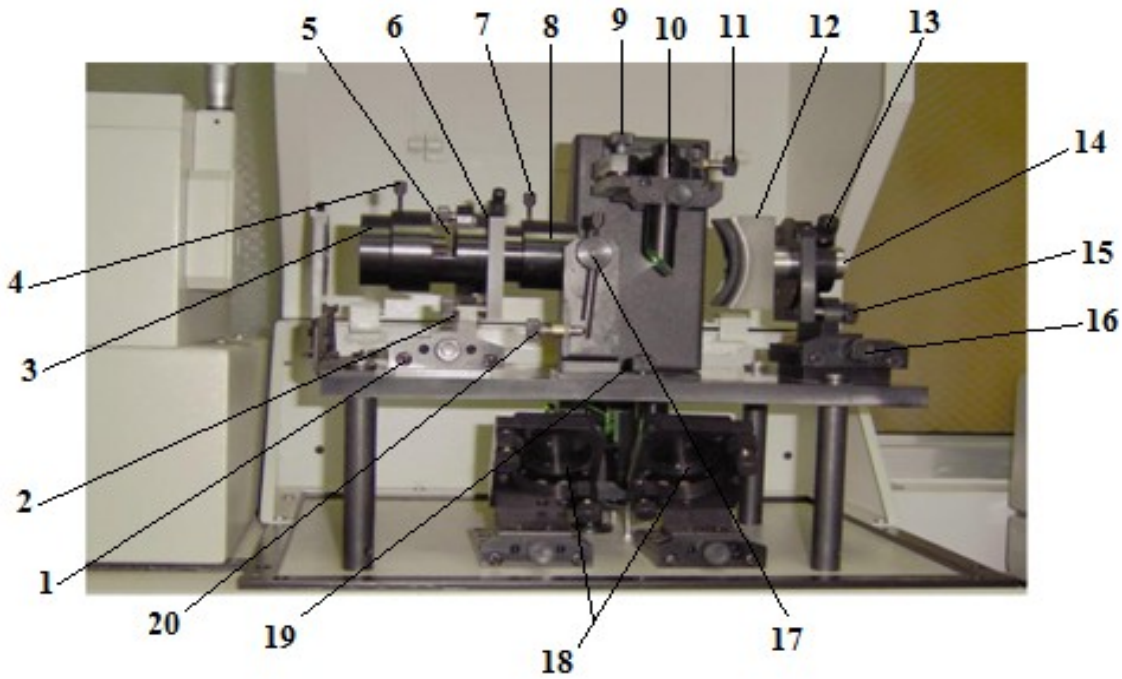

1. Adjustment screw 1 2. Adjustment screw 2 3. Object lens 1
4. Locking screw 1 5. Position of notch filter 6. Adjustment screw 3
7. Locking screw 2 8. Object len 2 9. Adjustment screw 4
10. Sample holder 11. Adjustment screw 5 12. Concave mirror
13. Adjustment screw 6 14. Locking screw 3 15. Adjustment screw 7
16. Adjustment screw 8 17. Small mirror holder 18. Normal incidence mirror
19. Locking screw 4 20. Adjustment screw 9

Figure 3.3: laser path in optical region and the manual adjustment.

The Raman program was operated by the computer. After the starting of the program, the work screen was appeared and there were number of steps:

(1) Step of software program settings where the data is set (working style, working range, work status), see Figure (3.4).

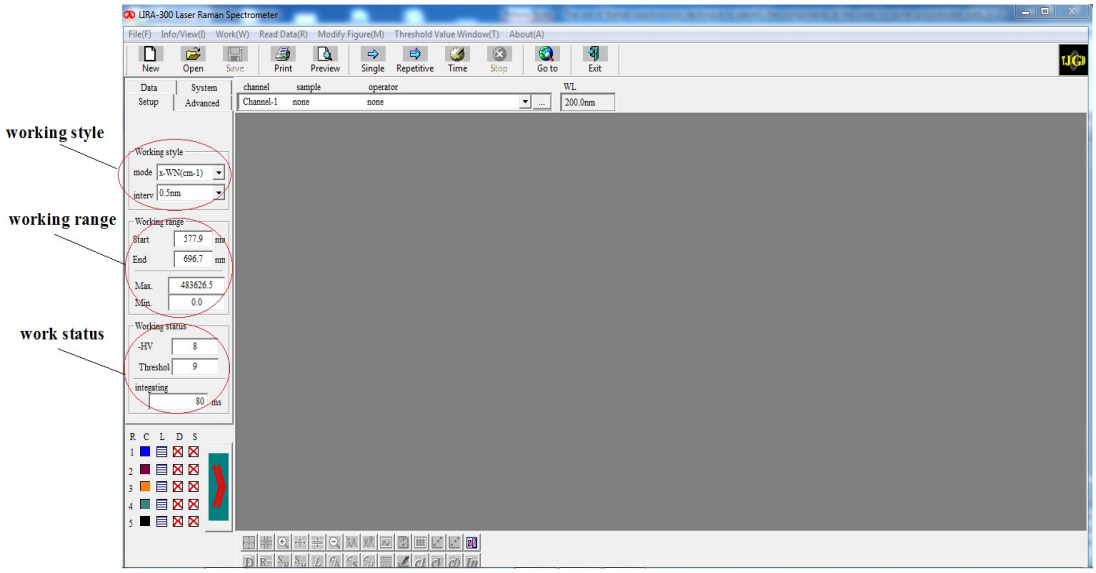

Figure 3.4: Software Program settings.

(2) Preparation Threshold was selected from the list on three stages, the first start of recording and secondly to determine the points and finally approve the form, where the value was recorded in the settings as shown in Figure (3.5).

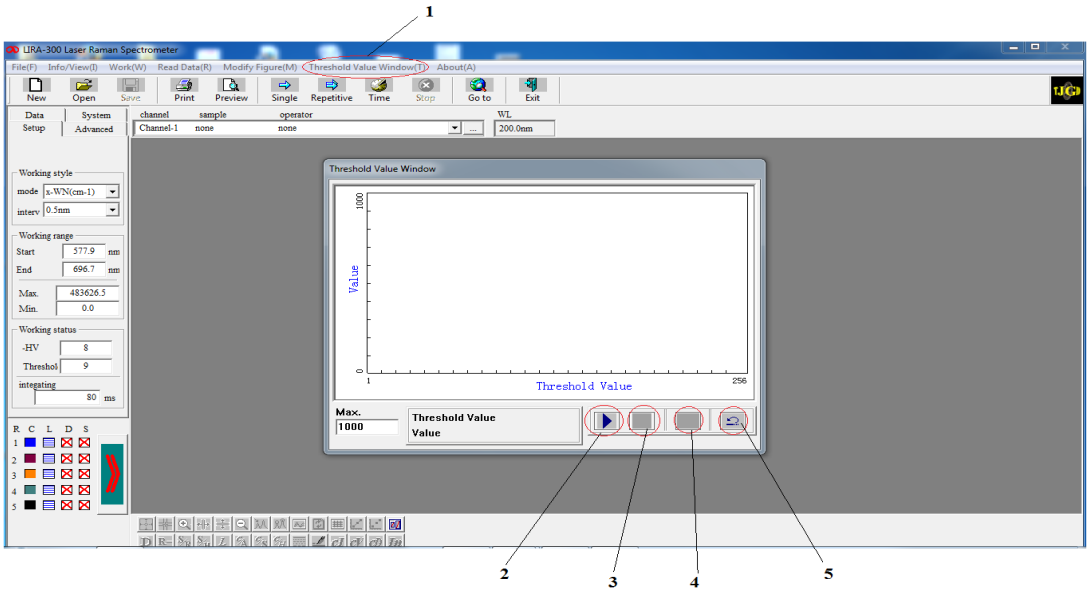

Figure 3.5: Preparation to calculate the Threshold.

1. Threshold selection 2. Start of recording 3. Stop of recording
4. determine the points 5. Close threshold window

(3)After setting all parameters, CCl_4 material was used to test the Raman spectrometer. It is the standard material for testing Raman Spectrometers. The Raman spectrum of CCl_4 is shown in Figure (3.6).

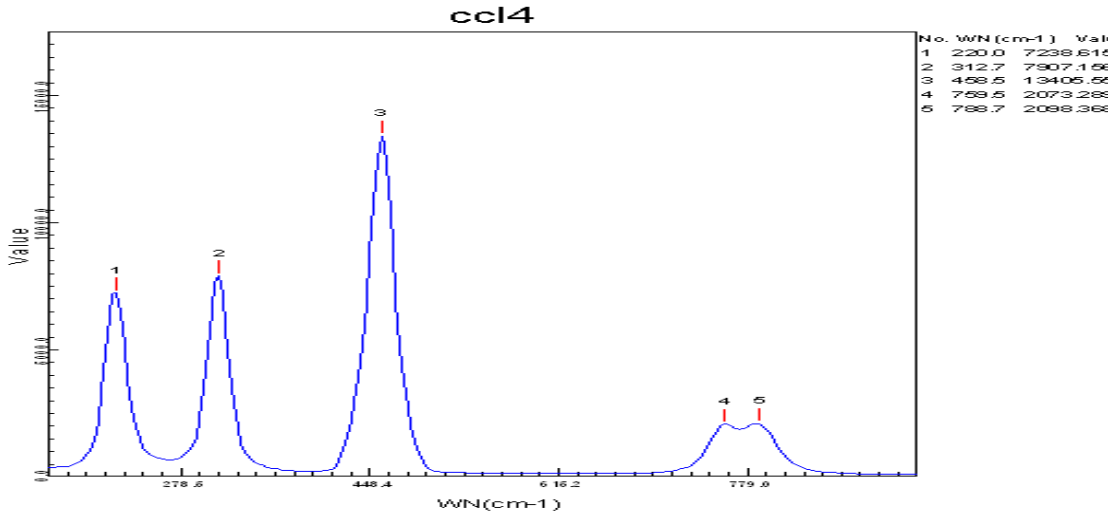

Figure 3.6: Raman spectrum of CCl_4 sample

After that, the samples of the underground water were investigated as follows:

(1) The sample was injected in the cuvette tube by using syringe (1 mL), and the unit of optical was closed to withhold outer light.

(2) Windows, door and all lights were closed to withhold outer, and also the vibrations and noise were reduced.

(3) Raman software program was operated by the computer device and all operating settings were checked.

(4) Raman spectrum was recorded by choosing single bottom, and then the spectrum was appeared on the work window, as shown in figure 3.7.

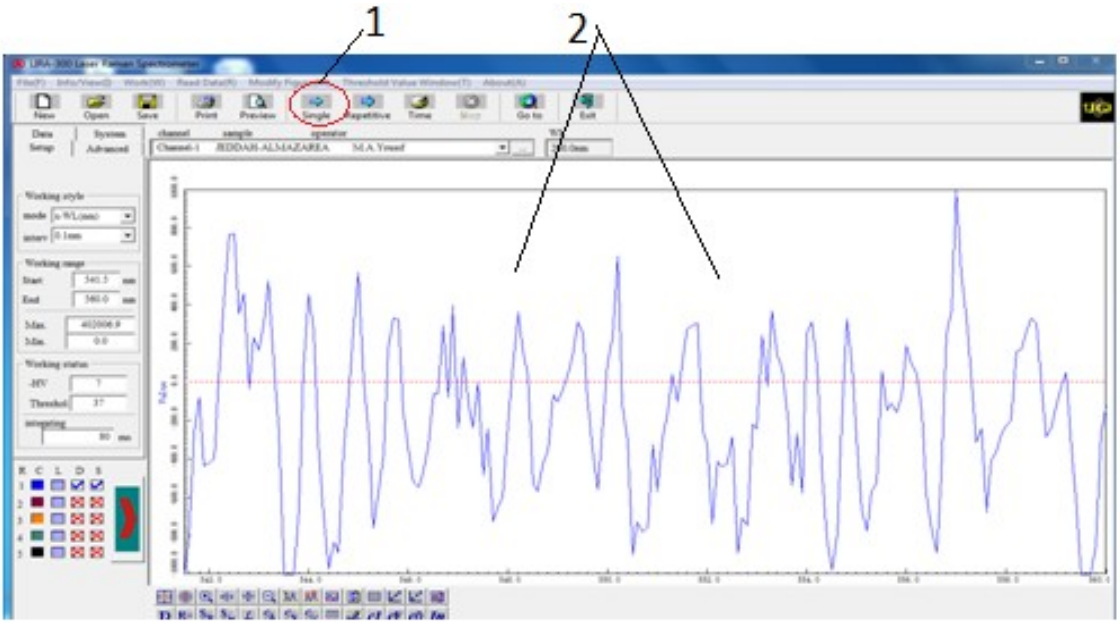

Figure 3.7: Spectrum shape in software program.

1. Single bottom 2. work window

(5) The same steps were repeated for all samples.

(6) The recorded spectra were analyzed using the standard data and the previously published work.

CHAPTER FOUR

RESULTS AND DISCUSSION

4.1 INTRODUCTION

The purpose of this study was to identify the components of ground water collected from some wells in the western region of Saudi Arabia using Laser Raman Spectrometer model LIRA – 300. The fourteen water samples were collected from ground wells in Jeddah region, Makah region and Madina region. The results of the investigation are presented in this chapter and discussed. At end of the chapter the main conclusions and recommendation are presented.

4.2 RESULTS AND DISCUSSION OF JEDDAH SAMPLES

Five water samples (S_1 – S_5) were collected from ground wells in Jeddah region. The results showed that these samples contain different materials, beside the water, with different amounts.

Figure 4.1 shows the Raman spectrum of a sample taken from a well in the area of Jeddah Ajuad (S_1) in the range from 367.2 to 3763.9 cm^{-1}. It shows clear peaks. By comparison with the vibrations recorded in some references, it was found that these vibrations describe the vibrations of water molecules and some components of other materials as listed in Table 4.1.

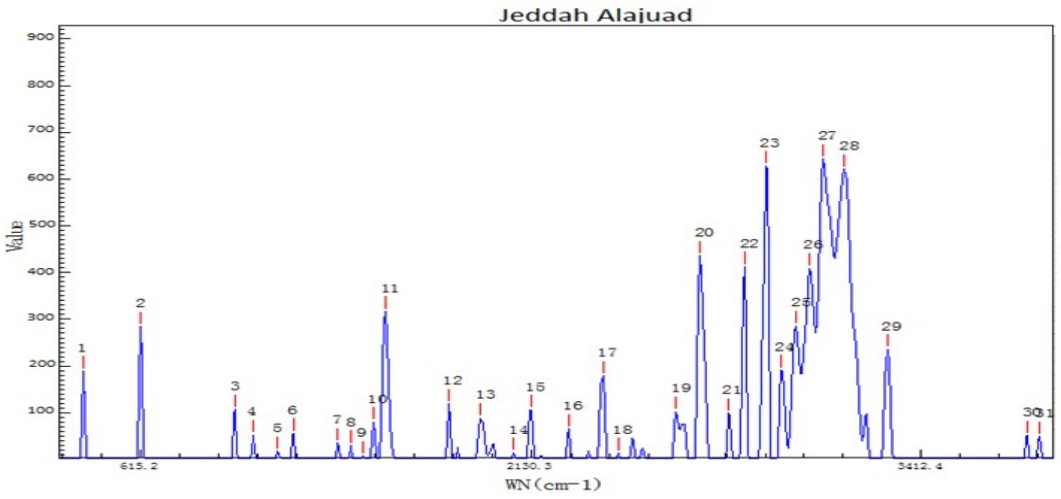

Figure (4.1) Raman spectrum of ground water sample S_1 collected from (Jeddah Ajuad) in the range from 367.2 to 3763.9 cm^{-1}.

Table (4.1): The wave number, intensities, and Functional Group/ Vibration of peaks in the Raman spectra of the ground water S_1 collected from Jeddah Ajuad.

No. of Peak	Wavenumber (cm^{-1})	Intensity (au)	Functional Group/ Vibration	References
1	367.2	189.424	X metal – O	(Ewen.S, Geoffrey D.2005) , (Robert M., Francis X., David J., 2005)
2	615.2	284.624	C = S	(Ewen.S, Geoffrey D.2005), (Robert M., Francis X., David J., 2005)

3	1009.7	107.198	Aromatic ring	(Lin-Vien, D.; et. al., 1991), (Ewen.S,Geoffrey D.2005), (George Socrates, 2004), (Robert M., Francis X., David J., 2005)
4	1079.1	52.731	Si – O – Si	(Ewen.S, Geoffrey D.2005), (Robert M., Francis X., David J., 2005)
5	1179.0	17.031	Si – O – C	(Ewen.S, Geoffrey D.2005), (Robert M., Francis X., David J., 2005)
6	1240.8	55.625	Sulfonic acid	(Ewen.S, Geoffrey D.2005), (Robert M., Francis X., David J., 2005)
7	1411.7	35.136	CH_2 , CH_3	(Lin-Vien, D.; et. al., 1991), (Ewen.S, Geoffrey D.2005), (Robert M., Francis X., David J., 2005)
8	1466.0	30.176	Aromatic ring	(Lin-Vien, D.; et. al., 1991), (Ewen.S, Geoffrey D.2005), (George Socrates, 2004), (Robert M., Francis X., David J., 2005)
9	1507.9	7.627	C = C	(Lin-Vien, D.; et. al., 1991), (Ewen.S, Geoffrey D.2005), (George Socrates, 2004), (Robert M., Francis X., David J., 2005)
10	1549.7	80.190	Aliphatic azo	(Ewen.S, Geoffrey D.2005), (Robert M., Francis X., David J., 2005)
11	1597.1	316.907	Aromatic/hetero ring	(Lin-Vien, D.; et. al., 1991), (Ewen.S, Geoffrey D.2005), (George Socrates, 2004), (Robert M., Francis X., David J., 2005)
12	1830.6	119.052	Anhydride	((Ewen.S, Geoffrey D.2005), (Robert M., Francis X., David J., 2005)
13	1950.6	88.712	-	-
14	2069.0	14.285	Isothiocyanate	(Ewen.S, Geoffrey D.2005), (Robert M., Francis X., David J., 2005)
15	2130.3	106.136	Thiocyanate	(Ewen.S, Geoffrey D.2005), (Robert M., Francis X., David J., 2005)
16	2262.6	64.756	Diazonium salt	(Ewen.S, Geoffrey D.2005), (Robert M., Francis X., David J., 2005)
17	2382.0	178.422	P – H	(Ewen.S, Geoffrey D.2005), (Robert M., Francis X., David J., 2005)

18	2435.7	14.139	-	-
19	2631.5	102.552	-	-
20	2709.5	435.845	Th iol	(Ewen.S, Geoffrey D.2005), (Robert M., Francis X., David J., 2005)
21	2802.1	98.926	CH_2	(Lin-Vien, D.; et. al., 1991), (Ewen.S, Geoffrey D.2005), (Robert M., Francis X., David J., 2005)
22	2858.2	412.409	$C – CH_3$	(Ewen.S, Geoffrey D.2005), (Robert M., Francis X., David J., 2005)
23	2924.0	628.086	CH_2	(Lin-Vien, D.; et. al., 1991), (Ewen.S, Geoffrey D.2005), (Robert M., Francis X., David J., 2005)
24	2974.2	191.291	Aromatic C – H	(Ewen.S, Geoffrey D.2005), (George Socrates, 2004), (Robert M., Francis X., David J., 2005)
25	3024.1	285.783	$= CH_2$	(Lin-Vien, D.; et. al., 1991), (Ewen.S, Geoffrey D.2005), (Robert M., Francis X., David J., 2005)
26	3063.8	409.052	$= CH_2$	(Lin-Vien, D.; et. al., 1991), (Ewen.S, Geoffrey D.2005), (Robert M., Francis X., David J., 2005)
27	3108.3	642.707	OH	(Ewen.S, Geoffrey D.2005), (Robert M., Francis X., David J., 2005)
28	3176.9	620.887	Amide , Amine	(Ewen.S, Geoffrey D.2005), (Robert M., Francis X., David J., 2005)
29	3307.5	235.570	Phenol	(Ewen.S, Geoffrey D.2005), (Robert M., Francis X., David J., 2005)
30	3727.7	51.026	-	-
31	3763.9	49.233	-	-

Figure 4.2 shows the Raman spectrum in the range from 974.9 to 3824.7cm^{-1} of a water sample S_2 taken from Almazara in Jeddah area. It shows clear peaks represent the vibration of water molecules and some components of other materials as illustrated in Table 4.2.

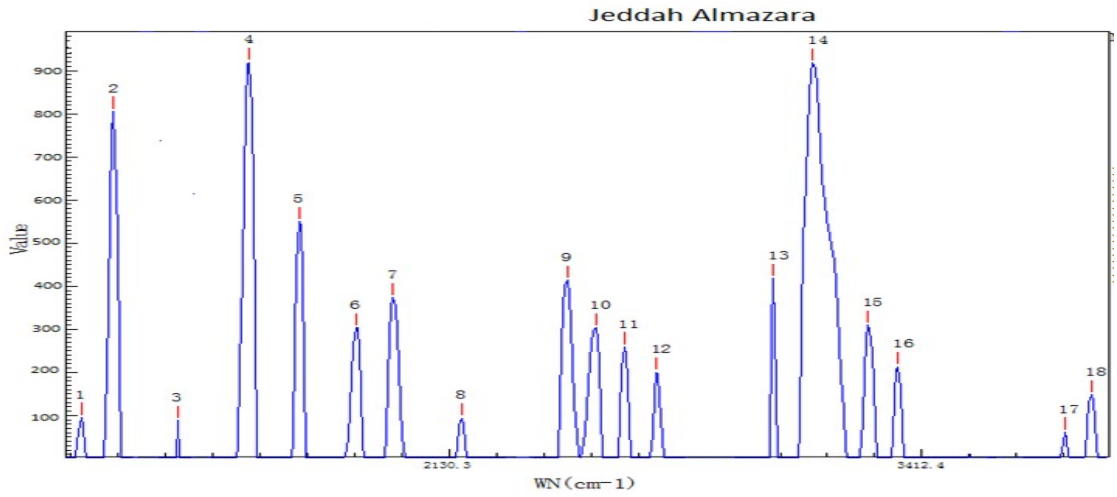

Figure (4.2) Raman spectrum of ground water sample S_2 collected from (Jeddah Almazara) in the range from 974.9 to 3824.7cm^{-1}.

Table (4.2): The wave number, intensities, and Functional Group/ Vibration of peaks in the Raman spectra of the ground water S_2 collected from Jeddah Almazara.

No. of Peak	Wavenumber (cm^{-1})	Intensity (au)	Functional Group/ Vibration	References
1	974.9	95.939	Aromatic ring	(Lin-Vien, D.; et. al., 1991), (Ewen.S, Geoffrey D.2005), (George Socrates, 2004), (Robert M., Francis X., David J., 2005)
2	1082.2	805.765	Si – O – C	(Ewen.S, Geoffrey D.2005), (Robert M., Francis X., David J., 2005)
3	1293.1	88.476	-	-
4	1522.9	919.309	C = C	(Lin-Vien, D.; et. al., 1991), (Ewen.S, Geoffrey D.2005), (George Socrates, 2004), (Robert M., Francis X., David J., 2005)
5	1676.6	549.584	C = C	(Lin-Vien, D.; et. al., 1991), (Ewen.S, Geoffrey D.2005), (George Socrates, 2004), (Robert M., Francis X., David J., 2005)
6	1850.7	303.524	C = C	(Lin-Vien, D.; et. al., 1991), (Ewen.S, Geoffrey D.2005), (George Socrates, 2004), (Robert M., Francis X., David J., 2005)
7	1964.8	373.570	-	-
8	2166.4	94.466	Thiocyanate	(Ewen.S, Geoffrey D.2005), (Robert M., Francis X., David J., 2005)

9	2470.5	413.683	-	-
10	2550.0	302.806	Th iol	(Ewen.S, Geoffrey D.2005), (Robert M., Francis X., David J., 2005)
11	2628.8	258.981	-	-
12	1717.2	200.584	Anhydride	(Ewen.S, Geoffrey D.2005), (Robert M., Francis X., David J., 2005)
13	3031.6	418.332	= CH_2	(Lin-Vien, D.; et. al., 1991), (Ewen.S, Geoffrey D.2005), (Robert M., Francis X., David J., 2005)
14	3135.3	917.323	OH	(Ewen.S, Geoffrey D.2005), (Robert M., Francis X., David J., 2005)
15	3276.3	309.899	Alkyne	(Ewen.S, Geoffrey D.2005), (Robert M., Francis X., David J., 2005)
16	3353.0	213.193	Phenol	(Ewen.S, Geoffrey D.2005), (Robert M., Francis X., David J., 2005)
17	3761.0	61.490	-	-
18	3824.7	147.950	-	-

In the Raman spectrum of the sample S_3 taken from a well in Jeddah-Alsafa (figure 4.3) there is a clear picture of the water components and some other materials. Table 4.3 illustrates the analysis of this spectrum.

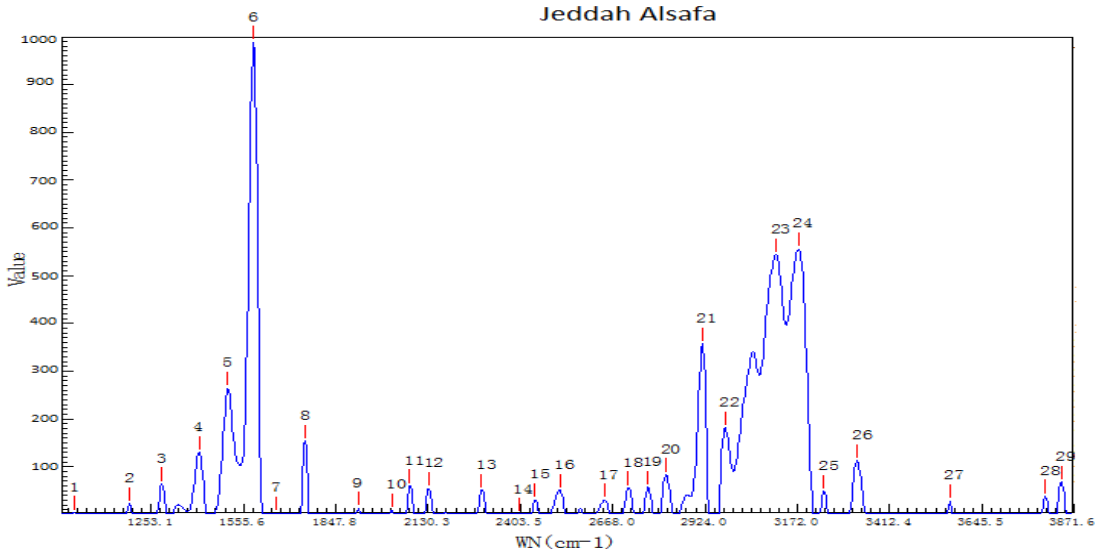

Figure (4.3): Raman spectrum of ground water sample S_3 collected from (Jeddah-Alsafa) in the range from 993.9 to 3840.4 cm^{-1}.

Table (4.3) The wave number, intensities, and Functional Group/ Vibration of peaks in the Raman spectrum of the ground water S_3 collected from Jeddah Alsafa.

No.	Wavenumber		Functional	

of Peak	(cm^{-1})	Intensity (au)	Group/ Vibration	References
1	993.9	4.346	Aromatic ring	(Lin-Vien, D.; et. al., 1991), (Ewen.S, Geoffrey D.2005), (George Socrates, 2004), (Robert M., Francis X., David J., 2005)
2	1182.1	22.715	Si – O – C	(Ewen.S, Geoffrey D.2005), (Robert M., Francis X., David J., 2005)
3	1290.0	64.370	-	-
4	1411.7	130.146	CH_2 , CH_3	(Lin-Vien, D.; et. al., 1991), (Ewen.S, Geoffrey D.2005), (Robert M., Francis X., David J., 2005)
5	1504.9	264.395	Aromatic ring	(Lin-Vien, D.; et. al., 1991), (Ewen.S, Geoffrey D.2005), (George Socrates, 2004), (Robert M., Francis X., David J., 2005)
6	1588.3	988.648	Aliphatic azo	(Ewen.S, Geoffrey D.2005), (Robert M., Francis X., David J., 2005)
7	1662.0	2.684	C = N	(Ewen.S, Geoffrey D.2005), (George Socrates, 2004), (Robert M., Francis X., David J., 2005)
8	1752.5	153.282	Lactone	(Ewen.S, Geoffrey D.2005), (Robert M., Francis X., David J., 2005)
9	1916.5	13.268	-	-
10	2121.3	9.363	Isothiocyanate	(Ewen.S, Geoffrey D.2005), (Robert M., Francis X., David J., 2005)
11	2074.6	60.049	Alkyne	(Ewen.S, Geoffrey D.2005), (Robert M., Francis X., David J., 2005)
12	2133.1	54.347	Azide	(Ewen.S, Geoffrey D.2005), (Robert M., Francis X., David J., 2005)
13	2289.9	50.717	-	-
14	2398.2	0.267	P – H	(Ewen.S, Geoffrey D.2005), (Robert M., Francis X., David J., 2005)
15	2446.4	30.645	-	-
16	2518.3	50.881	Th iol	(Ewen.S, Geoffrey D.2005), (Robert M., Francis X., David J., 2005)
17	2644.5	30.298	-	-
18	2712.1	55.579	Aldehyde	(Ewen.S, Geoffrey D.2005), (Robert M., Francis X., David J., 2005)
19	2766.2	56.932	N – CH_3	(Ewen.S, Geoffrey D.2005),

				(Robert M., Francis X., David J., 2005)
20	2817.4	83.639	C – CH_3	(Ewen.S, Geoffrey D.2005), (Robert M., Francis X., David J., 2005)
21	2916.4	357.039	CH_2	(Lin-Vien, D.; et. al., 1991), (Ewen.S, Geoffrey D.2005), (Robert M., Francis X., David J., 2005)
22	2979.2	181.612	Aromatic C – H	(Lin-Vien, D.; et. al., 1991), (Ewen.S, Geoffrey D.2005), (George Socrates, 2004), (Robert M., Francis X., David J., 2005)
23	3115.6	543.583	OH	(Ewen.S, Geoffrey D.2005), (Robert M., Francis X., David J., 2005)
24	3174.4	555.915	Amide , Amine	(Ewen.S, Geoffrey D.2005), (Robert M., Francis X., David J., 2005)
25	3242.5	48.588	Alcohol	(Ewen.S, Geoffrey D.2005), (Robert M., Francis X., David J., 2005)
26	3329.1	113.235	Phenol	(Ewen.S, Geoffrey D.2005), (Robert M., Francis X., David J., 2005)
27	3564.7	28.316	O - H	(Ewen.S, Geoffrey D.2005), (Robert M., Francis X., David J., 2005)
28	3802.2	38.187	-	-
29	3840.4	67.753	-	-

Figure (4.4) shows the Raman spectrum of the sample S_4 collected from omalgoura well in Jeddah area. The analysis of the spectrum illustrates that. These vibrations are consistent with the results of previous studies as listed in Table 4.4.

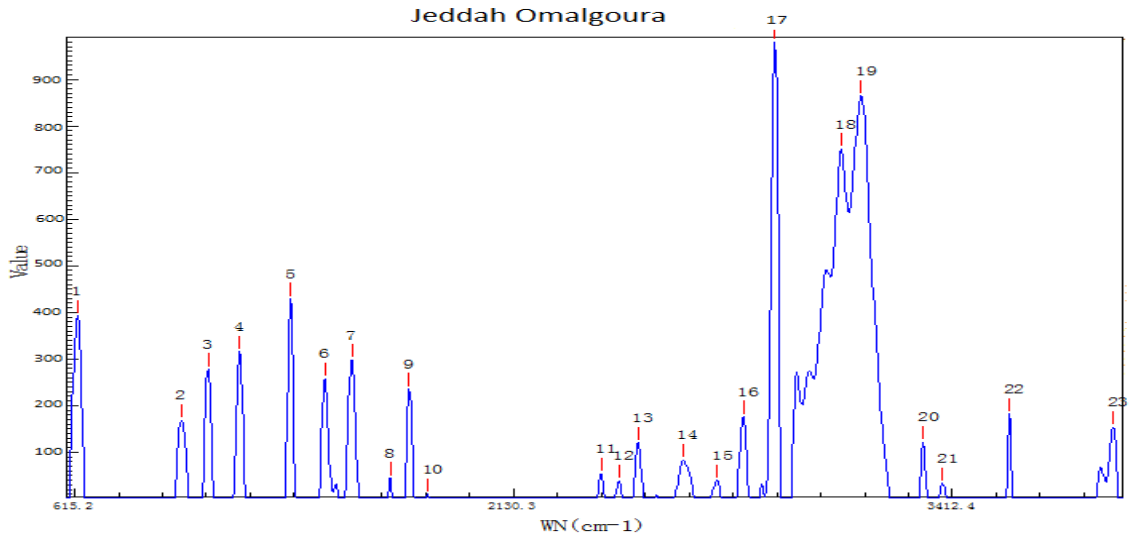

Figure (4.4) Raman spectrum in the range from 625.1 to 3833.7 cm^{-1} of ground water collected from S_4 (Jeddah Omalgora).

Table (4.4) the wavenumber, intensities, and Functional Group/ Vibration of peaks in the Raman spectrum of the ground water S_4 collected from Jeddah-Omalgora.

No. of Peak	Wavenumber (cm^{-1})	Intensity (au)	Functional Group/ Vibration	References
1	625.1	392.974	C = S	(Ewen.S, Geoffrey D.2005), (Robert M., Francis X., David J., 2005)
2	1006.6	168.601	Aromatic ring	(Lin-Vien, D.; et. al., 1991), (Ewen.S, Geoffrey D.2005), (George Socrates, 2004), (Robert M., Francis X., David J., 2005)
3	1104.1	278.486	Sulfonic acid	(Ewen.S, Geoffrey D.2005), (Robert M., Francis X., David J., 2005)
4	1216.1	315.769	-	-
5	1393.6	429.605	Si – O – C	(Ewen.S, Geoffrey D.2005), (Robert M., Francis X., David J., 2005)
6	1510.9	258.246	C = C	(Lin-Vien, D.; et. al., 1991), (Ewen.S, Geoffrey D.2005), (George Socrates, 2004), (Robert M., Francis X., David J., 2005)
7	1603.0	298.032	Aromatic/hetero ring	(Lin-Vien, D.; et. al., 1991), (Ewen.S, Geoffrey D.2005), (George Socrates, 2004), (Robert M., Francis X., David J., 2005)
8	1732.1	44.896	Ester	(Ewen.S, Geoffrey D.2005),

				(Robert M., Francis X., David J., 2005)
9	1793.1	235.723	Anhydride	(Ewen.S, Geoffrey D.2005), (Robert M., Francis X., David J., 2005)
10	1853.6	10.128	C = C	(Lin-Vien, D.; et. al., 1991), (Ewen.S, Geoffrey D.2005), (George Socrates, 2004), (Robert M., Francis X., David J., 2005)
11	2403.5	53.703	P – H	(Ewen.S, Geoffrey D.2005), (Robert M., Francis X., David J., 2005)
12	2457.1	39.191	-	-
13	2515.7	120.357	-	-
14	2649.7	83.397	-	-
15	2750.8	39.693	N – CH_3	(Ewen.S, Geoffrey D.2005), (Robert M., Francis X., David J., 2005)
16	2827.7	176.172	C – CH_3	(Ewen.S, Geoffrey D.2005), (Robert M., Francis X., David J., 2005)
17	2918.9	980.408	CH_2	(Lin-Vien, D.; et. al., 1991), (Ewen.S, Geoffrey D.2005), (Robert M., Francis X., David J., 2005)
18	3105.8	750.901	OH	(Ewen.S, Geoffrey D.2005), (Robert M., Francis X., David J., 2005)
19	3162.2	864.619	Amide , Amine	(Ewen.S, Geoffrey D.2005), (Robert M., Francis X., David J., 2005)
20	3333.9	121.918	Phenol	(Ewen.S, Geoffrey D.2005), (Robert M., Francis X., David J., 2005)
21	3386.3	32.947	Phenol	(Ewen.S, Geoffrey D.2005), ((Robert M., Francis X., David J., 2005)
22	3564.7	181.847	O – H	(Ewen.S, Geoffrey D.2005), (Robert M., Francis X., David J., 2005)
23	3833.7	153.959	-	-

Figure (4.5) illustrates the Raman spectrum of the groundwater collected from S_5 (Jeddah shakreen) in the range from 769.2 to 3838.1 cm^{-1}. Table (4.5) lists the analysis of this spectrum.

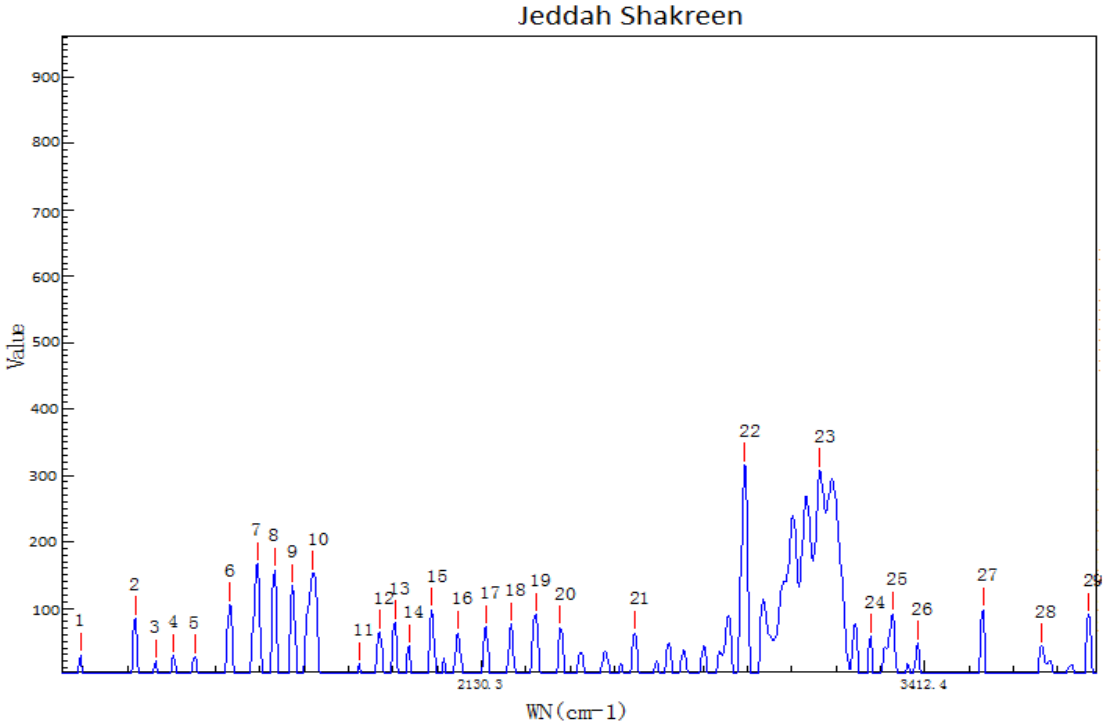

Figure (4.5) Raman spectrum of ground water collected from S_5 (Jeddah Shakreen) in the range from 769.2 to 3838.1 cm^{-1}

Table (4.5) the wavenumber, intensities, and Functional Group/ Vibration of peaks in the Raman spectra of the ground water S_5 collected from Jeddah Shakreen sample.

No. of Peak	Wavenumber (cm^{-1})	Intensity (au)	Functional Group/ Vibration	References
1	769.2	29.575	C - F	(Ewen.S, Geoffrey D.2005), (Robert M., Francis X., David J., 2005)
2	968.5	84.328	Aromatic ring	(Lin-Vien, D.; et. al., 1991), (Ewen.S, Geoffrey D.2005), (George Socrates, 2004), (Robert M., Francis X., David J., 2005)
3	1041.3	19.514	Sulfonic acid	(Ewen.S, Geoffrey D.2005), (Robert M., Francis X., David J., 2005)
4	1104.1	28.230	Sulfonamide	(Ewen.S, Geoffrey D.2005), (Robert M., Francis X., David J., 2005)
5	1179.0	26.940	Sulfonic acid	(Ewen.S, Geoffrey D.2005), (Robert M., Francis X., David J.,

				2005)
6	1302.2	105.502	CH_2	(Lin-Vien, D.; et. al., 1991), (Ewen.S, Geoffrey D.2005), (Robert M., Francis X., David J., 2005)
7	1396.6	166.729	Aromatic azo	(Ewen.S, Geoffrey D.2005), (Robert M., Francis X., David J., 2005)
8	1453.9	157.659	CH_2 , CH_3	(Lin-Vien, D.; et. al., 1991), (Ewen.S, Geoffrey D.2005), (Robert M., Francis X., David J., 2005)
9	1516.9	133.242	C = C	(Lin-Vien, D.; et. al., 1991), (Ewen.S, Geoffrey D.2005), (George Socrates, 2004), (Robert M., Francis X., David J., 2005)
10	1585.3	152.540	Aromatic/heter o ring	(Lin-Vien, D.; et. al., 1991), (Ewen.S, Geoffrey D.2005), (George Socrates, 2004), (Robert M., Francis X., David J., 2005)
11	1738.0	16.037	Ester	(Ewen.S, Geoffrey D.2005), (Robert M., Francis X., David J., 2005)
12	1804.6	63.829	Anhydride	(Ewen.S, Geoffrey D.2005), (Robert M., Francis X., David J., 2005)
13	1853.6	78.726	C = C	(Lin-Vien, D.; et. al., 1991), (Ewen.S, Geoffrey D.2005), (George Socrates, 2004), (Robert M., Francis X., David J., 2005)
14	1899.4	42.806	C = C	(Lin-Vien, D.; et. al., 1991), (Ewen.S, Geoffrey D.2005), (George Socrates, 2004), (Robert M., Francis X., David J., 2005)
15	1973.3	97.387	-	-
16	2055.0	62.660	Isothiocyanate	(Ewen.S, Geoffrey D.2005), (Robert M., Francis X., David J., 2005)
17	2144.2	71.735	Azide	(Ewen.S, Geoffrey D.2005), (Robert M., Francis X., David J., 2005)
18	2221.5	75.249	Aromatic nitrile	(Ewen.S, Geoffrey D.2005), (Robert M., Francis X., David J., 2005)
19	2298.1	90.121	P – H	(Ewen.S, Geoffrey D.2005), (Robert M., Francis X., David J., 2005)
20	2373.9	70.531	P – H	(Ewen.S, Geoffrey D.2005), (Robert M., Francis X., David J., 2005)
21	2573.4	62.664	Th iol	(Ewen.S, Geoffrey D.2005), (Robert M., Francis X., David J.,

				2005)
22	2916.4	315.583	CH_2	(Lin-Vien, D.; et. al., 1991), (Ewen.S, Geoffrey D.2005), (Robert M., Francis X., David J., 2005)
23	3127.9	307.520	OH	(Ewen.S, Geoffrey D.2005), (Robert M., Francis X., David J., 2005)
24	3266.6	57.764	Alkyne	(Ewen.S, Geoffrey D.2005), (Robert M., Francis X., David J., 2005)
25	3326.7	91.300	Amide , Amine	(Ewen.S, Geoffrey D.2005), (Robert M., Francis X., David J., 2005)
26	3393.4	47.349	Phenol	(Ewen.S, Geoffrey D.2005), (Robert M., Francis X., David J., 2005)
27	3567.0	97.917	O – H	(Ewen.S, Geoffrey D.2005), (Robert M., Francis X., David J., 2005)
28	3718.0	43.044	-	-
29	3838.1	90.297	-	-

Through the analysis of the five samples collected from Jeddah area it was found that the vibration modes of some materials are appeared in all the samples while other modes are appeared in some samples and disappeared in other samples. That is as follows:

1. X metal - O: appeared in the spectrum of (Ajuad) well, with intensity of 189.424 (au).

2. C=S: appeared in the spectra of (Ajuad and omalgoura) wells, with different intensities (284.624and 392.974) (au), respectively.

3. Aromatic ring: appeared in the spectra of all samples (Ajuad, Almazara, Safa, omalgoura, shakreen) wells, with intensities (107.198, 95.939, 264.39, 168.6, 84.328) (au), respectively.

4. Si – O – Si: appeared in the spectrum of (Ajuad) well, with intensity of 52.7(au).

5. Si – O – C: appeared in the spectra of the (Ajuad, Almazara, Safa, omalgoura) wells, with intensities (17.031, 805.76, 22.715, 429.6) (au), respectively.

6. Sulfonic acid: appeared in the spectra of (Ajuad, omalgoura, shakreen) wells, with different intensities (55.625, 278.486, (19.514, 26.94) (au), respectively.

7. CH_2, CH_3: appeared in the spectra of (Ajuad, Safa, omalgoura, shakreen) wells, with intensities (130.146, 357.039, 980.4, 105.5) (au), respectively.

8. C=C: appeared in the spectra of (Ajuad, Almazara, omalgoura, shakreen) wells, with different intensities (7.627, 919.309, 258.246, 133.242) (au), respectively.

9. Aliphatic azo: appeared in the spectra of (Ajuad and Safa) wells, with different intensities (80.19, 988.648) (au), respectively.

10. Aromatic/hetero ring: appeared in the spectra of (Ajuad, omalgoura, shakreen) wells, with different intensities (316.907, 298.032, 152.54) (au), respectively.

11. Anhydride: appeared in the spectra of (Ajuad, Almazara, omalgoura, shakreen) wells, with different intensities (119.052, 200.584, 235.723, 63.829) (au), respectively.

12. Isothiocyanate: appeared in the spectra of (Ajuad, Safa, shakreen) wells, with different intensities (14.285, 9.362, 62.66) (au), respectively.

13. Thiocyanate: appeared in the spectra of (Ajuad and Almazara) wells, with different intensities (106.136, 94.466) (au), respectively.

14. Diazonium salt: appeared in the spectrum of the recorded from Ajuad well, with intensity of 64.756 (au).

15. P – H: appeared in the spectra of (Ajuad, Safa, omalgoura, shakreen) wells, with different intensities (178.422, 0.267, 53.703, 90.121) (au), respectively.

16. Thiol: appeared in the spectra of (Ajuad, Almazara, Safa, shakreen) wells, with different intensities (435.845, 302.806, 50.881, 62.664) (au), respectively.

17. C – CH_3: appeared in the spectra of (Ajuad, Safa, omalgoura) wells, with different intensities (412.409, 83.639, 176.172) (au), respectively.

18. Aromatic C – H: appeared in the spectra of (Ajuad, Safa) wells, with different intensities (191.291, 181.612) (au), respectively.

19. = CH_2: appeared in the spectra of (Ajuad and Almazara) wells, with different intensities (409.05, 418.33) (au), respectively.

20. OH: appeared in the spectra of (Ajuad, Almazara, Safa, omalgoura, shakreen) wells, with different intensities (642.707, 917.323, 543.583, 750.901, 307.520) (au), respectively.

21. Amide, Amine: appeared in the spectra of (Ajuad, Safa, omalgoura, shakreen) wells, with different intensities (620.887, 555.915, 864.619, 91.3) (au), respectively.

22. Phenol: appeared in the spectra of (Ajuad, Almazara, Safa, omalgoura, shakreen) wells, with different intensities (235.57, 213.193, 113.235, 121.918, 47.34) (au), respectively.

23. Alkyne: appeared in the spectra of (Almazara, Safa, shakreen) wells, with different intensities (309.899, 60.049, 57.764) (au), respectively.

24. C = N, Lactone, Aldehyde, Alcohol: appeared in the spectrum of (Safa) well, with intensities (2.684, 153.28, 55.579, 48.588) (au), respectively.

25. Azide: appeared in the spectrum of (Safa and shakreen) wells, with different intensities (54.347, 71.735) (au), respectively.

26. N – CH_3: appeared in the spectrum of (Safa and omalgoura) wells, with different intensities (56.932, 39.693) (au), respectively.

27. O – H: appeared in the spectrum of the recorded from (Safa, omalgoura, shakreen) wells, with different intensities (28.316, 181.847, 97.917) (au), respectively.

28. Ester: appeared in the spectra of (omalgoura and shakreen) wells, with different intensities (44.896, 16.037) (au), respectively.

29. Sulfonamide, Aromatic azo, Aromatic nitrile: appeared in the spectrum of (shakreen) well, with intensities (28.230, 166.729, 75.249) (au), respectively.

Some vibrations modes in samples (S_1 – S_5), collected from Jeddah wells, indicate the presence of some components Like: benzene, hydroxide, mehylene, carbonyl, carboxylic acid, phosphoramides, trimethylamines, diazonium salts, hydroxyl and hydrophobic.

4.3 RESULTS AND DISCUSSION OF MAKAH SAMPLES

Five samples (S_6 – S_{10}) were collected from ground wells in Makah region. The samples were investigated by LIRA 300 Raman spectrometer. The results showed that the samples contain different materials, beside the water, with different amounts.

Figure 4.6 shows the Raman spectrum of a sample taken from a well in the area of Makah Alawaly (S_6) in the range from 1000.2 to 3752.9 cm^{-1}. It shows clear peaks and by comparison with the results recorded in some references, we found that these peaks are belong to the vibrations of water molecules and some other materials as listed in Table 4.6.

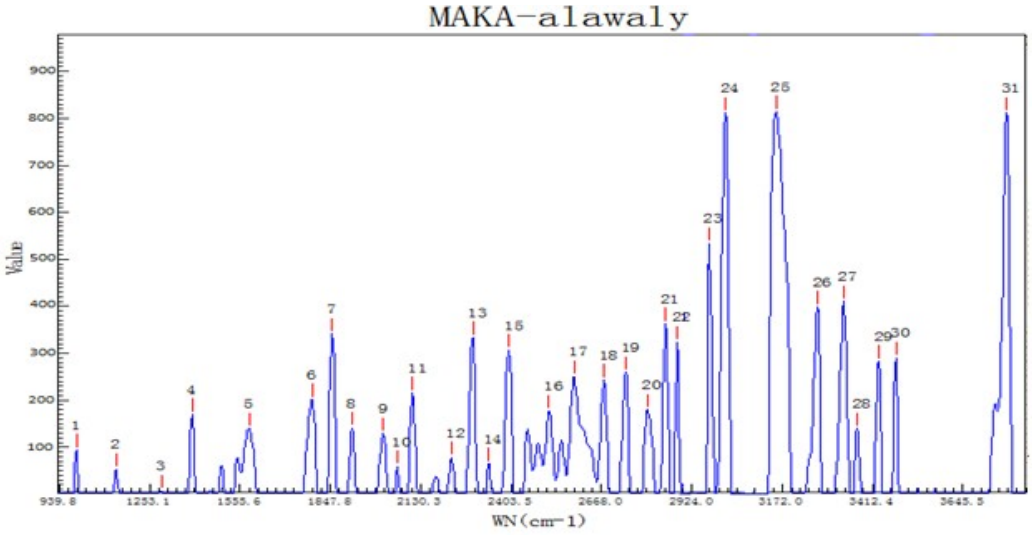

Figure (4.6) Raman spectrum in the range from 1000.2 to 3752.9 cm^{-1} of ground water sample S_6 collected from (Makah Alawaly).

Table (4.6) the wavenumber, intensities, and Functional Group/ Vibration of peaks in the Raman spectra of the ground water sample S_6 collected from Makah Alawaly.

No. of Peak	Wavenumber (cm^{-1})	Functional Group/ Vibration	Intensity (au)	References
1	1000.2	Aromatic ring	94.488	(Lin-Vien, D.; et. al., 1991), (Ewen.S,Geoffrey D.2005), (George Socrates, 2004), (Robert M., Francis X., David J., 2005)
2	1138.5	Si – O – C	53.224	(Ewen.S, Geoffrey D.2005) , (Robert M., Francis X., David J., 2005)
3	1293.1	-	7.192	(Ewen.S, Geoffrey D.2005) , (Robert M., Francis X., David J., 2005)
4	1396.6	Aromatic azo	170.115	(Ewen.S, Geoffrey D.2005) , (Robert M., Francis X., David J., 2005)
5	1585.3	Aliphatic azo	139.604	(Ewen.S, Geoffrey D.2005) , (Robert M., Francis X., David J., 2005)
6	1790.2	Anhydride	201.165	(Ewen.S, Geoffrey D.2005) , (Robert M., Francis X., David J., 2005)
7	1853.6	C = C	341.310	(Lin-Vien, D.; et. al., 1991), (Ewen.S,Geoffrey D.2005), (George

				Socrates, 2004), (Robert M., Francis X., David J., 2005)
8	1916.5	-	141.085	-
9	2015.7	-	129.160	-
10	2057.8	Isothiocyanate	59.173	(Ewen.S, Geoffrey D.2005) , (Robert M., Francis X., David J., 2005)
11	2105.3	Thiocyanate	216.162	(Ewen.S, Geoffrey D.2005) , (Robert M., Francis X., David J., 2005)
12	2224.2	Diazonium salt	77.948	(Ewen.S, Geoffrey D.2005) , (Robert M., Francis X., David J., 2005)
13	2289.9	-	333.592	-
14	2336.1	P – H	65.161	(Ewen.S, Geoffrey D.2005) , (Robert M., Francis X., David J., 2005)
15	2398.2	P – H	306.854	(Ewen.S, Geoffrey D.2005) , (Robert M., Francis X., David J., 2005)
16	2515.7	-	177.053	-
17	2589.5	Th iol	250.413	(Ewen.S, Geoffrey D.2005) , (Robert M., Francis X., David J., 2005)
18	2675.8	-	243.342	-
19	2737.9	Aldehyde	259.544	(Ewen.S, Geoffrey D.2005) , (Robert M., Francis X., David J., 2005)
20	2799.6	N – CH_3	179.957	(Ewen.S, Geoffrey D.2005) , (Robert M., Francis X., David J., 2005)
21	2850.6	O – CH_3	363.468	(Ewen.S, Geoffrey D.2005) , (Robert M., Francis X., David J., 2005)
22	2883.6	C – CH_3	324.213	(Ewen.S, Geoffrey D.2005) , (Robert M., Francis X., David J., 2005)
23	2971.7	CH = CH	533.932	(Ewen.S, Geoffrey D.2005) , (Robert M., Francis X., David J., 2005)
24	3016.7	= CH_2	811.670	(Ewen.S, Geoffrey D.2005) , (Robert M., Francis X., David J., 2005), (Lin-Vien, D.; et. al., 1991)
25	3154.9	Amide , Amine	814.534	(Ewen.S, Geoffrey D.2005) , (Robert M., Francis X., David J., 2005)
26	3266.6	Alkyne	398.559	(Ewen.S, Geoffrey D.2005) , (Robert M., Francis X., David J., 2005)
27	3336.3	Phenol	410.972	(Ewen.S, Geoffrey D.2005) , (Robert M., Francis X., David J., 2005)

28	3372.0	Phenol	139.458	(Ewen.S, Geoffrey D.2005) , (Robert M., Francis X., David J., 2005)
29	3428.9	OH	283.614	(Ewen.S, Geoffrey D.2005) , (Robert M., Francis X., David J., 2005)
30	3473.7	OH	290.446	(Ewen.S, Geoffrey D.2005) , (Robert M., Francis X., David J., 2005)
31	3752.9	-	811.734	-

Figure 4.7 shows the Raman spectrum in the range from 641.6 to 3833.7cm^{-1} of a water sample (S_7) taken from Alzaher well in Makah area. It shows clear peaks describe the vibration of water molecules and some other materials as illustrated in Table 4.7.

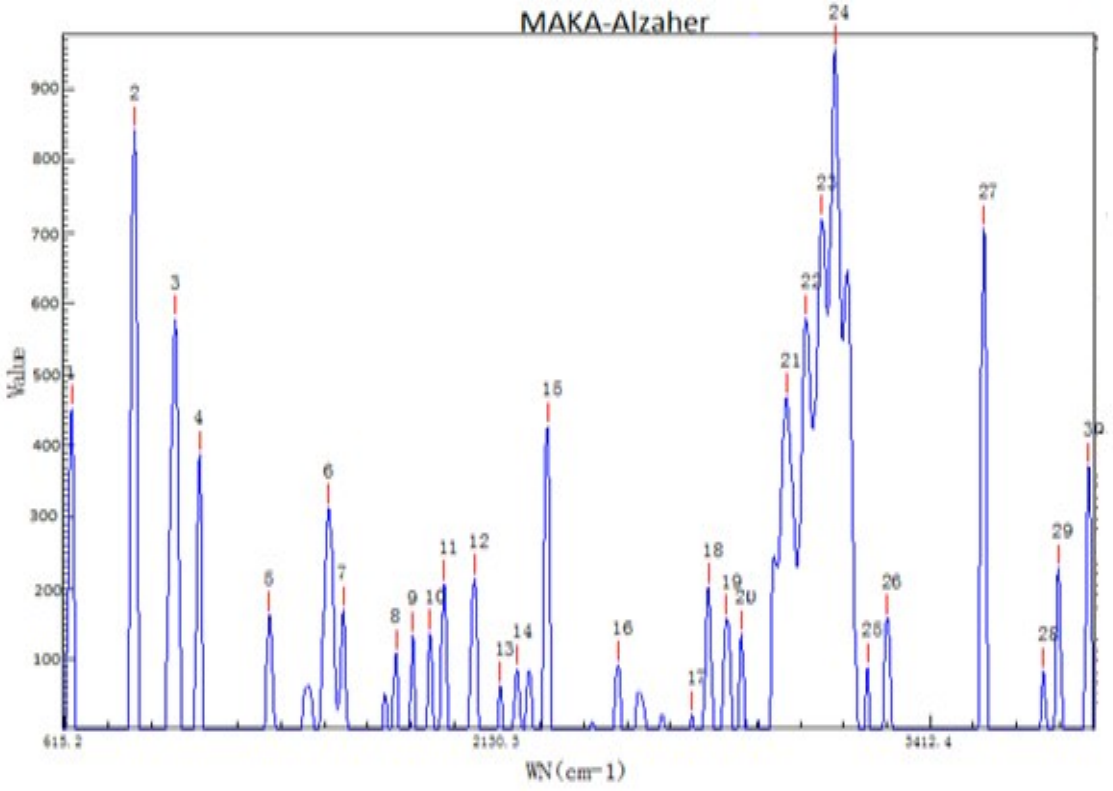

Figure (4.7) Raman spectrum of ground water sample S_7 collected from (Makah Alzaher) in the range from 641.6 to 3833.7cm^{-1}.

Table (4.7) the wavenumber, intensities, and Functional Group/ Vibration of peaks in the Raman spectra of the ground water sample S_7 collected from Makah Alzaher.

No. of Peak	Wavenumber (cm^{-1})	Functional Group/ Vibration	Intensity (au)	References
1	641.6	C = S	451.730	(Ewen.S, Geoffrey D.2005) ,(Robert M., Francis X., David J., 2005)
2	879.1	C – O – C	843.491	(Ewen.S, Geoffrey D.2005) ,(Robert M., Francis X., David J., 2005)
3	1028.7	Si – O – C	577.523	(Ewen.S, Geoffrey D.2005) ,(Robert M., Francis X., David J., 2005)
4	1116.7	Sulfonamide	387.953	(Ewen.S, Geoffrey D.2005) ,(Robert M., Francis X., David J., 2005)
5	1363.2	C – CH_3	161.855	(Ewen.S, Geoffrey D.2005) ,(Robert M., Francis X., David J., 2005)
6	1570.5	Aliphatic azo	312.935	(Ewen.S, Geoffrey D.2005) ,(Robert M., Francis X., David J., 2005)
7	1620.8	Carboxylic acid	169.043	(Ewen.S, Geoffrey D.2005) ,(Robert M., Francis X., David J., 2005)
8	1798.9	Anhydride	108.688	(Ewen.S, Geoffrey D.2005) ,(Robert M., Francis X., David J., 2005)
9	1853.6	C = C	133.835	(Lin-Vien, D.; et. al., 1991), (Ewen.S,Geoffrey D.2005), (George Socrates, 2004), (Robert M., Francis X., David J., 2005)
10	1910.8	--	136.369	--
11	1956.3	--	205.444	--
12	2055.0	Isothiocyanate	214.096	(Ewen.S, Geoffrey D.2005) ,(Robert M., Francis X., David J., 2005)
13	2138.7	Azide	63.198	(Ewen.S, Geoffrey D.2005) ,(Robert M., Francis X., David J., 2005)
14	2194.0	Alkyne	86.888	(Ewen.S, Geoffrey D.2005) ,(Robert M., Francis X., David J., 2005)
15	2289.9	P – H	426.701	(Ewen.S, Geoffrey D.2005) ,(Robert M., Francis X., David J., 2005)
16	2507.7	--	92.645	--
17	2732.7	Aldehyde	22.301	(Ewen.S, Geoffrey D.2005) ,(Robert M., Francis X., David J., 2005)
18	2781.6	N – CH_3	201.353	(Ewen.S, Geoffrey D.2005) ,(Robert M., Francis X., David J., 2005)
19	2835.3	O – CH_3	157.203	(Ewen.S, Geoffrey D.2005) ,(Robert M., Francis X., David J., 2005)
20	2878.5	C – CH_3	135.507	(Ewen.S, Geoffrey D.2005) ,(Robert M., Francis X., David J., 2005)
21	3009.3	CH – CH	467.880	(Ewen.S, Geoffrey D.2005) ,(Robert M., Francis X., David J., 2005)

22	3066.3	= CH_2	578.987	(Lin-Vien, D.; et. al., 1991), (Ewen.S, Geoffrey D.2005), (Robert M., Francis X., David J., 2005)
23	3110.7	OH	718.285	(Ewen.S, Geoffrey D.2005) ,(Robert M., Francis X., David J., 2005)
24	3147.5	OH	957.495	(Ewen.S, Geoffrey D.2005) ,(Robert M., Francis X., David J., 2005)
25	3240.1	Alcohol	89.004	(Ewen.S, Geoffrey D.2005) ,(Robert M., Francis X., David J., 2005)
26	3293.1	Alkyne	157.494	(Ewen.S, Geoffrey D.2005) ,(Robert M., Francis X., David J., 2005)
27	3557.7	O – H	704.422	(Ewen.S, Geoffrey D.2005) ,(Robert M., Francis X., David J., 2005)
28	3716.3	--	83.082	--
29	3754.9	--	228.451	--
30	3833.7	--	370.605	--

In the sample S_8 taken from Makah /Alhasanya (figure 4.8) there was a clear picture of the water components and some other materials. Table 4.8 illustrates the analysis of this spectrum.

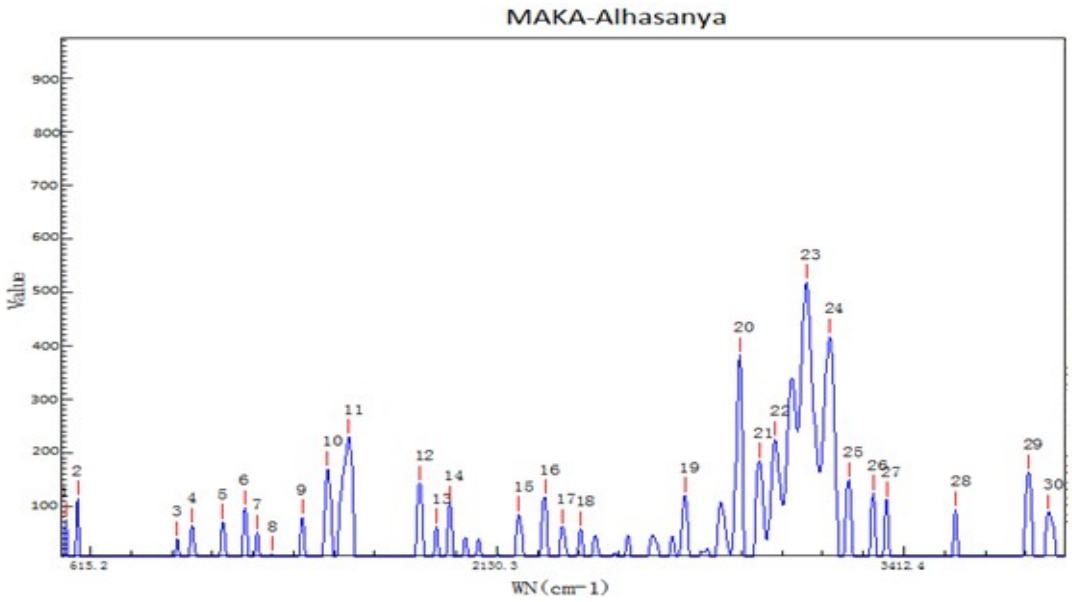

Figure (4.8) Raman spectrum of ground water sample S_8 collected from (Makah Alhasanya) in the range from 515.5 to 3822.4 cm^{-1}.

Table (4.8) the wavenumber, intensities, and Functional Group/ Vibration of peaks in the Raman spectrum of the ground water sample S_8 collected from Makah Alhasanya.

No.	Wavenumber	Functional		

of Peak	(cm^{-1})	Group/ Vibration	Intensity (au)	References
1	515.5	Si – O – Si	74.277	(Ewen.S, Geoffrey D.2005) , (Robert M., Francis X., David J., 2005)
2	565.5	C – CL	114.947	(Lin-Vien, D.; et. al., 1991), (Ewen.S,Geoffrey D.2005), (George Socrates, 2004), (Robert M., Francis X., David J., 2005)
3	962.1	Carboxylic acid dimer	38.604	(Ewen.S, Geoffrey D.2005) , (Robert M., Francis X., David J., 2005)
4	1022.4	Si – O – C	63.397	(Ewen.S, Geoffrey D.2005) , (Robert M., Francis X., David J., 2005)
5	1138.5	Si – O – Si	70.939	(Ewen.S, Geoffrey D.2005) , (Robert M., Francis X., David J., 2005)
6	1222.3	Sulfonic acid	96.783	(Ewen.S, Geoffrey D.2005) , (Robert M., Francis X., David J., 2005)
7	1271.6	-	51.426	-
8	1326.7	Nitro	10.827	(Ewen.S, Geoffrey D.2005) , (Robert M., Francis X., David J., 2005)
9	1438.9	CH_2 , CH_3	79.541	(Lin-Vien, D.; et. al., 1991), (Ewen.S, Geoffrey D.2005), (Robert M., Francis X., David J., 2005)
10	1531.8	C – (NO_2) asym	169.239	(Ewen.S, Geoffrey D.2005) , (Robert M., Francis X., David J., 2005)
11	1609.0	Aromatic/hetro ring	229.342	(Lin-Vien, D.; et. al., 1991), (Ewen.S,Geoffrey D.2005), (George Socrates, 2004), (Robert M., Francis X., David J., 2005)
12	1862.2	C = C	142.704	(Lin-Vien, D.; et. al., 1991), (Ewen.S,Geoffrey D.2005), (George Socrates, 2004), (Robert M., Francis X., David J., 2005)
13	1922.2	-	62.244	-
14	1967.6	-	105.059	-
15	2205.0	Diazonium salt	85.300	(Ewen.S, Geoffrey D.2005) , (Robert M., Francis X., David J., 2005)
16	2292.6	P – H	116.967	(Ewen.S, Geoffrey D.2005) , (Robert M., Francis X., David J., 2005)
17	2349.6	P – H	62.122	(Ewen.S, Geoffrey D.2005) , (Robert M., Francis X., David J.,

				2005)
18	2411.6	P – H	57.397	(Ewen.S, Geoffrey D.2005) , (Robert M., Francis X., David J., 2005)
19	2748.2	-	120.946	-
20	2918.9	CH_2	382.445	(Lin-Vien, D.; et. al., 1991), (Ewen.S, Geoffrey D.2005), (Robert M., Francis X., David J., 2005)
21	2979.2	Aromatic C - H	185.407	(Ewen.S, Geoffrey D.2005) , (Robert M., Francis X., David J., 2005)
22	3029.1	= CH_2	225.546	(Lin-Vien, D.; et. al., 1991), (Ewen.S, Geoffrey D.2005), (Robert M., Francis X., David J., 2005)
23	3123.0	OH	518.740	(Ewen.S, Geoffrey D.2005) , (Robert M., Francis X., David J., 2005)
24	3193.9	Amide , Amine	417.027	(Ewen.S, Geoffrey D.2005) , (Robert M., Francis X., David J., 2005)
25	3249.7	Alcohol	148.790	(Ewen.S, Geoffrey D.2005) , (Robert M., Francis X., David J., 2005)
26	3321.9	Alcohol	124.918	(Ewen.S, Geoffrey D.2005) , (Robert M., Francis X., David J., 2005)
27	3362.5	Phenol	112.563	(Ewen.S, Geoffrey D.2005) , (Robert M., Francis X., David J., 2005)
28	3562.4	O – H	94.263	(Ewen.S, Geoffrey D.2005) , (Robert M., Francis X., David J., 2005)
29	3766.2	-	163.537	-
30	3822.4	-	89.051	-

Figure (4.9) shows the Raman spectrum of the sample S_9 collected from Alhasanya 2 area in Makah. The vibrations of water molecules are appeared in the spectrum beside some other vibrations. These vibrations were consistent with many previous studies as listed in Table 4.9.

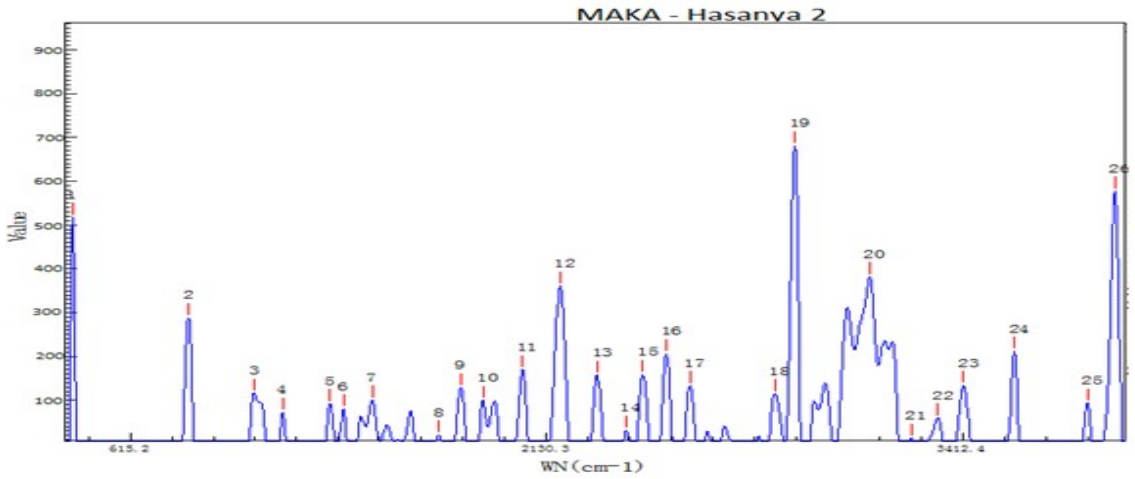

Figure (4.9) Raman spectrum in the range from 384.2 to 3833.7cm^{-1} of ground water sample S_9 collected from (Makah Alhasanya 2).

Table (4.9) the wavenumber, intensities, and Functional Group/ Vibration of peaks in the Raman spectrum of the ground water sample S_9 collected from Makah Alhasanya 2.

No. of Peak	Wavenumber (cm^{-1})	Functional Group/ Vibration	Intensity (au)	References
1	384.2	C – C aliphatic chain	617.633	(Lin-Vien, D.; et. al., 1991), (Ewen.S, Geoffrey D.2005), (Robert M., Francis X., David J., 2005)
2	843.7	C – O – C	288.411	(Ewen.S, Geoffrey D.2005) , (Robert M., Francis X., David J., 2005)
3	1094.7	Si – O – C	116.817	(Ewen.S, Geoffrey D.2005) , (Robert M., Francis X., David J., 2005)
4	1200.7	Sulfonamide	72.624	(Ewen.S, Geoffrey D.2005) , (Robert M., Francis X., David J., 2005)
5	1375.4	C – CH_3	92.652	(Ewen.S, Geoffrey D.2005) , (Robert M., Francis X., David J., 2005)
6	1423.8	CH_2 , CH_3	80.570	(Lin-Vien, D.; et. al., 1991), (Ewen.S, Geoffrey D.2005), (Robert M., Francis X., David J., 2005)
7	1528.8	C – (NO_2) asym	100.518	(Ewen.S, Geoffrey D.2005) , (Robert M., Francis X., David J.,

				2005)
8	1764.1	Acid chloride	20.938	(Ewen.S, Geoffrey D.2005) , (Robert M., Francis X., David J., 2005)
9	1839.2	C = C	128.557	(Lin-Vien, D.; et. al., 1991), (Ewen.S,Geoffrey D.2005), (George Socrates, 2004), (Robert M., Francis X., David J., 2005)
10	1916.5	-	99.756	-
11	2049.4	Isothiocyanate	169.538	(Ewen.S, Geoffrey D.2005) , (Robert M., Francis X., David J., 2005)
12	2174.7	Alkyne	361.129	(Ewen.S, Geoffrey D.2005) , (Robert M., Francis X., David J., 2005)
13	2298.1	P – H	157.455	(Ewen.S, Geoffrey D.2005) , (Robert M., Francis X., David J., 2005)
14	2390.1	P – H	31.592	(Ewen.S, Geoffrey D.2005) , (Robert M., Francis X., David J., 2005)
15	2446.4	-	158.829	-
16	2521.0	-	206.494	-
17	2594.8	Th iol	133.463	(Ewen.S, Geoffrey D.2005) , (Robert M., Francis X., David J., 2005)
18	2858.2	C – CH_3	115.276	(Ewen.S, Geoffrey D.2005) , (Robert M., Francis X., David J., 2005)
19	2918.9	CH_2	681.011	(Lin-Vien, D.; et. al., 1991), (Ewen.S, Geoffrey D.2005), (Robert M., Francis X., David J., 2005)
20	3142.6	OH	382.120	(Ewen.S, Geoffrey D.2005) , (Robert M., Francis X., David J., 2005)
21	3264.2	Alkyne	13.989	(Ewen.S, Geoffrey D.2005) , (Robert M., Francis X., David J., 2005)
22	3341.0	Phenol	59.843	(Ewen.S, Geoffrey D.2005) , (Robert M., Francis X., David J., 2005)
23	3414.7	OH	133.958	(Ewen.S, Geoffrey D.2005) , (Robert M., Francis X., David J., 2005)
24	3557.7	O – H	212.115	(Ewen.S, Geoffrey D.2005) , (Robert M., Francis X., David J., 2005)
25	3759.4	-	94.106	-
26	3833.7	-	577.463	-

Figure (4.10) illustrates Raman spectrum of the groundwater sample S_{10} collected from (Makah Kakya) in the range from 407.9 to 3831.4 cm^{-1}. Table (4.10) lists the analysis of this spectrum.

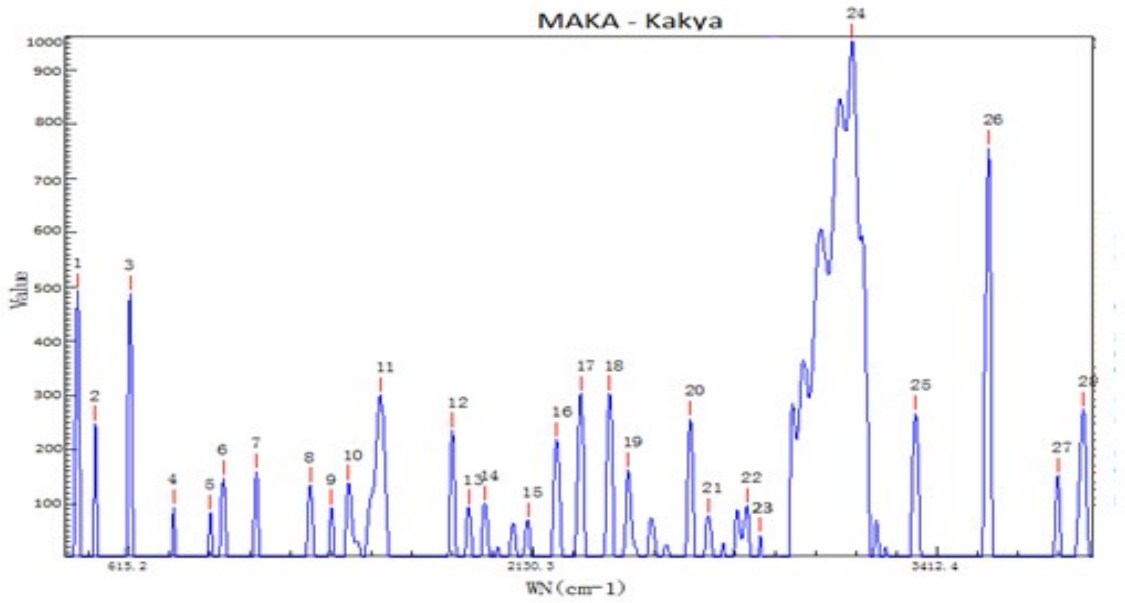

Figure (4.10) Raman spectrum of ground water sample S_{10} collected from (Makah Kakya) in the range from 407.9 to 3831.4 cm^{-1}.

Table (4.10) the wavenumber, intensities, and Functional Group/ Vibration of peaks in the Raman spectra of Makah Kakya sample (S_{10}).

No. of Peak	Wavenumber (cm^{-1})	Functional Group/ Vibration	Intensity (au)	References
1	407.9	X metal – O	492.385	(Ewen.S, Geoffrey D.2005) , (Robert M., Francis X., David J., 2005)
2	478.6	Si – O – Si	247.740	(Ewen.S, Geoffrey D.2005) , (Robert M., Francis X., David J., 2005)
3	621.8	C = S	487.665	(Ewen.S, Geoffrey D.2005) , (Robert M., Francis X., David J., 2005)
4	798.4	C – F	93.625	(Ewen.S, Geoffrey D.2005) , (Robert M., Francis X., David J., 2005)
5	943.0	Carboxylic acid dimer	83.419	(Ewen.S, Geoffrey D.2005) , (Robert M., Francis X., David J.,

				2005)
6	993.9	Aromatic ring	147.272	(Lin-Vien, D.; et. al., 1991), (Ewen.S, Geoffrey D.2005), (George Socrates, 2004), (Robert M., Francis X., David J., 2005)
7	1126.0	Si – O – C	159.837	(Ewen.S, Geoffrey D.2005) , (Robert M., Francis X., David J., 2005)
8	1329.7	Nitro	134.129	(Ewen.S, Geoffrey D.2005) , (Robert M., Francis X., David J., 2005)
9	1408.7	CH_2 , CH_3	93.180	(Lin-Vien, D.; et. al., 1991), (Ewen.S, Geoffrey D.2005), (Robert M., Francis X., David J., 2005)
10	1472.0	Aromatic ring	138.451	(Lin-Vien, D.; et. al., 1991), (Ewen.S, Geoffrey D.2005), (George Socrates, 2004), (Robert M., Francis X., David J., 2005)
11	1591.2	Aromatic/heter o ring	300.174	(Lin-Vien, D.; et. al., 1991), (Ewen.S, Geoffrey D.2005), (George Socrates, 2004), (Robert M., Francis X., David J., 2005)
12	1850.7	C = C	235.502	(Lin-Vien, D.; et. al., 1991), (Ewen.S, Geoffrey D.2005), (George Socrates, 2004), (Robert M., Francis X., David J., 2005)
13	1908.0	-	92.974	-
14	1964.8	-	100.317	-
15	2113.6	Si – H	69.394	(Ewen.S, Geoffrey D.2005) , (Robert M., Francis X., David J., 2005)
16	2213.2	Aromatic nitrile	218.074	(Ewen.S, Geoffrey D.2005) , (Robert M., Francis X., David J., 2005)
17	2295.3	P – H	302.805	(Ewen.S, Geoffrey D.2005) , (Robert M., Francis X., David J., 2005)
18	2390.1	P – H	303.699	(Ewen.S, Geoffrey D.2005) , (Robert M., Francis X., David J., 2005)
19	2451.8	-	162.745	-
20	2654.9	-	256.663	-
21	2712.1	Aldehyde	77.935	(Ewen.S, Geoffrey D.2005) , (Robert M., Francis X., David J., 2005)
22	2835.3	O – CH_3	95.975	(Ewen.S, Geoffrey D.2005) , (Robert M., Francis X., David J., 2005)
23	2878.5	C – CH_3	42.230	(Ewen.S, Geoffrey D.2005) , (Robert M., Francis X., David J., 2005)

24	3159.8	OH	952.969	(Ewen.S, Geoffrey D.2005) , (Robert M., Francis X., David J., 2005)
25	3350.6	Amide , Amine	267.175	(Ewen.S, Geoffrey D.2005) , (Robert M., Francis X., David J., 2005)
26	3562.4	O – H	756.067	(Ewen.S, Geoffrey D.2005) , (Robert M., Francis X., David J., 2005)
27	3759.4	-	152.061	-
28	3831.4	-	274.081	-

Through the analysis of the five samples collected from Makah area it was found that the vibration modes of some materials are appeared in all the samples while other modes are appeared in some samples and disappeared in other samples. That is as follows:

1. Aromatic ring: appeared in the spectra of (Alawaly, Kakya) wells, with intensities (94.488, 147.272) (au), respectively.

2. Si – O – C: appeared in the spectra of (Alawaly, Alzaher, Alhasanya, Alhasanya2, Kakya) wells, with different intensities (53.224, 577.523, 63.397, 116.817, 159.837) (au), respectively.

3. Aromatic azo: appeared in the spectra of (Alawaly) well, with intensity of (170.115) (au).

4. Aliphatic azo: appeared in the spectra of (Alawaly, Alzaher) wells, with different intensities (139.604, 312.935) (au), respectively.

5. Anhydride: appeared in the spectra of the (Alawaly, Alzaher) wells, with intensities (201.165, 108.688) (au), respectively.

6. C=C: appeared in the spectra of (Alawaly, Alzaher, Alhasanya, Alhasanya2, Kakya) wells, with different intensities (341.310, 133.835, 142.704, 128.557, 235.502) (au), respectively.

7. Isothiocyanate: appeared in the spectra of (Alawaly, Alzaher, Alhasanya2) wells, with intensities (59.173, 214.096, 169.538) (au), respectively.

8. Thiocyanate: appeared in the spectra of (Alawaly) well, with intensity of (216.162) (au).

9. Diazonium salt: appeared in the spectra of (Alawaly, Alhasanya) wells, with different intensities (77.948, 85.3) (au), respectively.

10. P – H: appeared in the spectra of (Alawaly, Alzaher, Alhasanya, Alhasanya2, Kakya) wells, with different intensities (306.854, 426.701, 116.967, 157.455, 303.699) (au), respectively.

11. Th iol: appeared in the spectra of (Alawaly, Alhasanya2) wells, with different intensities (250.413, 133.463) (au), respectively.

12. Aldehyed: appeared in the spectra of (Alawaly, Alzaher, Kakya) wells, with different intensities (259.544, 22.301, 77.935) (au), respectively.

13. N-CH_3: appeared in the spectra of (Alawaly, Alzaher) wells, with different intensities (179.957, 201.353) (au), respectively.

14. O-CH_3: appeared in the spectra of (Alawaly, Alzaher, Kakya) wells, with different intensities (363.468, 157.203, 95.975) (au), respectively.

15. C-CH_3: appeared in the spectra of (Alawaly, Alzaher, Alhasanya2, Kakya) wells, with different intensities (324.213, 161.855, 115.276, 42.230) (au), respectively.

16. CH = CH: appeared in the spectra of (Alawaly, Alzaher) wells, with different intensities (533.932, 467.880) (au), respectively.

17. = CH_2: appeared in the spectra of (Alawaly, Alzaher, Alhasanya) wells, with different intensities (811.670, 578.987, 225.546) (au), respectively.

18. Amide, Amine: appeared in the spectra of (Alawaly, Alhasanya, Kakya) wells, with different intensities (814.534, 417.027, 267.175) (au), respectively.

19. Alkyne: appeared in the spectra of (Alawaly, Alzaher, Alhasanya2) wells, with different intensities (398.559, 157.494, 361.129) (au), respectively.

20. Phenol: appeared in the spectra of (Alawaly, Alhasanya, Alhasanya2) wells, with different intensities (410.972, 112.563, 59.843) (au), respectively.

21. OH: appeared in the spectra of (Alawaly, Alzaher, Alhasanya, Alhasanya2, Kakya) wells, with different intensities (290.446, 957.495, 518.740, 382.120, 952.968) (au), respectively.

22. C=S: appeared in the spectra of (Alzaher, Kakya) wells, with different intensities (451.730, 487.665) (au), respectively.

23. C-O-C: appeared in the spectra of (Alzaher, Alhasanya2) wells, with different intensities (843.491, 288.411) (au), respectively.

24. Sulfonamide: appeared in the spectra of (Alzaher, Alhasanya2) wells, with different intensities (387.953, 72.624) (au), respectively.

25. Aliphatic azo: appeared in the spectra of (Alzaher) well, with intensity of (312.935) (au).

26. Carboxylic acid: appeared in the spectra of (Alzaher) well, with intensity of 169.043 (au).

27. Anhydride: appeared in the spectra of (Alzaher) well, with intensity of 108.688 (au).

28. Azide: appeared in the spectra of (Alzaher) well, with intensity of 63.198 (au).

29. Alcohol: appeared in the spectra of (Alzaher, Alhasanya) wells, with different intensities (89.004, 148.790) (au), respectively.

30. O-H: appeared in the spectra of (Alzaher, Alhasanya, Alhasanya2, Kakya) wells, with different intensities (704.422, 94.263, 212.115, 756.067) (au), respectively.

31. Si-O-Si: appeared in the spectra of (Alhasanya, Kakya) wells, with different intensities (74.277, 247.740) (au), respectively.

32. C-CL: appeared in the spectra of (Alhasanya) well, with intensity of 114.947 (au).

33. Carboxylic acid dimer: appeared in the spectra of (Alhasanya, Kakya) wells, with different intensities (38.604, 83.419) (au), respectively.

34. Sulfonic acid: appeared in the spectra of (Alhasanya) well, with intensity of 96.783 (au).

35. Nitro: appeared in the spectra of (Alhasanya, Kakya) wells, with different intensities (10.827, 134.129) (au), respectively.

36. CH_2, CH_3: appeared in the spectra of (Alhasanya, Alhasanya2, Kakya) wells, with different intensities (79.541, 80.570, 93.180) (au), respectively.

37. C-(NO_2) asym: appeared in the spectra of (Alhasanya, Alhasanya2) wells, with different intensities (169.239, 100.518) (au), respectively.

38. Aromatic/hetro ring: appeared in the spectra of (Alhasanya, Kakya) wells, with different intensities (229.342, 300.174) (au), respectively.

39. CH_2: appeared in the spectra of (Alhasanya, Alhasanya2) wells, with different intensities (382.445, 681.011) (au), respectively.

40. Aromatic C-H: appeared in the spectra of (Alhasanya) well, with intensity of 185.407 (au).

41. C-C aliphatic chain: appeared in the spectra of (Alhasanya2) well, with intensity of 617.633 (au).

42. Acid chloride: appeared in the spectra of (Alhasanya2) well, with intensity of 20.938 (au).

43. C-F: appeared in the spectra of (Kakya) well, with intensity of 93.625 (au).

44. Si-H: appeared in the spectra of (Kakya) well, with intensity of 69.394 (au).

45. Aromatic nitrile: appeared in the spectra of (Kakya) well, with intensity of 218.074 (au).

46. X metal - O: appeared in the spectra of (Kakya) well, with intensity of 492.385 (au).

Some vibrations modes in samples (S_6 – S_{10}), collected from Makah wells, indicate the presence of some components Like: diazonium salts, benzene, hydroxide, mehylene, carbonyl, carboxylic acid, phosphoramides, trimethylamines, hydroxyl and hydrophobic.

4.4 RESULTS AND DISCUSSION OF MADINA SAMPLES

Four samples (S_{11} – S_{14}) were collected from ground wells in Madina region. The samples were investigated by LIRA 300 Raman spectrometer. The results showed that the samples contain different materials, beside the water, with different amounts.

Figure 4.11 shows the Raman spectrum of a sample taken from a well in the area of Madina Alarak (S_{11}) in the range from 1003.4 to 3782.0 cm^{-1}. It shows clear peaks and by comparison with the results recorded in some references, we found that these peaks are belong to the vibrations of water molecules and some other materials as listed in Table 4.11.

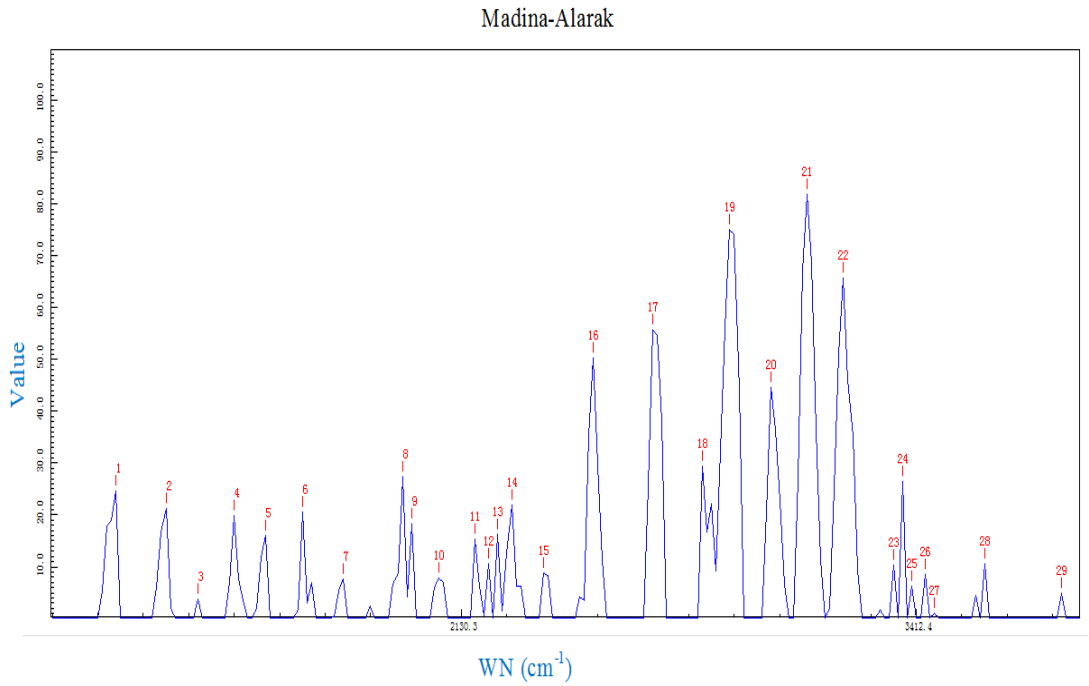

Figure (4.11) Raman spectrum of ground well water sample S_{11} collected from (Madina Alarak) in the range from 1003.4 to 3782.0 cm^{-1}.

Table (4.11) the wave number, intensities, and Functional Group/ Vibration of peaks in the Raman spectra of the ground water sample S_{11} collected from Madina Alarak.

References	Intensity (au)	Functional Group/ Vibration	Wavenumber (cm^{-1})	No. of Peak
) ,(Lin-Vien, D.; et. al., 1991) George) ,(Ewen.S, Geoffrey D.2005 Robert M.,) ,(Socrates, 2004 (Francis X., David J., 2005	24.615	Aromatic rings	1003.4	1
), (Ewen.S, Geoffrey D.2005) Robert M., Francis X., David J., (2005	21.195	Sulfonamide	1175.8	2
-	3.690	-	1283.9	3
) ,(Lin-Vien, D.; et. al., 1991)) ,(Ewen.S, Geoffrey D.2005 Robert M., Francis X., David J., (2005	19.800	CH_2, CH_3	1405.7	4
-	16.065	-	1510.9	5
) ,(Lin-Vien, D.; et. al., 1991) George) ,(Ewen.S,Geoffrey D.2005 Robert M.,) ,(Socrates, 2004 (Francis X., David J., 2005	20.520	C = C	1629.6	6

) ,(Ewen.S, Geoffrey D.2005) Robert M., Francis X., David J., (2005	7.695	Lactone	1761.2	7
-	27.405	-	1947.8	8
-	18.315	-	1976.1	9
), (Ewen.S, Geoffrey D.2005) Robert M., Francis X., David J., (2005	7.920	Isothiocyanate	2060.6	10
), (Ewen.S, Geoffrey D.2005) Robert M., Francis X., David J., (2005	15.300	Alkyne	2171.9	11
), (Ewen.S, Geoffrey D.2005) Robert M., Francis X., David J., (2005	10.575	Aromatic Nitrile	2213.2	12
), (Ewen.S, Geoffrey D.2005) Robert M., Francis X., David J., (2005	16.290	Nitrile	2240.7	13
-	21.825	-	2281.7	14
), (Ewen.S, Geoffrey D.2005) Robert M., Francis X., David J., (2005	8.820	P – H	2376.6	15
-	50.220	-	2523.6	16
), (Ewen.S, Geoffrey D.2005) Robert M., Francis X., David J., (2005	55.755	Aldehyde	2693.9	17
), (Ewen.S, Geoffrey D.2005) Robert M., Francis X., David J., (2005	29.385	$O – CH_3$	2835.3	18
Ewen.S, Geoffrey D.2005) , (Robert M., Francis X., David J., 2005)	74.970	$C – CH_3$	2911.4	19
), (Ewen.S, Geoffrey D.2005) Robert M., Francis X., David J., (Lin-Vien, D.; et. al., 1991) ,(2005	44.595	$CH_2 =$	3024.1	20
), (Ewen.S, Geoffrey D.2005) Robert M., Francis X., David J., (2005	81.855	OH	3123.0	21
), (Ewen.S, Geoffrey D.2005) Robert M., Francis X., David J., (2005	65.700	Alcohol	3220.7	22
-	10.350	-	3353.0	23
Ewen.S, Geoffrey D.2005) , (Robert M., Francis X., David J., 2005)	26.415	Phenol	3376.8	24
Ewen.S, Geoffrey D.2005) , (Robert M., Francis X., David J., 2005)	6.345	Amide, Amine	3400.5	25
), (Ewen.S, Geoffrey D.2005) Robert M., Francis X., David J., (2005	8.640	OH	3436.0	26
), (Ewen.S, Geoffrey D.2005) Robert M., Francis X., David J.,	1.125	OH	3459.6	27

(2005				
-	10.620	-	3587.9	28
-	4.815	-	3782.0	29

Figure 4.12 shows the Raman spectrum in the range from 1585.3 to 3849.3 cm^{-1} of a water sample (S_{12}) taken from a well Aldeara in Madina area which shows clear peaks describe the vibration of water molecules and some components to other materials as illustrated in Table 4.12.

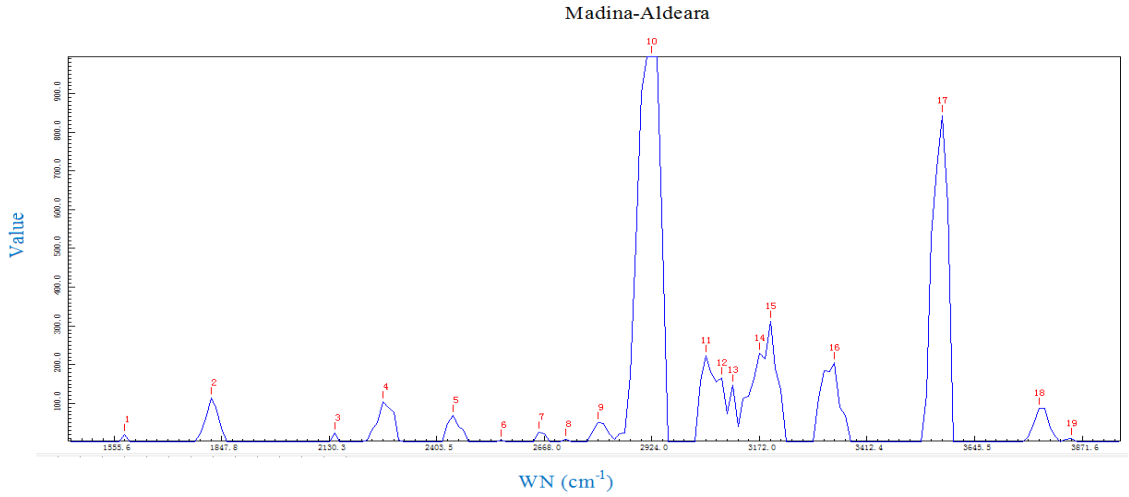

Figure (4.12) Raman spectrum of ground water sample S_{12} collected from (Madina Aldeara) in the range from 1585.3 to 3849.3cm^{-1}.

Table (4.12) the wave number, intensities, and Functional Group/ Vibration of peaks in the Raman spectra of the ground water sample S_{12} collected from Madina Aldeara.

References	Intensity (au)	Functional Group/ Vibration	Wavenumber (cm^{-1})	No. of Peak
Robert), (Ewen.S, Geoffrey D.2005) (M., Francis X., David J., 2005	19.980	Aliphatic azo	1585.3	1
Robert), (Ewen.S, Geoffrey D.2005) (M., Francis X., David J., 2005	113.265	Anhydride	1819.1	2
	24.075	Azide	2144.2	3
Ewen.S, Geoffrey D.2005) ,(Robert M., Francis X., David J., 2005)	104.130	Diazonium salt	2268.1	4
-	68.715	-	2443.8	5
Robert), (Ewen.S, Geoffrey D.2005)	4.860	Th iol	2563.2	6

(M., Francis X., David J., 2005				
-	26.550	-	2654.9	7
Robert), (Ewen.S, Geoffrey D.2005) (M., Francis X., David J., 2005	7.155	Aldehyde	2719.8	8
Ewen.S, Geoffrey D.2005) ,(Robert M., Francis X., David J., 2005)	50.220	N – CH_3	2797.0	9
Robert), (Ewen.S, Geoffrey D.2005) (M., Francis X., David J., 2005	1232.730	C – CH_3	2924.0	10
Ewen.S, Geoffrey D.2005) ,(Robert M., Francis X., David J., 2005), (Lin-Vien, D.; et. al., 1991)	222.930	CH_2 =	3049.0	11
Robert), (Ewen.S, Geoffrey D.2005) (M., Francis X., David J., 2005	164.880	Aromatic C – H	3086.1	12
Robert), (Ewen.S, Geoffrey D.2005) (M., Francis X., David J., 2005	148.140	OH	3110.7	13
Ewen.S, Geoffrey D.2005) ,(Robert M., Francis X., David J., 2005)	229.320	Amide, Amine	3172.0	14
Ewen.S, Geoffrey D.2005) ,(Robert M., Francis X., David J., 2005)	311.850	Amide, Amine	3196.4	15
Ewen.S, Geoffrey D.2005) ,(Robert M., Francis X., David J., 2005)	204.255	Phenol	3341.0	16
-	842.985	-	3576.3	17
-	86.850	-	3782.0	18
-	9.675	-	3849.3	19

In the sample (S_{13}) taken from Madina /Almaboath (figure 4.13) there was a clear picture of the water components and some other materials. Table 4.13 illustrates the analysis of this spectrum.

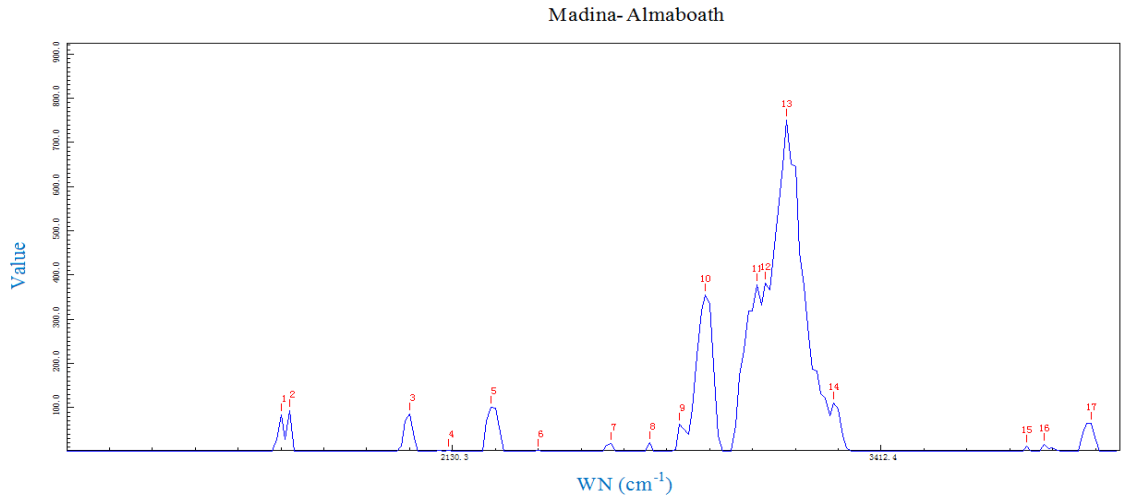

Figure (4.13) Raman spectrum of ground water sample S_{13} collected from (Madina Almaboath) in the range from 1555.6 to 3971.2cm^{-1}.

Table (4.13) the wave number, intensities, and Functional Group/ Vibration of peaks in the Raman spectrum of the ground water sample S_{13} collected from Madina Almaboath.

References	Intensity (au)	Functional Group/ Vibration	Wavenumber (cm^{-1})	No. of Peak
Ewen.S, Geoffrey D.2005) ,(Robert M., Francis X., David J., 2005)	83.160	Aliphatic azo	1555.6	1
) ,(Lin-Vien, D.; et. al., 1991) George) ,(Ewen.S,Geoffrey D.2005 Robert M., Francis) ,(Socrates, 2004 (X., David J., 2005	93.240	Aromatic / Hetro ring	1585.3	2
-	84.870	-	1990.3	3
Robert), (Ewen.S, Geoffrey D.2005) (M., Francis X., David J., 2005	3.870	Si – H	2116.4	4
Robert), (Ewen.S, Geoffrey D.2005) (M., Francis X., David J., 2005	101.295	Diazonium salt	2254.4	5
Robert), (Ewen.S, Geoffrey D.2005) (M., Francis X., David J., 2005	3.240	P – H	2403.5	6
-	18.225	-	2628.8	7
-	19.305	-	2745.6	8
Robert), (Ewen.S, Geoffrey D.2005) (M., Francis X., David J., 2005	61.515	O – CH_3	2835.3	9
Ewen.S,) ,(Lin-Vien, D.; et. al., 1991) Robert M.,) ,(Geoffrey D.2005 (Francis X., David J., 2005	355.680	CH_2	2911.4	10
Ewen.S, Geoffrey D.2005) ,(Robert M., Francis X., David J., 2005), (Lin-Vien, D.; et. al., 1991)	377.685	CH_2 =	3061.4	11
Robert), (Ewen.S, Geoffrey D.2005) (M., Francis X., David J., 2005	382.185	OH	3086.1	12
Robert), (Ewen.S, Geoffrey D.2005) (M., Francis X., David J., 2005	750.690	OH	3147.5	13
Ewen.S, Geoffrey D.2005) ,(Robert M., Francis X., David J., 2005)	109.530	Alkyne	3281.1	14
-	11.880	-	3804.5	15
-	16.110	-	3849.3	16
-	64.215	-	3971.2	17

Figure (4.14) shows the Raman spectrum of the sample S_{14} collected from a well in the Alabar area in Madina. The vibrations of water molecules are appeared in the spectrum beside some other vibrations. These vibrations were consistent with many previous studies as listed in Table 4.14.

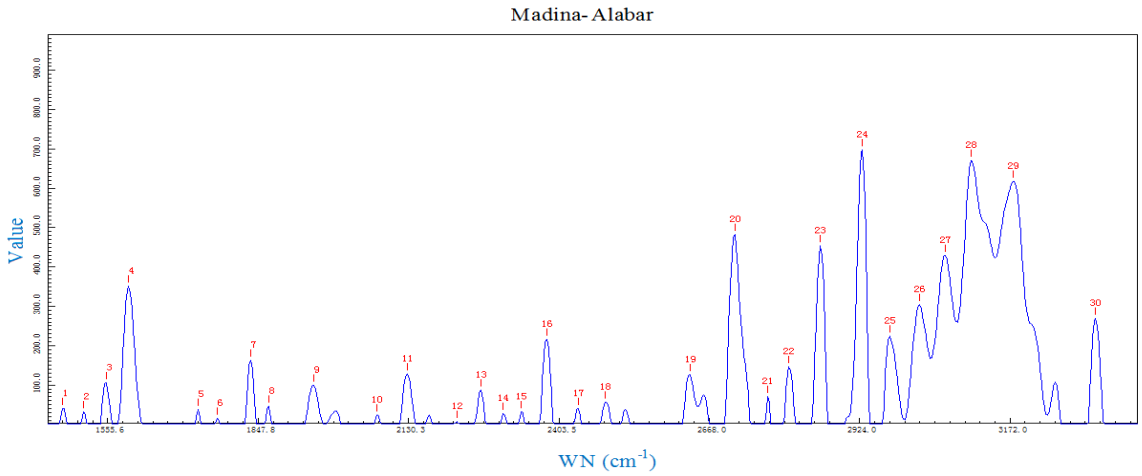

Figure (4.14) Raman spectrum in the range from 1466.0 to 3309.9cm^{-1} of ground water sample S_{14} collected from (Madina Alabar).

Table (4.14) the wavenumber, intensities, and Functional Group/ Vibration of peaks in the Raman spectrum of the ground water sample S_{14} collected from Madina Alabar.

References	Intensity (au)	Functional Group/ Vibration	Wavenumber (cm^{-1})	No. of Peak
(Lin-Vien, D.; et. al., 1991), (Ewen.S, Geoffrey D.2005), (George Socrates, 2004), (Robert M., Francis X., David J., 2005)	40.722	Aromatic ring	1466.0	1
-	31.190	-	1507.9	2
), (Ewen.S, Geoffrey D.2005) Robert M., Francis X., David J., (2005	105.957	Aliphatic azo	1552.6	3
), (Ewen.S, Geoffrey D.2005) Robert M., Francis X., David J., (2005	350.549	Nitro	1597.1	4
) ,(Ewen.S, Geoffrey D.2005) Robert M., Francis X., David J., (2005	37.352	Aliphatic ester	1732.1	5
) ,(Ewen.S, Geoffrey D.2005) Robert M., Francis X., David J., ((2005	15.852	Lactone	1769.9	6
-	162.959	-	1833.5	7
-	46.346	-	1867.9	8
-	98.864	-	1953.5	9
), (Ewen.S, Geoffrey D.2005)	23.499	Isothiocyanat	2071.8	10

Robert M., Francis X., David J., (2005		e		
) ,(Ewen.S, Geoffrey D.2005) Robert M., Francis X., David J., (2005	128.634	Azide	2127.5	11
) ,(Lin-Vien, D.; et. al., 1991)) ,(Ewen.S, Geoffrey D.2005 Robert) ,(George Socrates, 2004 M., Francis X., David J., 2005	6.263	Aromatic Nitrile	2218.7	12
), (Ewen.S, Geoffrey D.2005) Robert M., Francis X., David J., (2005	87.734	Isocyanate	2262.6	13
), (Ewen.S, Geoffrey D.2005) Robert M., Francis X., David J., (2005	28.202	P – H	2303.5	14
), (Ewen.S, Geoffrey D.2005) Robert M., Francis X., David J., (2005	31.690	P – H	2336.1	15
), (Ewen.S, Geoffrey D.2005) Robert M., Francis X., David J., (2005	217.010	P – H	2382.0	16
-	39.018	-	2438.4	17
-	56.905	-	2486.4	18
-	126.117	-	2634.1	19
), (Ewen.S, Geoffrey D.2005) Robert M., Francis X., David J., (2005	481.873	Aldehyde	2712.1	20
), (Ewen.S, Geoffrey D.2005) Robert M., Francis X., David J., (2005	71.527	$N – CH_3$	2768.8	21
) ,(Lin-Vien, D.; et. al., 1991)) ,(Ewen.S, Geoffrey D.2005 Robert M., Francis X., David J., 2005	145.896	CH_2	2804.7	22
), (Ewen.S, Geoffrey D.2005) Robert M., Francis X., David J., (2005	453.543	$C – CH_3$	2858.2	23
) ,(Lin-Vien, D.; et. al., 1991)) ,(Ewen.S, Geoffrey D.2005 Robert M., Francis X., David J., (2005	696.694	CH_2	2929.0	24
), (Ewen.S, Geoffrey D.2005) Robert M., Francis X., David J., (2005	223.762	Aromatic C – H	2974.2	25
), (Ewen.S, Geoffrey D.2005) Robert M., Francis X., David J., (Lin-Vien, D.; et. al., 1991) ,(2005	303.500	CH_2 =	3024.1	26
), (Ewen.S, Geoffrey D.2005) Robert M., Francis X., David J., (Lin-Vien, D.; et. al., 1991) ,(2005	428.811	CH_2 =	3066.3	27
), (Ewen.S, Geoffrey D.2005) Robert M., Francis X., David J.,	670.669	OH	3108.3	28

(2005				
), (Ewen.S, Geoffrey D.2005) Robert M., Francis X., David J., (2005	618.755	Amide, Amine	3176.9	29
), (Ewen.S, Geoffrey D.2005) Robert M., Francis X., David J., (2005	270.332	Amide, Amine	3309.9	30

Through the analysis of the four samples collected from Madina area it was found that the vibration modes of some materials are appeared in all the samples while other modes are appeared in some samples and disappeared in other samples. That is as follows:

1. Aromatic ring: appeared in the spectra of (Alarak, Alabar) wells, with intensities (24.615, 40.722) (au), respectively.

2. Sulfonamide, CH_2 and CH_3, C = C, Alcohol, Nitrile: appeared in the spectra of Alarak well, with intensities (21.195, 19.8, 20.520, 65.7, 16.290) (au), respectively.

3. Isothiocyanate: appeared in the spectra of (Alarak, Alabar) wells, with different intensities (7.920, 23.499) (au), respectively.

4. Alkyne: appeared in the spectra of (Alarak, Almaboath) wells, with different intensities (15.300, 109.530) (au), respectively.

5. Aromatic nitrile: appeared in the spectrum of (Alarak, Alabar) wells, with different intensities (10.575, 6.263) (au), respectively.

6. P – H: appeared in the spectra of (Alarak, Almaboath, Alabar) wells, with different intensities (8.820, 3.240, 217.01) (au), respectively.

7. Aldehyed: appeared in the spectra of (Alarak, Aldeara, Alabar) wells, with different intensities (55.755, 7.155, 481.873) (au), respectively.

8. O - CH_3: appeared in the spectra of (Alarak, Almaboath) wells, with different intensities (29.385, 61.515) (au), respectively.

9. C - CH_3: appeared in the spectra of (Alarak, Aldeara, Alabar) wells, with different intensities (74.970, 1232.730, 453.543) (au), respectively.

10. = CH2: appeared in the spectra of (Alarak, Aldeara, Almaboath, Alabar) wells, with different intensities (44.959, 222.930, 377.685, 428.811) (au), respectively.

11. OH: appeared in the spectra of (Alarak, Aldeara, Almaboath, Alabar) wells, with different intensities (81.853, 148.140, 750.690, 670.669) (au), respectively.

12. Lactone: appeared in the spectra of (Alarak, Alabar) wells, with different intensities (7.695, 15.852) (au), respectively.

13. Phenol: appeared in the spectra of (Alarak, Aldeara) wells, with different intensities (26.415, 204.255) (au), respectively.

14. Amide, Amine: appeared in the spectra of (Alarak, Aldeara, Alabar) wells, with different intensities (6.345, 311.850, 618.755) (au), respectively.

15. Aliphatic azo: appeared in the spectra of (Aldeara, Almaboath, Alabar) wells, with different intensities (19.980, 83.160, 105.957) (au), respectively.

16. Anhydride, Th iol: appeared in the spectra of Aldeara well, with intensities (113.265, 4.860) (au), respectively.

17. Azide: appeared in the spectra of (Aldeara, Alabar) wells, with different intensities (24.075, 128.634) (au), respectively.

18. Diazonium salt: appeared in the spectra of (Aldeara, Almaboath) wells, with different intensities (104.130101.295) (au), respectively.

19. N - CH_3: appeared in the spectra of (Aldeara, Alabar) wells, with different intensities (50.220, 71.527) (au), respectively.

20. Aromatic C-H: appeared in the spectra of (Aldeara, Alabar) wells, with different intensities (222.930, 223.762) (au), respectively.

21. Aromatic/hetro ring, Si - H: appeared in the spectra of Aldeara well, with intensities (93.240, 3.870) (au), respectively.

22. CH_2: appeared in the spectra of (Aldeara, Alabar) wells, with different intensities (355.680, 696.694) (au), respectively.

23. Aliphatic Ester, Isocyanate, Nitro: appeared in the spectra of Alabar well, with intensities (37.352, 87.734, 350.549) (au), respectively.

Some vibrations modes in samples (S_{11} – S_{14}), collected from Madina wells, indicate the presence of some components Like: carboxylic acid, phosphoramides, diazonium salts, benzene, hydroxide, mehylene, carbonyl, trimethylamines, hydroxyl and hydrophobic.

4.5 CONCLUSIONS

From the obtained results, one can conclude that:

- This study provides valuable the contents of the groundwater in western area in Kingdom of Saudi Arabia.
- Significant differences in the peaks intensities and Raman shift were recorded in the spectra of the samples.
- Some peaks indicate the presence of some components Like: benzene, hydroxide, acid, phosphoramides, trimethylamines, and diazonium salts.
- Certain dangerous molecules were identified like: Phenol, Isothiocyanate and Thiocyanate.

4.6 RECOMMENDATIONS

By the end of this research one can recommend the followings:

1- The usage of Laser Raman Spectroscopy to provide information about the contents of the ground water in other areas of Kingdom of Saudi Arabia.

2- The usage of Laser Raman Spectroscopy to identify and determine the concentrations of contaminates materials in water.

3- Applying laser Raman spectroscopy to characterize and identify the groundwater components in Sudan.

REFERENCES

Anna Yu. Likhacheva, et.al., (2011), *Raman spectroscopy of natural cordierite at high water pressure up to 5 GPa*, (wileyonlinelibrary.com) DOI :10.1002/jrs.3060.

Bruno Robert, (2009), *Resonance Raman Spectroscopy*, Review, photosynth Res: 101:147-155, DIO 1007/s11120-009-9440-4.

Ewen S. , Geoffery D., (2005), *Modern Raman Spectroscopy*, John Wiely and Sons, Ltd. ISBN 0-471-49668-5.

Fangyuan Han, Weimin Liu, Chong Fang, (2013), *Excited-state proton transfer of photoexcited pyranine in water observed by femtosecond stimulated Raman spectroscopy*, Journal of Chemical Physics 422 (2013) 204–219.

George Socrates, (2004), *Infrared and Raman Characteristic Group Frequencies*: Tables and Charts, 3rd Edition, John Wiley & Sons. Inc, ISBN: 978-0-470-09307-8.

Ivana –Duriˇckovi´c, et.al., (2010), *Water–ice phase transition probed by Raman Spectroscopy*, (wileyonlinelibrary.com) DOI 10.1002/jrs.2841.

J. Kauppinen, J. Partanen (2001), *Fourier Transforms in Spectroscopy* (Wiley, New York).

J.L. Kinsey (1977), *Laser-induced fluorescence*. Ann. Rev. Phys. Chem. 28, 349.

J.R. Lakowicz (1991), *Topics in Fluorescence Spectroscopy*, (Plenum, New York).

John R. et al. (2003), *Introductory Raman Spectroscopy*, (Second edition), Elsevier, ISBN: 978-0-12-254105-6.

K. A. Vereschagin., et.al., (2007), *Coherent anti-stokes Raman spectroscopy investigation of collisional broadening of the hydrogen Q-branch transitions by water at high temperatures*, J. Raman Spectrosc. 2008; 39: 722–725 (www.interscience.wiley.com) DOI: 10.1002/jrs.1930.

Kazuhiro Ito, et.al., (2002), *Non-destructive method for the quantification of the average particle diameter of latex as water-based emulsions by near-*

infrared Fourier transform Raman spectroscopy, J. Raman Spectrosc. 2002; 33: 466–470, (www.interscience.wiley.com). DOI: 10.1002/jrs.860.

Lin-Vien, D.; et. al., (1991), *The Handbook of Infrared and Raman Characteristic Frequencies of Organic Molecules*, 1st ed.; Academic Press: San Diego.

Lambda Scientific Pty Ltd, (2016), *LIRA-300 Laser Raman Spectrometer*, Available at: (http://www.lambdasci.com/uploads/brochures/catalog.pdf), [29 July 2016].

Martin Mulvihill, et.al., (2008), *Surface-Enhanced Raman Spectroscopy for Trace Arsenic Detection in Contaminated Water*, Angew. Chem. Int. Ed. 2008, 47, 6456 –6460 DOI: 10.1002/anie.200800776.

Monsuru O. Gborigi, et.al. , (2005), *Raman spectroscopy of a hydrated CO_2/water composite*, Journal of Petroleum Science and Engineering 56 (2007) 65–74.

M. Pastorczak, et.al., (2009), *Water–Polymer interactions in PVME hydrogels – Raman spectroscopy studies*, Journal of Polymer 50 (2009) 4535–4542.

P. Larkin, (2011), *Infrared and Raman Spectroscopy*; Principles and Spectral Interpretation, Elsevier.

Phodchanee Phongpa-Ngan, et.al., (2014), *Raman spectroscopy to assess water holding capacity in muscle from fast and slow growing broilers*, LWT -Food Science and Technology 57 (2014) 696e700.

P. Sobron, et.al., (2007), *Modeling the physico-chemistry of acid sulfate waters through Raman spectroscopy of the system $FeSO_4$–H_2SO_4–H_2O, J.* Raman Spectrosc. 2007; 38: 1127–1132 (www.interscience.wiley.com) DOI: 10.1002/jrs.1729.

P. Schmidt, J. Dybal, M. Trchova, (2006), *Investigations of the hydrophobic and hydrophilic interactions in polymer–water systems by ATR FTIR and Raman spectroscopy*, Journal of Vibrational Spectroscopy 42 (2006) 278–283.

Qiang Sun, (2009), *The Raman OH stretching bands of liquid water*, Journal of Vibrational Spectroscopy 51 (2009) 213–217.

Richard L. (2000), *Raman Spectroscopy for Chemical Analysis*, the Ohio State University Columbus, Ohio/ILEY Interscience a John Wiley & Sons, INC., Publication New York/ by John Wiley & Sons, IncAll rights reseved. Published simultaneously in Canada.

Robert M., Francis X., David J., (2005), *Spectromtric Idendification of Organic Compounds*, seven edition, John Wiley & Sons.Inc, ISBN 0-471-39362-2,USA.

S. Burikov, et.al., (2010), *Identification And Determination Of Concentration Of Salts In Natural Waters By Raman Spectroscopy Using Artificial Neural Networks*, American Institute of Physics 978-0-7354-0818-0/10.

Stephen J. et al., (2002), *Water and the environment, American Geological Institute*, ISBN 0-922152-63-2.

Vinceza Crupi. et. al., (2007), *a new insight on the hydrogen bonding structures of nanoconfined water*: a Raman study. Published online 14 December 2007 in Wiley InterScience, DOI: 10.1002/jrs.1857.

W. Demtroder, (2008), *laser spectroscopy*, Fourth edition, Springer-Verlag Berlin Heidelberg, ISBN 978-3-540-73415-4.

Xuesong Song, et. al., (2013), *Detection of herbicides in drinking water by surface-enhanced Raman spectroscopy coupled with gold nanostructures*, Published online: 30 July 2013, Springer Science New York, DOI 10.1007/s11694-013-9145-4.

Yang Zhaoa, et.al., (2014), *Molecular vibrational dynamics in water studied by femtosecond coherent anti-Stokes Raman spectroscopy*, Journal of Chemical Physics Letters 613 (2014) 1–4.

Zhiyun Li, et. al., (2014), *Raman Spectroscopy for In-Line Water Quality Monitoring — Instrumentation and Potential*, Sensors, 14, 17275-17303; DOI: 10.3390/s140917275.